

Manuscript Number: EJMECH-D-19-02351R1

Title: Design, synthesis and biological evaluation of novel TR $\beta$  selective agonists sustained by ADME-Toxicity analysis

Article Type: Full Paper

Keywords: Triiodothyronine, thyronamine, TR $\beta$  selective agonist, fatty-liver disorder, ADME-T

Corresponding Author: Professor Simona Rapposelli, Ph.D

Corresponding Author's Institution: University of Pisa

First Author: Massimiliano Runfola

Order of Authors: Massimiliano Runfola; Simona Sestito; Lorenza Bellusci; Valeria La Pietra; Vincenzo Maria D'amore; Marta Anna Kowalik; Grazia Chiellini; Sheraz Gul; Andrea Perra; Amedeo columbano; luciana Marinelli; Ettore Novellino; Simona Rapposelli, Ph.D

Abstract: Although triiodothyronine (T<sub>3</sub>) induces several beneficial effects on lipid metabolism, its use is hampered by toxic side-effects, such as tachycardia, arrhythmia, heart failure, bone and muscle catabolism and mood disturbances. Since the  $\alpha$  isoform of thyroid hormone receptors (TRs) is the main cause of T<sub>3</sub>-related harmful effects, several efforts have been made to develop selective agonists of the  $\beta$  isoform that could induce some beneficial effects (i.e. lowering triglyceride and cholesterol levels reducing obesity and improving metabolic syndrome), while overcoming most of the adverse T<sub>3</sub>-dependent side effects. Herein, we describe the drug discovery process sustained by ADME-Toxicity analysis that led us to identify novel agonists with selectivity for the isoform TR $\beta$  and an acceptable off-target and absorption, distribution metabolism, excretion and toxicity (ADME-Tox) profile. Within the small series of compounds synthesized, derivatives 1 and 3, emerge from this analysis as "potentially safe" to be engaged in preclinical studies. In in vitro investigation proved that both compounds were able to reduce lipid accumulation in HepG2 and promote lipolysis with comparable effects to those elicited by T<sub>3</sub>, used as reference drug. Moreover, a preliminary in vivo study confirmed the apparent lack of toxicity, thus suggesting compounds 1 and 3 as new potential TR $\beta$ -selective thyromimetics.

Dear Editor,

We deeply appreciate your wonderful jobs on our manuscript **Design, synthesis and biological evaluation of novel TR $\beta$  selective agonists sustained by ADME-Toxicity analysis** (*EJMECH-D-19-02351*). We have revised and submitted back the revised manuscript according to the reviewers' comments. Our response to the reviewer's comments point-by-point is appended at the letter.

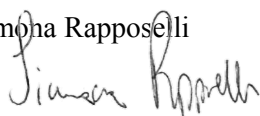
Hope we have addressed all the reviewers' concerns and our revised manuscript will meet all the requirements of the publication on the *European Journal of Medicinal Chemistry*.

Thank you very much for your consideration!

Sincerely yours,

The corresponding author

Simona Rapposelli

A handwritten signature in black ink, appearing to read 'Simona Rapposelli', written in a cursive style.

Reviewers' comments:

**Reviewer #3:** It is a very well written manuscript on a nice piece of work which is both substantial and comprehensive.

**Reply:** We would like to thank the Reviewer for the positive comments on our manuscript.

**Reviewer #4:** Rapposelli and co-workers report their effort towards the development of TRbeta agonists with specificity for the liver.

This manuscript is very well written, with clear objectives, strong rationale and a clear design and optimization strategy. Notably, efforts were made to discard CYP inhibitors and toxic compounds (off-targets) early in the process. I cannot comment on the biology which is outside of my expertise, but from what I read/understood, this manuscript deserves to be published in EJMC.

**Reply:** Thank you for the positive comments

Minor comments:

1. The Figures should be revised. The molecules are too small and there is way too much empty space. For example, Figure 2 shows molecules that are smaller than in the other figures while Scheme 3 could be reorganized to make it more compact.

**Reply:** We revised the Figure 2 as suggested. The Scheme 3 has been re-organized and now is more compacted.

2. It looks like the J. Med. Chem. format was used. In EJMC, Schemes and Figure should have a single legend at the bottom and not footnotes with the scheme number at the top and the references should be in square brackets. There might be other rules that I am not aware of.

**Reply:** Thank you for your suggestion. Indeed the manuscript was not formatted following the European Journal of Medicinal Chemistry. The revised manuscript has been properly corrected following the Elsevier Guidelines. Also the references have been properly revised.

#### **Editor's comments:**

Data in Brief (optional):

We invite you to convert your supplementary data (or a part of it) into an additional journal publication in Data in Brief, a multi-disciplinary open access journal. Data in Brief articles are a fantastic way to describe supplementary data and associated metadata, or full raw datasets deposited in an external repository, which are otherwise unnoticed.

You can submit to Data in Brief via the European Journal of Medicinal Chemistry submission system when you upload your revised European Journal of Medicinal Chemistry manuscript. To do so, complete the template and follow the co-submission instructions found here: [www.elsevier.com/dib-template](http://www.elsevier.com/dib-template). If your European Journal of Medicinal Chemistry manuscript is accepted, your Data in Brief submission will automatically be transferred to Data in Brief for editorial review and publication.

**Reply:** Following the Editor Suggestions, we converted part of supplementary data in a "Data in Brief" publication.

We are submitting Data in Brief via European Journal of Medicinal Chemistry submission system as indicated above

Reviewers' comments:

**Reviewer #3:** It is a very well written manuscript on a nice piece of work which is both substantial and comprehensive.

**Reply:** We would like to thank the Reviewer for the positive comments on our manuscript.

**Reviewer #4:** Rapposelli and co-workers report their effort towards the development of TRbeta agonists with specificity for the liver.

This manuscript is very well written, with clear objectives, strong rationale and a clear design and optimization strategy. Notably, efforts were made to discard CYP inhibitors and toxic compounds (off-targets) early in the process. I cannot comment on the biology which is outside of my expertise, but from what I read/understood, this manuscript deserves to be published in EJMC.

**Reply:** Thank you for the positive comments

Minor comments:

1. The Figures should be revised. The molecules are too small and there is way too much empty space. For example, Figure 2 shows molecules that are smaller than in the other figures while Scheme 3 could be reorganized to make it more compact.

**Reply:** We revised the Figure 2 as suggested. The Scheme 3 has been re-organized and now is more compacted.

2. It looks like the J. Med. Chem. format was used. In EJMC, Schemes and Figure should have a single legend at the bottom and not footnotes with the scheme number at the top and the references should be in square brackets. There might be other rules that I am not aware of.

**Reply:** Thank you for your suggestion. Indeed the manuscript was not formatted following the European Journal of Medicinal Chemistry. The revised manuscript has been properly corrected following the Elsevier Guidelines. Also the references have been properly revised.

**Editor's comments:**

Data in Brief (optional):

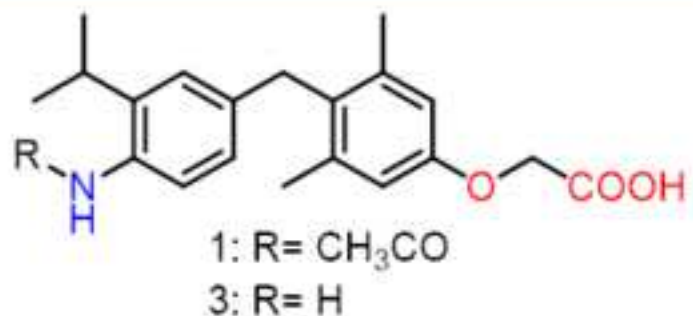
We invite you to convert your supplementary data (or a part of it) into an additional journal publication in Data in Brief, a multi-disciplinary open access journal. Data in Brief articles are a fantastic way to describe supplementary data and associated metadata, or full raw datasets deposited in an external repository, which are otherwise unnoticed.

You can submit to Data in Brief via the European Journal of Medicinal Chemistry submission system when you upload your revised European Journal of Medicinal Chemistry manuscript. To do so, complete the template and follow the co-submission instructions found here: [www.elsevier.com/dib-template](http://www.elsevier.com/dib-template). If your European Journal of Medicinal Chemistry manuscript is accepted, your Data in Brief submission will automatically be transferred to Data in Brief for editorial review and publication.

**Reply:** Following the Editor Suggestions, we converted part of supplementary data in a "Data in Brief" publication.

We are submitting Data in Brief via European Journal of Medicinal Chemistry submission system as indicated above

## New selected thyromimetics



2 compounds

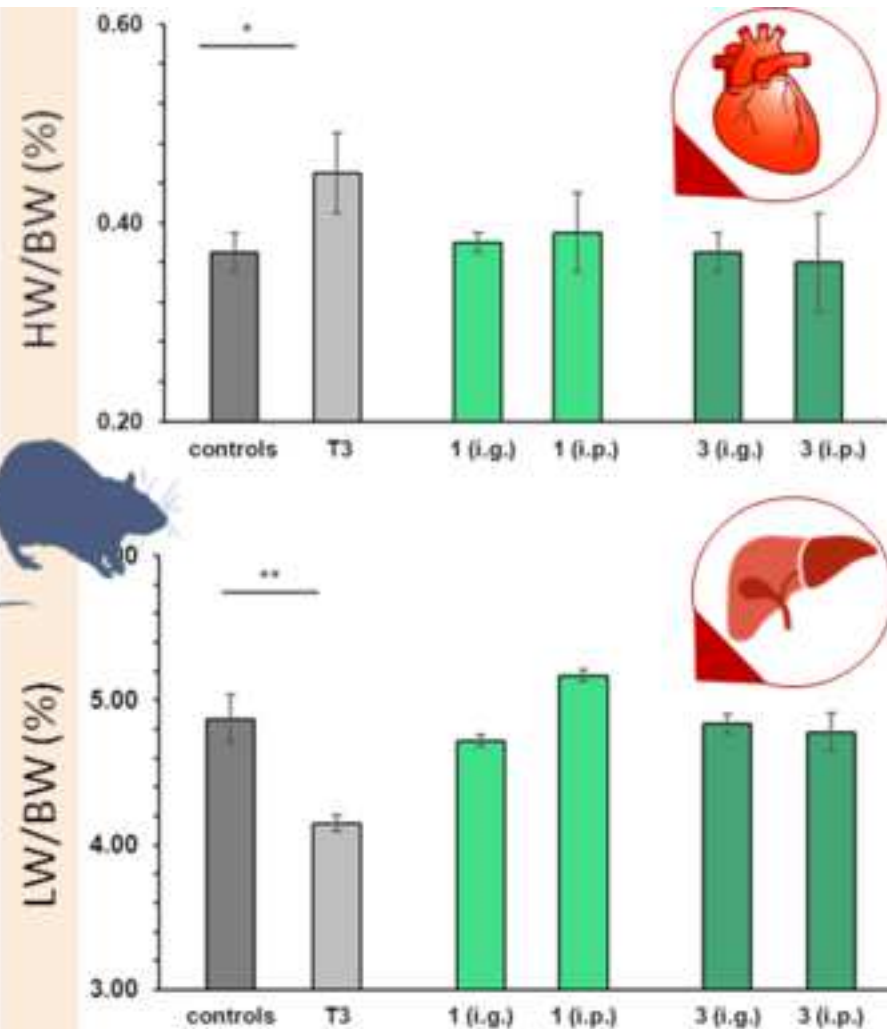
In vitro efficacy

6 compounds

ADME-TOX profiling

11 compounds

New thyromimetics library



## HIGHLIGHTS

- A novel series of thyromimetics was developed and their ADME-Toxicity profile was assessed.
- To simulate the interaction of selected compounds with the putative receptor-binding site in silico docking-studies were performed
- Compounds **1** and **3** proved to be TR $\beta$  selective agonists and promote lipolysis through the activation of AMPK/ACC pathway
- Preliminary in vivo studies of thyromimetics **1** and **3** confirm a safe-profile of both compounds, lacking both cardio- and hepatotoxicity.



1 **Design, synthesis and biological evaluation of novel TR $\beta$  selective agonists**  
2 **sustained by ADME-Toxicity analysis**

3 *Massimiliano Runfola<sup>1#</sup>, Simona Sestito<sup>1#</sup>, Lorenza Bellusci<sup>2</sup>, Valeria La Pietra<sup>3</sup>, Vincenzo Maria*  
4 *D'Amore<sup>3</sup>, Marta Anna Kowalik<sup>4</sup>, Grazia Chiellini<sup>2\*</sup>, Sheraz Gul<sup>5</sup>, Andrea Perra<sup>4</sup>, Amedeo*  
5 *Columbano<sup>4</sup>, Luciana Marinelli<sup>3</sup>, Ettore Novellino<sup>3</sup>, Simona Rapposelli<sup>1,6\*</sup>*

6 <sup>1</sup>Department of Pharmacy, University of Pisa, Pisa, 56126, Italy;

7 <sup>2</sup>Department of Pathology, University of Pisa, Pisa, 56126, Italy;

8 <sup>3</sup>Department of Pharmacy, University of Naples Federico II, Italy;

9 <sup>4</sup>Department of Biomedical Sciences, Unit of Oncology and Molecular Pathology, University of  
10 Cagliari, Cagliari, Italy;

11 <sup>5</sup>Fraunhofer Institute for Molecular Biology & Applied Ecology – ScreeningPort, Hamburg,  
12 Germany;

13 <sup>6</sup>Interdepartmental Research Centre for Biology and Pathology of Aging, University of Pisa,  
14 Pisa, Italy.

15

16 # M.R and S.S equally contributed;

17 \*For S.R.: phone, +39 050 2219582; fax, +39 050 2219577; Email: [simona.rapposelli@unipi.it](mailto:simona.rapposelli@unipi.it)

18 \*For G.C.: phone, +39 050 2218662; E-mail, [grazia.chiellini@unipi.it](mailto:grazia.chiellini@unipi.it)

19

20 **KEYWORDS:** Triiodothyronine, thyronamine, TR $\beta$  selective agonist, fatty-liver disorder, liver  
21 regeneration

22

23

24

25

26

27

28

29

30

31

32

33

34 **HIGHLIGHTS**

- 35
- 36
- 37
- 38
- 39
- 40
- 41
- 42
- 43
- A novel series of thyromimetics was developed and their ADME-Toxicity profile was assessed.
  - To simulate the interaction of selected compounds with the putative receptor-binding site in silico docking-studies were performed
  - Compounds **1** and **3** proved to be TR $\beta$  selective agonists and promote lipolysis through the activation of AMPK/ACC pathway
  - Preliminary in vivo studies of thyromimetics **1** and **3** confirm a safe-profile of both compounds, lacking of both cardio- and hepatotoxicity.

## 44 **ABSTRACT**

45 Although triiodothyronine (T3) induces several beneficial effects on lipid metabolism, its use is  
46 hampered by toxic side-effects, such as tachycardia, arrhythmia, heart failure, bone and muscle  
47 catabolism and mood disturbances. Since the  $\alpha$  isoform of thyroid hormone receptors (TRs) is  
48 the main cause of T3-related harmful effects, several efforts have been made to develop selective  
49 agonists of the  $\beta$  isoform that could induce some beneficial effects (i.e. lowering triglyceride and  
50 cholesterol levels reducing obesity and improving metabolic syndrome), while overcoming most  
51 of the adverse T3-dependent side effects. Herein, we describe the drug discovery process  
52 sustained by ADME-Toxicity analysis that led us to identify novel agonists with selectivity for  
53 the isoform TR $\beta$  and an acceptable off-target and absorption, distribution metabolism, excretion  
54 and toxicity (ADME-Tox) profile. Within the small series of compounds synthesized, derivatives  
55 **1** and **3**, emerge from this analysis as “potentially safe” to be engaged in preclinical studies. In *in*  
56 *vitro* investigation proved that both compounds were able to reduce lipid accumulation in HepG2  
57 and promote lipolysis with comparable effects to those elicited by T3, used as reference drug.  
58 Moreover, a preliminary *in vivo* study confirmed the apparent lack of toxicity, thus suggesting  
59 compounds **1** and **3** as new potential TR $\beta$ -selective thyromimetics.

60

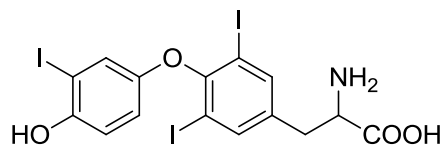
## 61 **INTRODUCTION**

62 Thyroid hormones (THs) are essential regulatory molecules for normal growth and development  
63 and for maintaining metabolic homeostasis<sup>1</sup>. Most of the activities elicited by THs are mediated  
64 by nuclear thyroid hormones receptors (TRs), which are members of the nuclear hormone  
65 receptor family and act as ligand-activated transcription factors. There are two main TR isoforms  
66 encoded on separate genes, namely TR $\alpha$  and TR $\beta$ . Both TR isoforms bind 3,5,3'-triiodothyronine  
67 (T3) and mediate TH-regulated gene expression through interactions with DNA response  
68 elements and with a complex array of transcriptional cofactors, including corepressors (CoRs),  
69 coactivators (CoAs), integrators like CREB-binding protein (CBP), and general transcription  
70 factors (GTFs)<sup>2</sup>. TH/TR binding exerts profound effects in several physiological processes. In  
71 the central nervous system (CNS) THs signaling is involved in development and maintenance of  
72 brain function, influencing various activities such as neuronal and glial cell differentiation,  
73 myelination, and neurogenesis<sup>3, 4</sup>. In the liver, THs influence hepatic lipid metabolism through

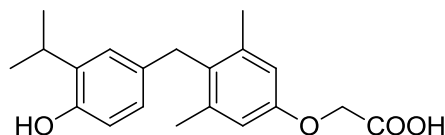
74 multiple pathways, with insightful effects on energy expenditure<sup>5</sup>, fat oxidation<sup>6</sup> and cholesterol  
75 metabolism<sup>7</sup>. Conversely, alteration of cellular TH signaling in the liver plays a key role in the  
76 onset or progression of several liver-associated diseases, such as non-alcoholic fatty liver disease  
77 (NAFLD), and hepatocellular carcinoma (HCC)<sup>8</sup>. Therefore, modulating the function of THs  
78 offers the potential to treat a wide variety of liver diseases and cancer, as well. Unfortunately, the  
79 use of THs as therapeutic agents is hampered by the lack of selectivity and the consequent  
80 adverse side effects (such as increased heart rate, cardiac hypertrophy, muscle wasting, and  
81 reduced bone density) that are mainly due to their binding to TR $\alpha$  receptors. In order to  
82 overcome these drawbacks, selective activation of the  $\beta$  thyroid hormone receptor (TR $\beta$ ) is an  
83 appropriate method to develop new treatments for several chronic diseases with a reduced side  
84 effect profile.

85 During the past two decades, a number of selective TR $\beta$  agonists have been developed. These  
86 include the analogues Sobetrome (GC-1), KB-141 and the Hep-Direct prodrug VK2809 that  
87 exhibit most of the beneficial properties of T3 in the absence of deleterious effects<sup>9-11</sup>. GC-1  
88 emerged in 1995<sup>9</sup> as the first halogen free thyromimetics. It was shown to bind preferentially to  
89 TR $\beta$  vs TR $\alpha$  and was initially studied as an hypocholesterolemic compound able to stimulate  
90 hepatic pathways without harmful side effects<sup>12</sup>. Due to the beneficial effects of GC-1 and  
91 KB2115, the latter known as Eprotirome, entered human clinical trials for dyslipidaemia, and  
92 yielded encouraging results in the absence of harmful effects typically associated with THs high  
93 levels (for reviews, see Tancevski *et al.* 2011<sup>13</sup>, Meruvu *et al.* 2013<sup>14</sup>). The progression of GC-1  
94 was discontinued despite a promising phase I trial for the treatment of lipid metabolism disorders  
95 and obesity, with no phase II trials being planned. Additional applications of GC-1 have been  
96 proposed in orphan indications and this drug is now in phase I/II trial for a rare disease (X-  
97 Linked Adrenoleukodystrophy) (Clinicaltrial.gov Identifier: NCT03196765). Eprotirome,  
98 progressed to phase III clinical trial but was terminated due to unexpected side effects in animal  
99 studies<sup>15</sup>. Another selective thyromimetic, namely Resmetirom (MGL-3196) was designed as a  
100 liver-specific TR $\beta$  agonist able to reduce hepatic lipid synthesis and has progressed to phase II  
101 trials (ClinicalTrials.gov Identifier: NCT02912260). In addition, VK2809 is a novel liver-  
102 directed thyroid receptor beta agonist pro-drug<sup>16</sup> that possesses selectivity for liver tissue, and  
103 after undergoing cleavage by a cytochrome P450 enzyme is able to release the potent TR binds  
104 to TR $\beta$  selective thyromimetic MB07344 (**Figure 1**). Currently, VK2809 has progressed to

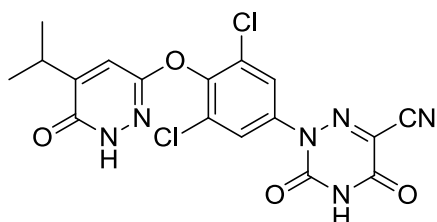
105 Phase 2 clinical trial in patients with primary hypercholesterolemia and non-alcoholic fatty liver  
106 disease (NAFLD). (ClinicalTrials.gov identifier: NCT02927184). Although many thyromimetics  
107 are currently in clinical trials, none have been approved by FDA (**Figure 1**).



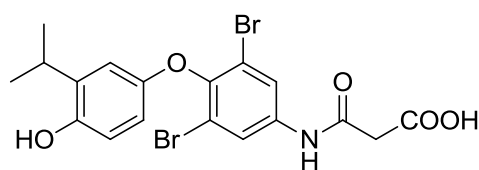
T3



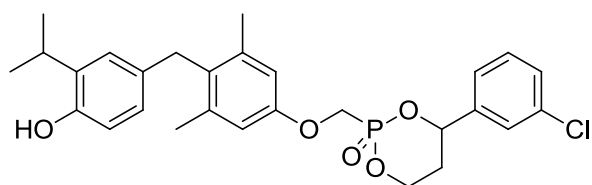
Sobetirome (GC-1)



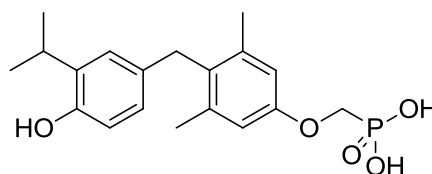
Resmetirom, MGL-3196



Eprotirome (KB2115)



VK2809



MB07344

108

109 **Figure 1.** Structures of TR $\beta$  agonists which have been progressed in drug discovery.

110

111 Despite the challenges with progressing TR $\beta$  selective agonists due to their side effect profiles,  
112 their use to treat other human pathologies could be explored as part of drug repositioning  
113 strategies. Accordingly, the identification of novel agonists with selectivity for both the TR $\beta$  and  
114 the liver could represent a valid strategy to regulate metabolic disorders. This paper reports the  
115 results of the design and synthesis of a novel series of TR $\beta$  agonists. The thyromimetic-  
116 analogues were evaluated for their off-target and ADME-Tox properties and the most optimal  
117 compounds progressed to *in vitro* profiling in a nuclear receptor coregulator assay  
118 (Thermofisher®) and for their ability to promote lipolysis in human hepatoma cells (HepG2).

119 Further investigation to determine the cellular pathways involved in their lipid-lowering ability  
120 was also carried-out. Additionally, to rationalize the pharmacological results, *in silico* docking  
121 studies on selected compounds were also performed in order to simulate their interaction with the  
122 putative receptor-binding site. Finally, we performed preliminary *in vivo* studies to assess the  
123 effect of two thyromimetics (compound **3** and its pro-drug **1**), which were shown to be associated  
124 with the most optimal off-target and ADME-Tox profile, to determine their ability to modulate  
125 cholesterol serum levels, triglycerides, glucose, bilirubin and transaminases in rats.

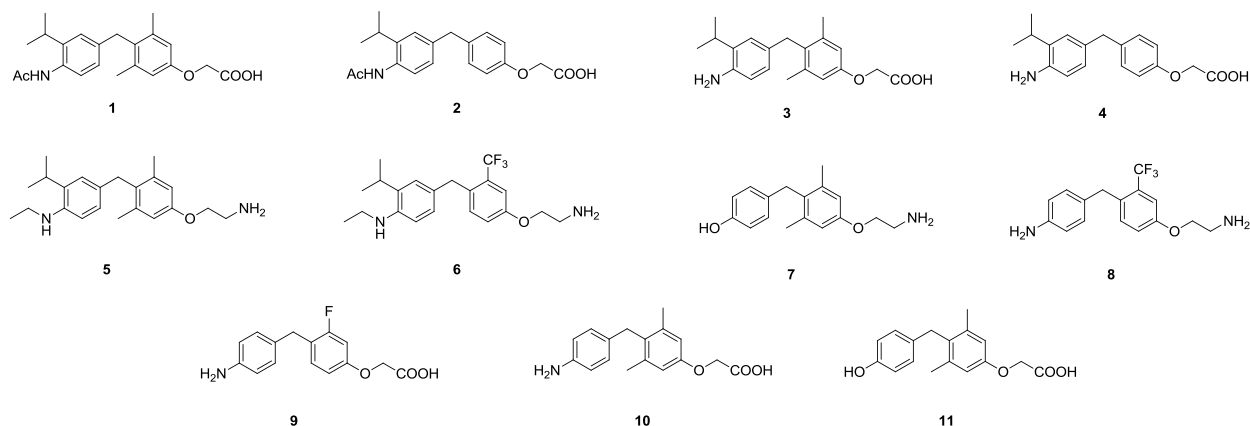
126

## 127 **RESULTS & DISCUSSION**

### 128 **Rational design of new thyromimetic molecules**

129 Our search for therapeutic agents focused on the design and synthesis of agonists endowed with  
130 high selectivity for TR $\beta$  and enhanced hepato-specificity. To this end, we designed and  
131 synthesized a new class of thyromimetics based on a diphenylmethane scaffold. This moiety has  
132 been widely recognized as an effective replacement for the biaryl-ether core of THs<sup>16-20</sup>. Notably,  
133 in previously developed diphenylmethane-based thyromimetics, the oxyacetic acid side chain  
134 was shown to have a critical role in conferring TR $\beta$  selectivity<sup>19</sup>. On the basis of this finding, we  
135 designed compounds **1-4** and **9-11** (**Figure 2**). In compounds **3**, **4**, **9** and **10**, the hydroxyl group  
136 at the 4'-position in T3 was replaced by an amino group. This type of modification generates the  
137 zwitterion that could be detrimental for the bioavailability of the molecule. Hence, we  
138 synthesized the corresponding acetamide-analogues of **3** and **4**, namely **1** and **2**, which could  
139 represent potential pro-drugs with improved drug-like properties. Oral administration of these  
140 pro-drugs, by first pass metabolism through the liver, should lead to an efficient generation of the  
141 corresponding parent compounds. Based on our previous experience gained during the  
142 development of SG-compounds as thyronamine analogues of T1AM, it is known that the  
143 oxyethylamine sidechain represents a valid precursor of the oxyacetic group that is formed  
144 following the metabolic activation by MAOs<sup>18</sup>. Therefore, we synthesized the derivatives **5-8** as  
145 possible precursors of the corresponding thyromimetics with an oxyacetic structure. The two  
146 iodine atoms present in the T3 inner ring have been replaced with hydrogen atoms (**2** and **4**),  
147 with two methyl groups (**1**, **3**, **5**, **7**, **10** and **11**) or with a hydrogen and CF<sub>3</sub> (or H and F) as in

148 compounds **6**, **8** and **9**. As to the iodine atom in the outer ring of T3, it has been replaced by an  
149 isopropyl group (**1-6**) or by a hydrogen atom (**7-11**).



150

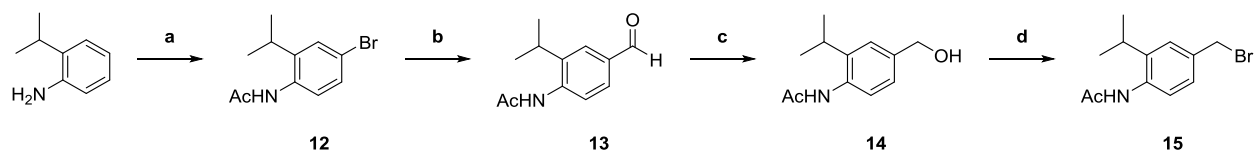
151 **Figure 2.** Structures of novel thyromimetics **1-11** with a biphenylmethane scaffold.

152

### 153 Chemistry

154 A crucial component in our synthetic procedures is the synthesis of the biphenylmethane scaffold  
155 which was obtained with the palladium (0)-catalyzed Suzuki-Miyaura cross coupling reaction  
156 between the substituted benzylbromide and selected phenyl boronic acid derivatives. The  
157 Suzuki-Miyaura reaction was performed under standard or microwave-assisted conditions, with  
158 yields ranging from 22% and 60% as reported in **Table 1**. In particular, benzylbromide **15**, which  
159 was not commercially available, was obtained as shown in **Scheme 1**. A one-pot reaction  
160 between 2-isopropylaniline, acetic anhydride, and bromine was carried out in acetic acid  
161 providing the bromobenzene derivative **12** with high yields. Then, formylation of **12** with n-BuLi  
162 and DMF at  $-78\text{ }^{\circ}\text{C}$  led to benzaldehyde-derivative **13**, which was reduced with  $\text{NaBH}_4$  to  
163 provide the benzylic alcohol **14**. Finally, **15** was obtained by bromination of **14**, using  $\text{CBr}_4$  and  
164  $\text{PPh}_3$  (Appel reaction).

### 165 Scheme 1.

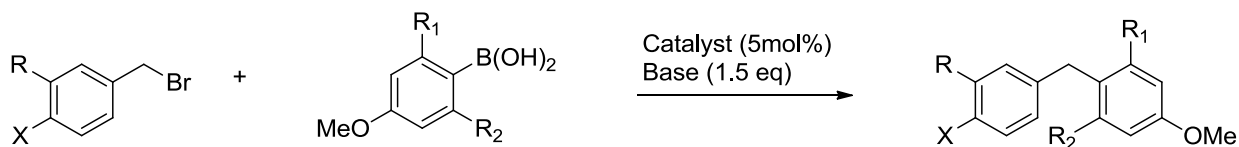


166  
167

**a Reagents and conditions.** (a) 1:  $\text{Ac}_2\text{O}$ ,  $\text{AcOH}$ ,  $117\text{-}118\text{ }^{\circ}\text{C}$ , 1 h; 2:  $\text{Br}_2$ ,  $\text{AcOH}$ ,  $65\text{ }^{\circ}\text{C}$ , 30' (b)

168 n-BuLi, DMF, THF, -78 °C → rt, 3 h; (c) NaBH<sub>4</sub>, MeOH, 0 °C → rt, 12 h; (d) CBr<sub>4</sub>, PPh<sub>3</sub>,  
 169 DCM, 0 °C → rt, 12 h.

170



A: R=H, X=NO<sub>2</sub>  
 B: R=iPr, X=NHAc

Substrate

Product

Substrate<sup>a</sup>

Entry	R <sub>1</sub>	R <sub>2</sub>	Product	Base	Catalyst	Solvent	Temp.	Time	Yield <sup>d</sup>
B <sup>b</sup>	Me	Me	<b>16</b>	K <sub>2</sub> CO <sub>3</sub>	PdCl <sub>2</sub>	acetone/H <sub>2</sub> O	40 °C	6h	60%
B <sup>b</sup>	H	H	<b>17</b>	K <sub>2</sub> CO <sub>3</sub>	PdCl <sub>2</sub>	Acetone/H <sub>2</sub> O	100 °C	10 <sup>c</sup>	30%
B <sup>b</sup>	CF <sub>3</sub>	H	<b>18</b>	K <sub>2</sub> CO <sub>3</sub>	Pd(PPh <sub>3</sub> ) <sub>4</sub>	1,4 dioxane	90 °C	12h	22%
A <sup>a</sup>	F	H	<b>24</b>	Ba(OH) <sub>2</sub> ·8H <sub>2</sub> O	Pd(PPh <sub>3</sub> ) <sub>4</sub>	1,2-DME/H <sub>2</sub> O	110 °C	20 <sup>c</sup>	39%
A <sup>a</sup>	CF <sub>3</sub>	H	<b>25</b>	K <sub>2</sub> CO <sub>3</sub>	Pd(PPh <sub>3</sub> ) <sub>4</sub>	1,4 dioxane	90 °C	6h	52%
A <sup>a</sup>	Me	Me	<b>26</b>	K <sub>2</sub> CO <sub>3</sub>	PdCl <sub>2</sub>	acetone/H <sub>2</sub> O	rt	72h	32%

171 **Table 1. Cross-Coupling Reactions.** <sup>a</sup> commercially available starting material; <sup>b</sup> compound **15**;  
 172 <sup>c</sup> reaction was performed using a microwave reactor; <sup>d</sup> yields refer to products after compound  
 173 purification which was performed by flash chromatography (for further information on eluent  
 174 mixture, consult **SI**).

175

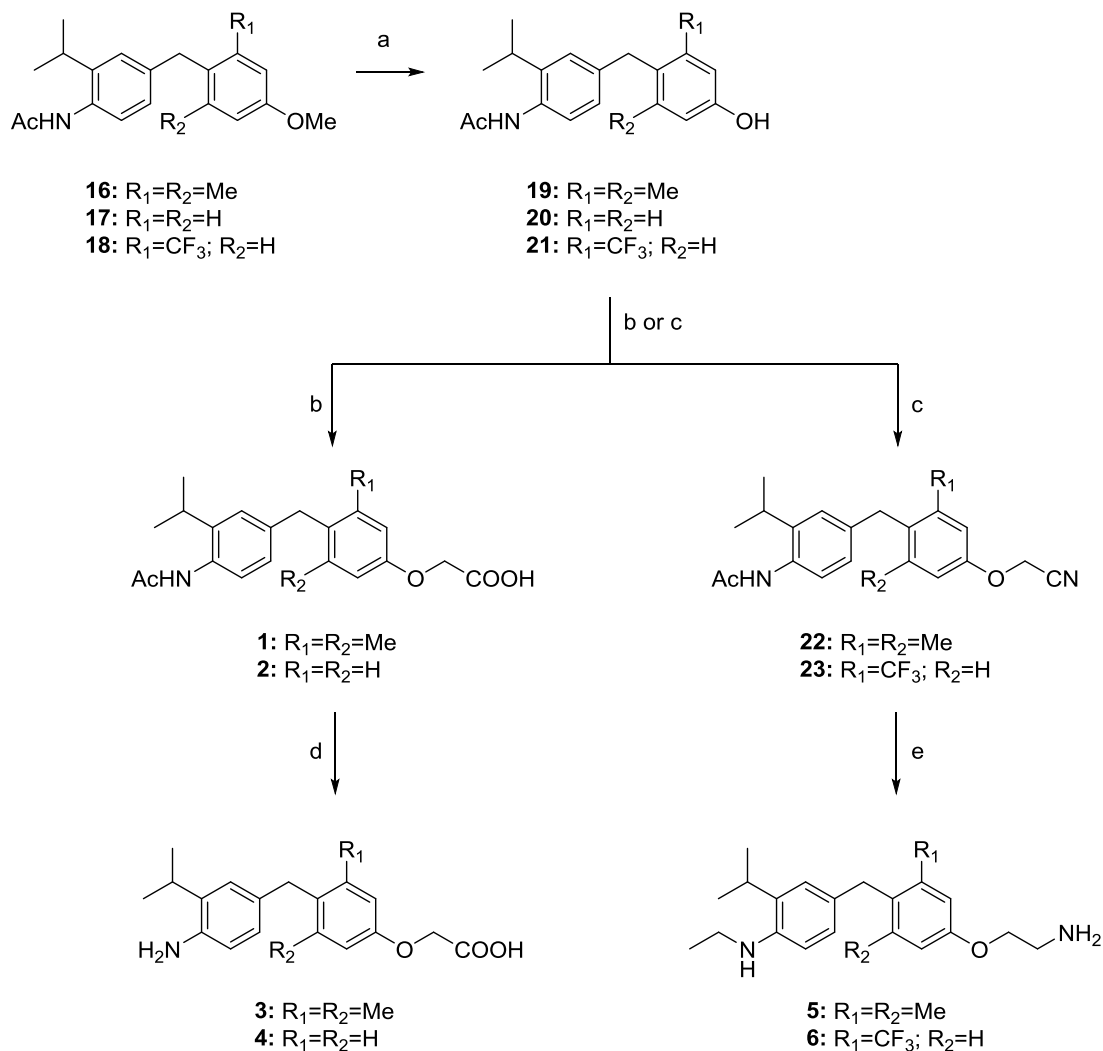
176 **Scheme 2** illustrates the synthetic procedure to obtain compounds **1-6**. Briefly, phenol  
 177 derivatives **19-21** were obtained by demethylation of purified cross coupling products **16-18** by  
 178 using BBr<sub>3</sub>. The following O-alkylation reaction of **20** and **21** with bromoacetic acid led to  
 179 compound **1** and **2**, which have undergone deacetylation in presence of hydrochloric acid at  
 180 concentrated grade to provide desired compound **3** or **4**. Compounds **5** and **6** were obtained by



181 reaction of phenolic derivative **19** or **21** with bromoacetonitrile, followed by reduction of  
182 intermediates **22** and **23** in presence of  $\text{LiAlH}_4$  and  $\text{AlCl}_3$ .

183 **Scheme 2<sup>a</sup>**

184



185

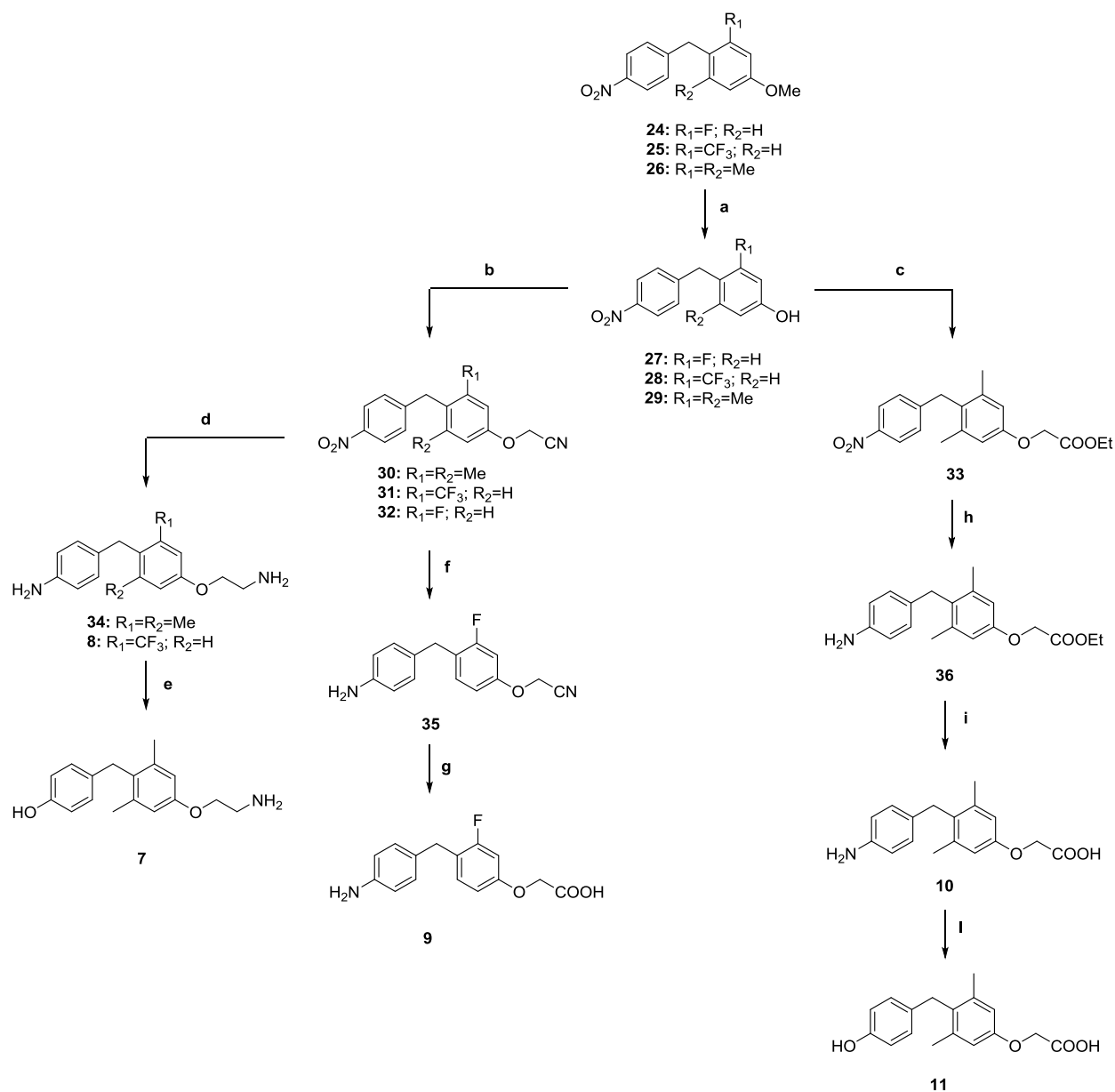
186 <sup>a</sup> **Reagents and conditions.** (a)  $\text{BBr}_3$ , DCM,  $-10\text{ }^\circ\text{C}$ , 1 h; (b)  $\text{BrCH}_2\text{COOH}$ , DMF,  $\text{Cs}_2\text{CO}_3$ , rt, 1  
187 h; (c)  $\text{BrCH}_2\text{CN}$ , DMF,  $\text{Cs}_2\text{CO}_3$ , rt, 30'; (d)  $\text{HCl}_{37\%}$ ,  $\text{H}_2\text{O}$ ,  $120\text{ }^\circ\text{C}$ , 12 h; (f)  $\text{LiAlH}_4$ ,  $\text{AlCl}_3$ , THF,  
188 rt  $\rightarrow 66\text{ }^\circ\text{C}$ , 12 h.

189

190 Compounds **7-11** were obtained according to the synthetic procedure reported in **Scheme 3**.  
191 Briefly, purified cross-coupling products **24-26** were treated with  $\text{BBr}_3$  to afford the phenol

192 derivatives **27-29** which have undergone O-alkylation reaction with bromoacetonitrile or ethyl  
 193 bromoacetate leading to intermediates **30-32** and **33**, respectively. Compound **9** was obtained by  
 194 selective nitro-group reduction (**35**), followed by acid hydrolysis with HCl at concentrated grade.  
 195 Treatment of **33** with hydrazine and FeCl<sub>3</sub> led to ethyl ester **36** which was converted to  
 196 compound **10** by mild saponification. Finally, the conversion of amine moiety of **10** to a phenolic  
 197 group using diazonium salt led to compound **11**.

198 **Scheme 3<sup>a</sup>**



199  
 200 <sup>a</sup> **Reagents and conditions:** (a) BBr<sub>3</sub>, DCM, -10 °C, 1 h; (b) BrCH<sub>2</sub>CN, DMF, Cs<sub>2</sub>CO<sub>3</sub>, rt, 20', 1  
 201 h (c) BrCH<sub>2</sub>COOEt, DMF, Cs<sub>2</sub>CO<sub>3</sub>, rt, 1 h; (d) LiAlH<sub>4</sub>, AlCl<sub>3</sub>, THF, rt → 66 °C, 12 h; (e)

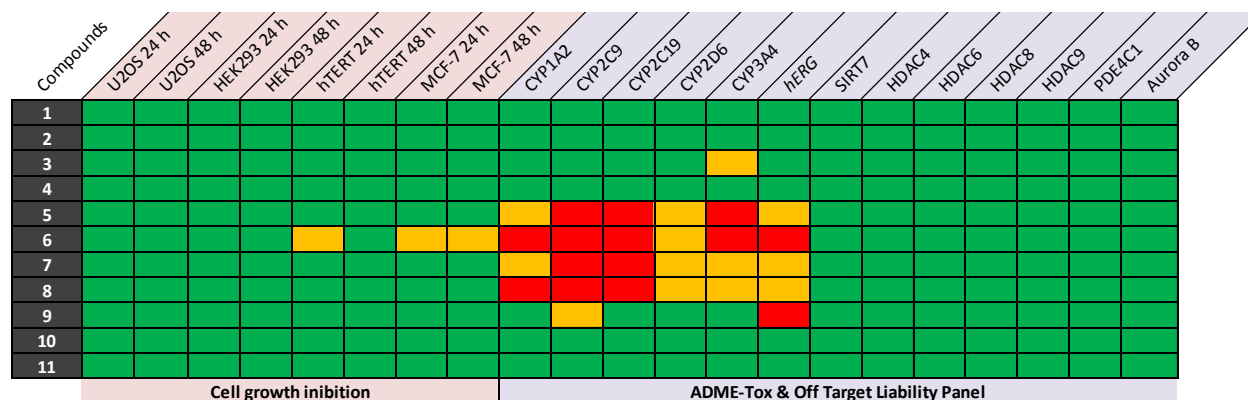
202 H<sub>2</sub>SO<sub>4</sub>, NaNO<sub>2</sub>, H<sub>2</sub>O, 100 °C, 1 h (f) H<sub>2</sub>, Pd/C, MeOH, 12 h; (g) HCl<sub>37%</sub>, H<sub>2</sub>O, 100 °C, 4 h; (h)  
 203 Pd/C, EtOH, 150', rt (i) NaOH<sub>10%</sub>, MeOH, 66 °C, 1 h; (l) H<sub>2</sub>SO<sub>4</sub>, NaNO<sub>2</sub>, H<sub>2</sub>O, 100 °C, 1 h.

204

### 205 Off-target and ADME-Tox profiling

206 In order to identify the most promising compound for progression in the drug discovery process,  
 207 the novel thyromimetics **1-11** were screened *in vitro* at 10 μM against a panel of early ADME-  
 208 Tox assays comprising cytotoxicity (U2OS, HEK, hTERT and MCF-7), cardiotoxicity (*h*ERG),  
 209 cytochrome P450 inhibition (CYP1A2, CYP2C9, CYP2C19, CYP2D6 and CYP3A4), and off-  
 210 targets (Aurora B kinase, phosphodiesterase (PDE4C1) and epigenetic enzymes (SIRT7,  
 211 HDAC4, HDAC6, HDAC8 and HDAC9), see **Figure 3**. At first, the cytotoxicity of **1-11** were  
 212 determined after 24 h or 48 h of treatment in the four cell-lines. Reassuringly, only compound **6**  
 213 was associated with a low degree of cytotoxicity at 10 μM (65 % at 24 h and 53 % at 48 h)  
 214 towards MCF-7 cell-line (see **Supporting Information** for details).

215



216

217

% Inhibition at 10 μM [compound]	Classification
<50	Acceptable profile
51-90	A flag that requires remedial action
>91	Major issue that requires significant attention

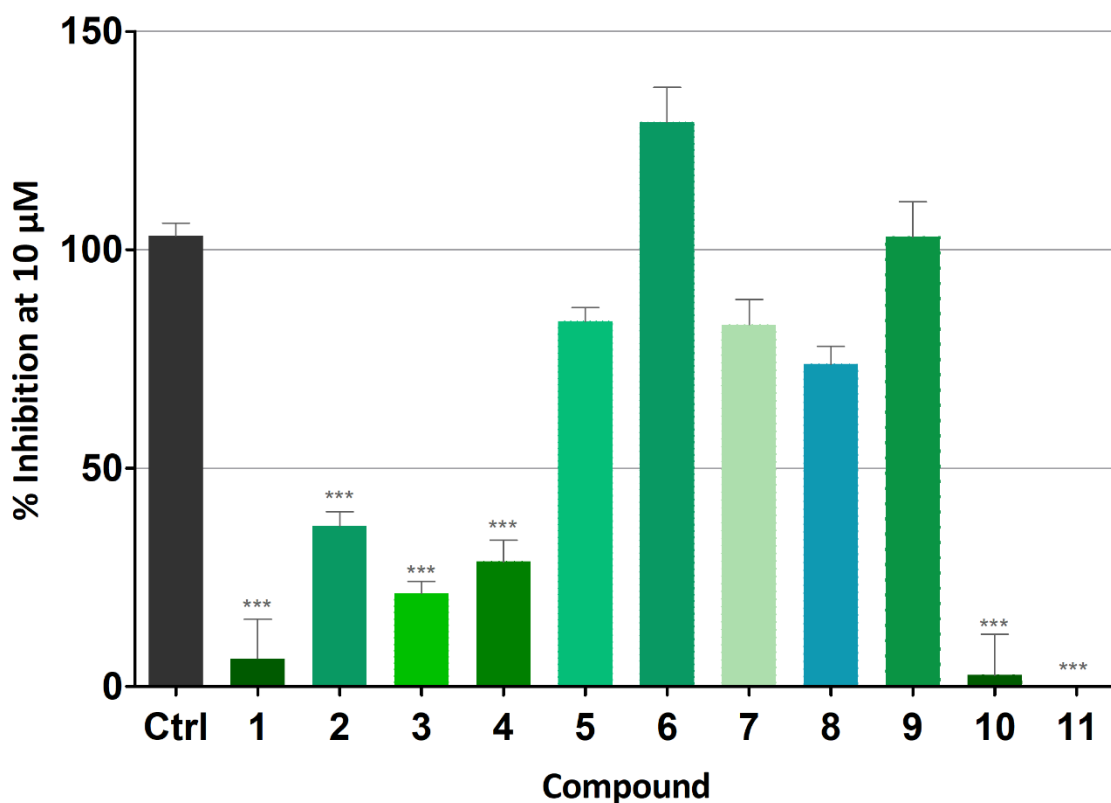
218

219 **Figure 3. Off-target and ADME-Tox profile of compounds 1-11.** All compounds were  
 220 screened at 10 μM in triplicate. A traffic-light system was used to characterize the effect of the  
 221 new thyromimetics in the *in vitro* off-target and ADME-Tox assays.

222

223 The ADME-Tox profile of a compound is a major factor when selecting the best candidate(s) to  
 224 progress in the drug discovery value chain. Among several enzymes responsible for xenobiotic

225 transformation, the cytochrome P450 (CYP450) enzyme plays a key role in phase I oxidative  
226 metabolism and most of drug biotransformation are essentially achieved by five isoforms:  
227 CYP1A2, CYP2C9, CYP2C19, CYP2D6, and CYP3A4<sup>21</sup>. Interestingly, while the carboxylic  
228 compounds were associated with minimal adverse effect on CYP450 enzyme activity,  
229 compounds **5-8** yielded considerably more inhibition against all CYP450 enzymes, probably as a  
230 consequence of the oxyethylamine moiety. In order to assess the off-target liability of newly  
231 synthesized molecules, all compounds were tested against several well-known off-targets. For  
232 this study, enzymes belonging to different classes were selected. SIRT7, HDAC4, HDAC6,  
233 HDAC8 and HDAC9 were chosen as representatives of an undesirable epigenetic  
234 modulation<sup>22,23</sup>. No compounds were associated with adverse inhibition of these targets.  
235 Moreover, the new synthesized molecules were also shown to be inactive against Aurora B  
236 kinase and PDE4C1 enzymes which are known to be essential for cell growth and whose  
237 inhibition has been involved in tumorigenesis. Finally, the ability of the newly synthesized  
238 molecules to modulate *h*ERG ion-channel activity was assessed using the Predictor *h*ERG FP  
239 assay (Thermofisher<sup>®</sup>). The *h*ERG ion-channel plays a key role in cardiac action potential and  
240 represents one of the main reasons for failure of clinical candidates or, even worse, a cause for  
241 withdrawal of drugs from the market. For this reason, it is considered important to assess the  
242 effect of compounds on *h*ERG ion-channel activity at an early stage of drug discovery process.  
243 Compounds **1-4**, **10** and **11** did not significantly alter the *h*ERG ion-channel activity, such that  
244 the percentage of inhibition was <40 % at 10  $\mu$ M. More importantly, compound **1**, **10**, and **11**  
245 were shown to inhibit *h*ERG ion-channel activity <25 % at 10  $\mu$ M (**Figure 4**). Overall, the off-  
246 target and ADME-Tox profiling led to the identification of 6 compounds (**1**, **2**, **3**, **4**, **10**, **11**) with  
247 the most optimal profiles for progression. Next, we proceeded with biological evaluation to  
248 assess their agonist activity against TR $\alpha$  and TR $\beta$ .  
249



250

251 **Figure 4. *h*ERG ion-channel inhibition profile of compounds 1-11.** All compounds were  
 252 tested at 10  $\mu$ M in triplicate, and raw data were normalized to positive control (**Ctrl** =  
 253 Compound E-4051) and negative control (DMSO) and the % Inhibition of the *h*ERG ion-channel  
 254 activity calculated. Results were compared to control using the One-Way ANOVA test. \*\*\*  
 255  $p < 0.005$ .

256

### 257 Nuclear receptor activation

258 The activity of compounds **1-4** and **10-11** on TR $\alpha$  and TR $\beta$  was assessed using the  
 259 LanthaScreen<sup>TM</sup> TR-FRET Nuclear Receptor Coregulator Assay (service provided by Invitrogen  
 260 Corporation, USA) in 10-point dose-response experiments for each compound. Among the tested  
 261 compounds, only **3** and **11** were active against TR $\alpha$  and TR $\beta$ . Interestingly, compound **11**  
 262 activated both TR isoforms with EC<sub>50</sub> towards TR $\alpha$  and TR $\beta$  of respectively 54 and 32 nM.  
 263 Apart from ability to activate the receptors, the selectivity towards the TR $\beta$  isoform is pivotal in  
 264 order to avoid side effects related to TR $\alpha$  activation *in vivo*. Above all, compound **3** was shown

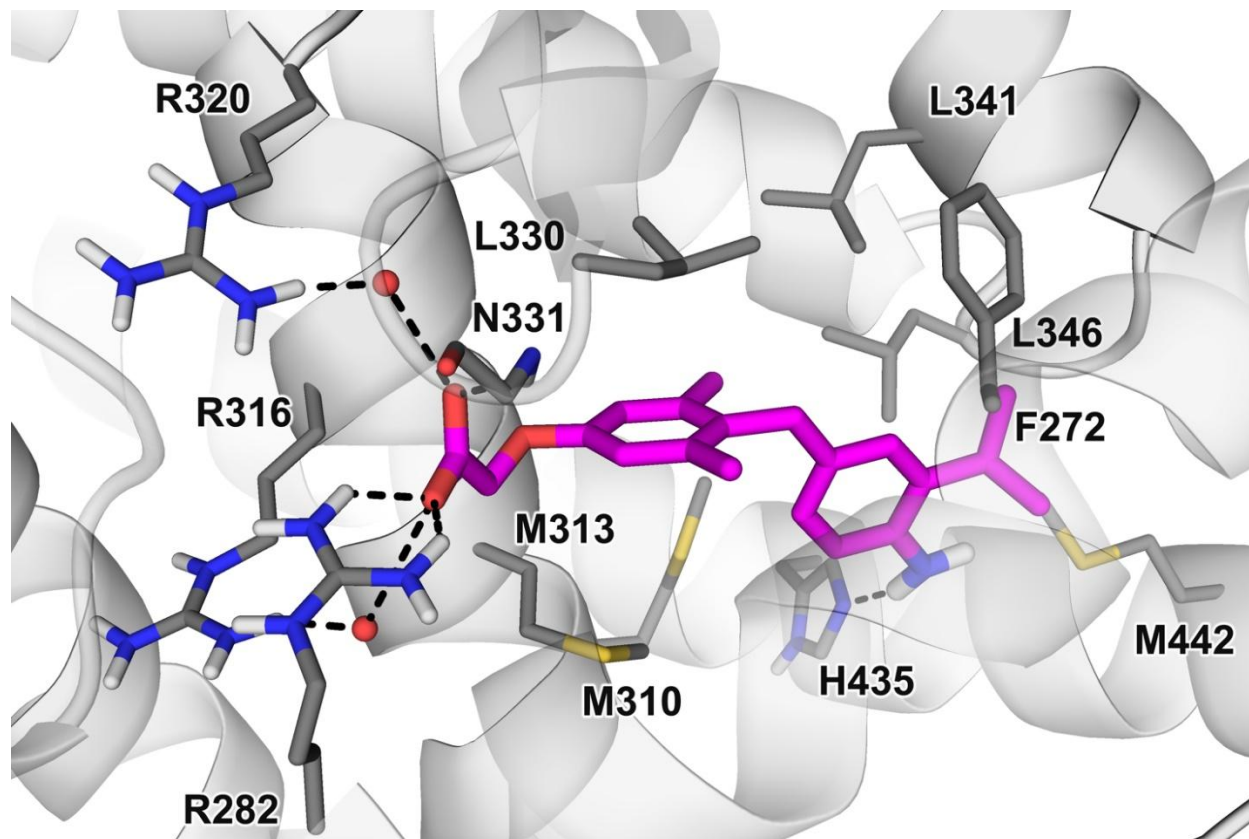
265 to be a TR $\beta$  agonist with EC<sub>50</sub> value 458 nM, whereas it only activated TR $\alpha$  to 30 % (at 1 $\mu$ M)  
266 (see **Supporting Information** for details). Based upon these results, compound **3** was selected  
267 for further biological investigations. In addition, compound **1** was also selected for further study,  
268 as it was originally designed as pro-drug of compound **3**, and more importantly, it was also found  
269 to possess an acceptable off-target and ADME-Tox profile.

270

### 271 **Computational studies**

272 In order to elucidate the activity and the preferential binding of compound **3** for TR $\beta$  with respect  
273 to TR $\alpha$ , docking calculations were carried out with the aid of Glide 6.7 (Maestro packaging) into  
274 the ligand-binding-cavity (LBC) of the two receptors, using the structures co-crystallized with  
275 GC-1, PDB: 3ILZ and 3IMY, respectively (See Experimental Section for X-ray selection).  
276 Bearing in mind the importance of water-mediated interactions for GC-1, which is a potent  
277 thyromimetic as well as a very close analogue of **3**, our calculations were performed retaining  
278 crystal water molecules within 3 Å of the ligand. As for TR $\beta$ , the best ranked docking pose  
279 predicted for **3** (**Figure 5**) is highly superimposable with the crystal structure of GC-1 into the  
280 thyroid receptor. Specifically, the ligand carboxylate forms a H-bond with the backbone NH  
281 group of the N331 and engages two charge-reinforced H-bonds with the guanidinium group of  
282 R282. Moreover, water-mediated contacts are found with the R316 and R320 side chains. As for  
283 the dimethyl phenyl moiety, it establishes many van der Waals interactions with the LBC  
284 lipophilic side chains of L330, I275, I353, M313 and M310 and, thanks to the 3,5 di-methyl  
285 substitutions, it is locked in the active perpendicular conformation with respect to the terminal  
286 phenyl ring<sup>24</sup>. Other profitable lipophilic interactions are detected between the latter and the  
287 L341, F272, I276, L346 side chains and between the iso-propyl substituent with the residues  
288 F269, F272, M442, L346 and F451. Finally, the **3** amino group H-bonds the imidazoline nitrogen  
289 atom of the H435. Of note, when the zwitterionic form of **3** is docked into the receptor,  
290 numerous bad contacts are found between the cationic amino group and the surrounding  
291 lipophilic residues of the LBC, which might be responsible of the lower activity of **3** with respect  
292 to its hydroxyl analogue GC-1 (data from the literature). Moreover, the bulkiness of the residues  
293 F269, F455 and F439 does not allow a proper accommodation of the 4'-NH-acetyl group of  
294 compound **1**, generating intramolecular steric clashes and hampering the formation of an H-bond

295 with H435, justifying the loss of activity of this prodrug (see **Figure SI2** together with comments  
296 on the other derivatives of the series that can be found in **Supporting Information**).  
297



298  
299 **Figure 5. Binding mode of compound 3 in the TRβ LBC.** The receptor is displayed in grey  
300 cartoon, while the ligand and the main protein residues are depicted in magenta and gray sticks  
301 respectively. H3 helix and the N331 loop are in transparency and non-polar hydrogens are  
302 omitted for sake of clarity. H-bonds are shown as black dashed lines.

303  
304 As for the selectivity profile of **3**, in TRα a pose very similar to the co-crystallized structure of  
305 GC-1 with the receptor is found. This outcome is not surprising since it is known that only a  
306 single residue mutation (S277 in TRα versus N331 in TRβ) differentiates within the TRα and  
307 TRβ binding pockets, and this mutation does not alter the overall shape and characteristics of the  
308 two clefts. However, a deeper analysis shows that our ligand is not able to interact with R262  
309 (R316 in TRβ) and just one water-mediated contact is found with the R228 side chain (R282 in  
310 TRβ). In this regards, crystallographic analysis and MD studies<sup>25,26</sup>, have demonstrated that this

311 single mutation is able to affect the orientation of one of the interacting arginines (R228 in TR $\alpha$   
312 and R282 in TR $\beta$ ). Specifically, in TR $\beta$ , the N331 side chain interacts with the R282  
313 guanidinium, which in turn is permanently and optimally oriented toward the ligand carboxylate  
314 allowing GC-1 to stabilize a rich H-bonds network with the three surrounding arginines,  
315 justifying its preferential binding to TR $\beta$ . As described above, analogously to GC-1,  
316 thyromimetic compound **3** is able to establish a broad and stable interaction pattern with TR $\beta$   
317 arginines, including strong and direct contacts with R282, while part of these interactions are lost  
318 in TR $\alpha$ . Reasonably, this might in part justify the preferential binding of **3** to TR $\beta$  with respect to  
319 TR $\alpha$ . Also, it is known that in TR $\beta$  LBC, the residues lining the outer ring of thyromimetics  
320 (especially the M442 residue)<sup>27</sup>, are more flexible with respect to their corresponding TR $\alpha$   
321 residues, so that large 3'-substituents and certain 4'-substituents<sup>28</sup>, increment selectivity toward  
322 this isoform. Thus, it is possible that **3**, possessing the novel combination of 3'-iPr e 4'-NH<sub>2</sub>  
323 substituents on the outer ring, it is better accommodated within the TR $\beta$  pocket.

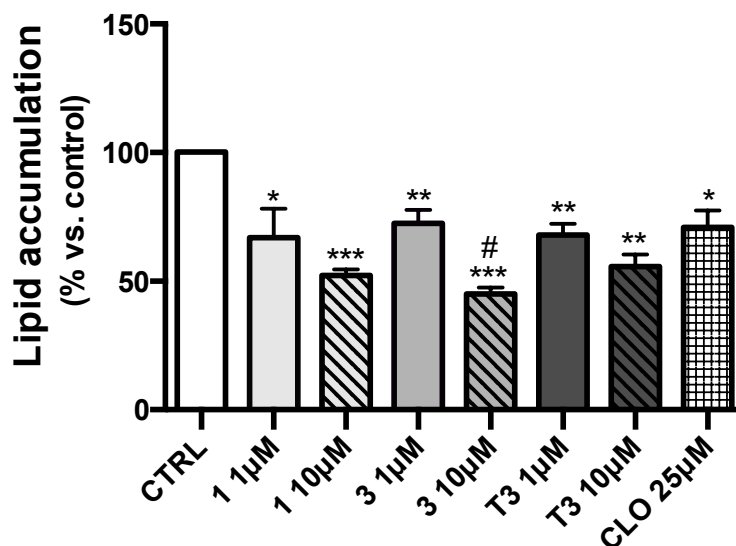
324

### 325 **Effects on lipid metabolism**

326 Abnormal accumulation of lipids in hepatocytes is a prominent aspect in several liver diseases  
327 such as NAFLD (non-alcoholic fatty liver spectrum disease) and alcoholic steato-hepatitis  
328 (ASH)<sup>29</sup>. In order to investigate whether the new thyromimetic molecules **1** and **3** could promote  
329 lipolysis, and whether derivative **1** is capable of efficiently delivering the corresponding parent  
330 compound **3**, we evaluated their effect on lipid metabolism in the human hepatoma cells HepG2.  
331 Initially HepG2 cells were incubated for 24 h with **1** and **3** at 1  $\mu$ M and 10  $\mu$ M, with T3 as  
332 reference drug (**Figure 6**). Oil-red O staining was used to monitor intracellular lipid  
333 accumulation (**Figure 7**). Cloroquine (CLO) 25  $\mu$ M was used as positive controls.

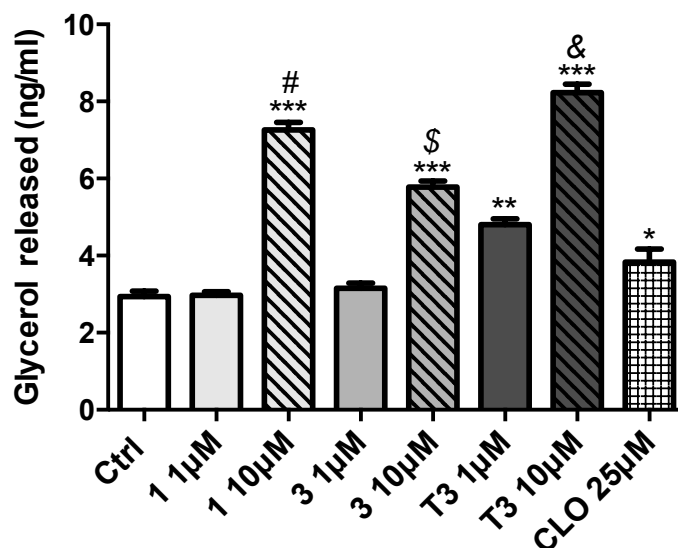
334





335  
 336 **Figure 6. Effects of 1 and 3 on total lipid accumulation in HepG2 cells.** Cells were treated  
 337 for 24 h with **1**, **3** or T3 at 1 and 10 µM). 25 µM Cloroquine (CLO) was used as positive control.  
 338 Oil red O stained intercellular oil droplets were eluted with isopropanol and quantified by  
 339 spectrophotometry analysis at 510 nm. Values represent the mean ± SEM of 4 to 8 experiments.  
 340 The groups were compared using the One-Way ANOVA followed by Tukey's range test.  
 341 \*p<0.05 vs. Ctrl; \*\*p<0.01 vs. Ctrl; \*\*\*p<0.005 vs. Ctrl; #p<0.05 vs. C3 1µM.

342



343  
 344 **Figure 7. Thyromimetic-derivatives 1 and 3 induce lipolysis in HepG2 cells.** Glycerol  
 345 released in the culture medium (0.5 ml) of HepG2 cells after 24 h treatment with **1**, **3** and T3 at 1

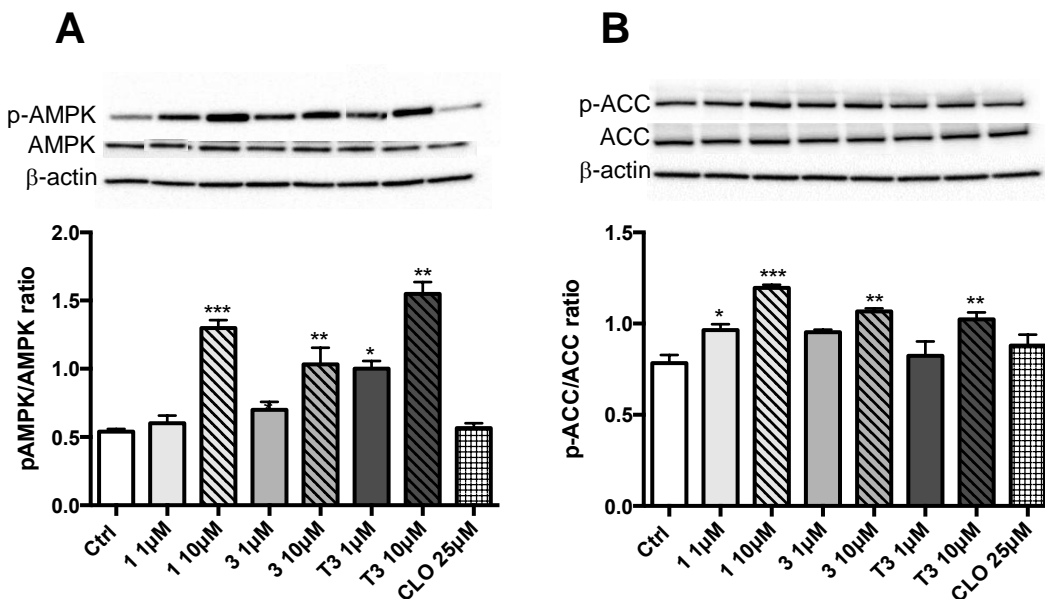
346 and 10  $\mu$ M. 25  $\mu$ M Cloroquine (CLO) was used as positive control. Values represent the mean  $\pm$   
347 SEM of 4 to 8 experiments. The groups were compared using the One-Way ANOVA followed  
348 by Tukey's range test. \* $p < 0.05$  vs. Ctrl; \*\* $p < 0.01$  vs. Ctrl; \*\*\* $p < 0.005$  vs. Ctrl; # $p < 0.005$  vs.  
349 compound **1** 1  $\mu$ M; \$ $p < 0.01$  vs. compound **3** 1  $\mu$ M; & $p < 0.01$  vs. T3 1  $\mu$ M.

350  
351 Oil Red O staining revealed that the newly designed compound **3** reduced total lipid  
352 accumulation into lipid droplets with a potency comparable or even higher than equimolar doses  
353 of T3 (**Figure 6**). This result also shows that compound **1** exerts the same effect of **3** in reducing  
354 lipid accumulation, whereas the increase in glycerol released levels seems to be more efficient  
355 when compared with **3**. This result let us to speculate that thyromimetic derivative **1** is a pro-  
356 drug which possesses improved drug-like properties when compared to **3** (zwitterionic molecule)  
357 and this contributes to increase the bioavailability of the molecule inside the hepatocytes. Further  
358 pharmacokinetic investigations need to be carried out in the near future to confirm our  
359 hypothesis.

360  
361 **Effects on AMPK/ACC pathway**

362 Thyroid hormone mediates lipogenesis, fatty acid  $\beta$ -oxidation, cholesterol synthesis and the  
363 reverse cholesterol transport pathway through different mechanisms such as (a) the induction of  
364 genes transcription involved in metabolism as well as (b) the activation of alternative cellular  
365 pathways implicated in the direct catabolism of fatty acids, such as autophagy<sup>30,31</sup>. Hepatic  
366 autophagy regulates lipid metabolism through elimination of triglyceride accumulation in liver  
367 and prevents the development of steatosis<sup>30,32</sup>. The 5' AMP-activated protein kinase (AMPK) is a  
368 serine/threonine protein kinase which plays a central role in regulating cellular metabolism and  
369 energy balance in mammalian cells<sup>33</sup>. Once activated, AMPK triggers several pathways such as  
370 glycolysis, fatty acid oxidation, and lipolysis. The overall effect on lipid metabolism is  
371 stimulation of fatty acid oxidation (FAO) and inhibition of cholesterol and triglycerides  
372 synthesis<sup>34</sup>. Since AMPK is a regulator of autophagy<sup>35,36</sup>, we investigated AMPK as a possible  
373 target of thyromimetic analogues **1** and **3**. In particular, we examined the protein levels of  
374 phosphorylated AMPK (p-AMPK), and its target phosphorylated acetyl-CoA carboxylase (p-  
375 ACC), a rate-limiting enzyme in cholesterol and fatty acid biosynthesis. As shown in **Figure 8**,  
376 both compounds, when tested at the higher concentration (i.e. 10  $\mu$ M), induced a significant

377 enhancement of pAMPK/AMPK and pACC/ACC ratios. Consistently, the effect induced by  
 378 thyromimetic analogue **1** in the pACC/ACC ratio was more pronounced than that observed with  
 379 the thyroid hormone T3.  
 380

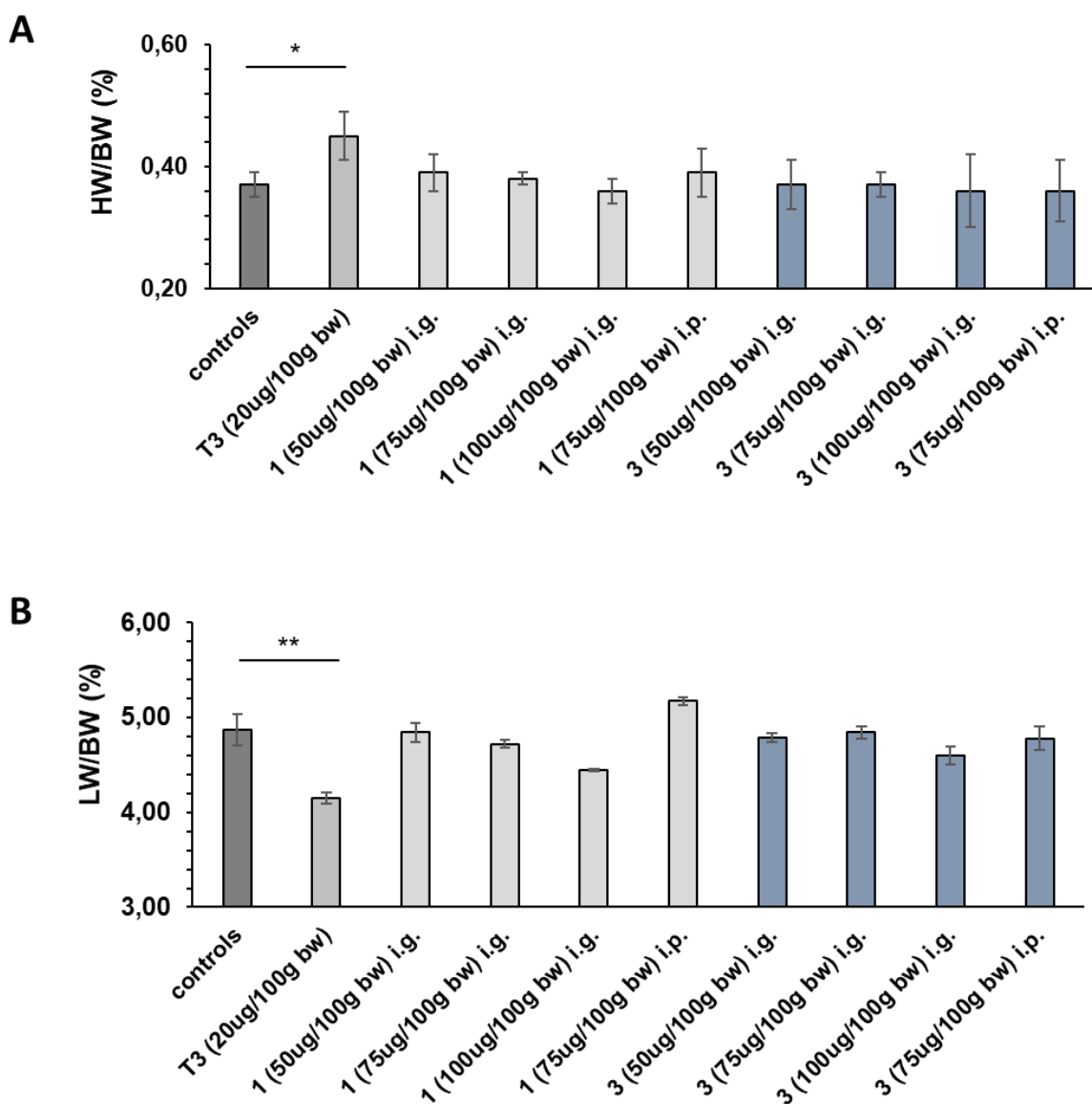


381  
 382  
 383 **Figure 8. Derivatives 1 and 3 regulate metabolism in HepG2 cells via AMPK/ACC pathway.** (A)  
 384 Representative immunoblotting images and quantitative analysis of AMPK phosphorylation. (B)  
 385 Representative immunoblotting images and quantitative analysis of ACC phosphorylation. \*  $p < 0.05$  vs.  
 386 Ctrl; \*\*  $p < 0.01$  vs. Ctrl; \*\*\*  $p < 0.005$  vs. Ctrl.

387  
 388 **Lack of hepatic toxicity and cardiac hypertrophy in thyromimetics-treated rats**

389 Our *in vitro* results showed that compound **3** and its pro-drug **1** efficiently reduced lipid  
 390 accumulation, suggesting their potential therapeutic use in pathological conditions, such as  
 391 NAFLD. To assess their effect *in vivo* we treated F344 male rats for 3 days with daily  
 392 intragastric (IG) administrations of **1** or **3** (50, 75 and 100  $\mu$ g/100g b.w.). Two additional groups  
 393 treated with the vehicle or with T3 (20  $\mu$ g/100g b.w.) were included. As shown in **Figure 9A**,  
 394 despite the brief exposure, T3 caused a significant increase of heart weight, as well as of the  
 395 heart/body weight ratio. No such effect was found in the heart of animals treated with **1** or **3** at  
 396 all doses used (**Figure 9A**), showing that the preferential binding to - and activation of -  
 397 TR $\beta$  does not result in cardiac hypertrophy. As to the liver, while T3 treatment caused a

398 significant reduction of the liver weight/body weight ratio, neither **1** nor **3** caused change in liver  
 399 weight. Similar results were obtained when the two thyromimetics were administered at the dose  
 400 of 75  $\mu\text{g}/100\text{ g}$  b.w. intraperitoneally for 3 days (**Figure 9B**). Notably, no change in the serum  
 401 levels of markers of liver injury, such as transaminases or bilirubin was observed following  
 402 administration of the two thyromimetics. Interestingly, the two novel drugs did not exhibit any  
 403 significant effect on serum levels of cholesterol and glucose, whereas compound **1** induces a  
 404 significant reduction of triglycerides when compared to controls and to T3 (**Table 2**).  
 405



406  
 407

408 **Figure 8: Effect of T3, 1 and 3 on liver/body weight ratio.** F344 male rats were treated for 3  
 409 days with daily intragastric (IG) injections of **1** or **3** (50, 75 and 100 µg/100 g b.w.) or T3 (20  
 410 µg/100 g b.w.). A control group received the vehicle (DMSO 5% in corn oil). Additional two  
 411 groups received daily injections of either **1** or **3** at the dose of 75 ug/100 g b.w. intraperitoneally  
 412 for 3 days. \*\*P<0.01.

413

414

---

Treatment	AST/GOT (U/L)	ALT/GPT (U/L)	Bilirubin (mg/dl)	Glucose (mg/dl)	Cholesterol (mg/dl)	TGs (mg/dl)
Controls	153 ± 11	46 ± 4	1.4 ± 0.2	151 ± 13.5	67.2 ± 2.5	86.8 ± 10.4
T3	159 ± 11	53 ± 4.1	1.4 ± 0.3	139 ± 4.4	65.2 ± 7.1	90.2 ± 9.3
<b>1</b> i.g. (50 ug/100 g)	141 ± 11	46 ± 3.1	1.1 ± 0.3	129 ± 14	68.0 ± 5.2	70.4 ± 7.6
<b>1</b> i.g. (75 ug/100 g)	133 ± 8	46 ± 1.7	0.9 ± 0.1	132 ± 7.6	71.4 ± 6.6	67.0 ± 12.0
<b>1</b> i.g. (100 ug/100 g)	108 ± 7	37 ± 2.5	1.1 ± 0.2	164 ± 12	67.6 ± 8.1	62.8 ± 6.1*
<b>3</b> i.g. (50 ug/100 g)	134 ± 6	41 ± 2.1	1.3 ± 0.3	136 ± 6	69.5 ± 9.4	68.3 ± 9.1
<b>3</b> i.g. (75 ug/100 g)	119 ± 6	43 ± 3.3	1.6 ± 0.2	153 ± 18	68.6 ± 5.6	74.0 ± 12.8
<b>3</b> i.g. (100 ug/100 g)	102 ± 5	42 ± 4.6	1.0 ± 0.2	166 ± 5.1	70.2 ± 7.0	67.8 ± 12.5
<b>1</b> i.p. (75 ug/100 g)	134 ± 10	38 ± 2.9	1.5 ± 0.4	132 ± 14	71.4 ± 3.1	74.2 ± 9.0
<b>3</b> i.p. (75 ug/100 g)	123 ± 10	36 ± 1.7	1.1 ± 0.2	129 ± 9	69.6 ± 1.2	79.6 ± 9.7

---

415 Values are expressed as means ± S.D. of 3 to 4 animals per group. \*Significantly different from Controls for at least; p < 0.05.

416 **Table 2.** Effect of thyromimetics **1** and **3** and T3 on rat Serum Levels of AST/GOT, ALT/GPT,  
 417 Bilirubin, Cholesterol and Triglycerides (TGs) after the treatment with **1** or **3** (i.g., 50, 75 and 100  
 418 µg/100 g b.w; or i.p. 75 µg/100 g b.w.) or T3 (20 µg/100 g b.w.) for 3 days.

419

## 420 CONCLUSION

421 Compound **3** and its pro-drug **1** showed encouraging off-target and ADME-Tox profile that  
 422 prompted us to explore them as TRβ selective thyromimetics. The biochemical-based nuclear  
 423 receptor assay allowed us to consider compound **3** as a potential TRβ selective agonist able to  
 424 influence lipid metabolism and fat oxidation in hepatocytes. Indeed, our *in vitro* assays showed  
 425 that both compound **3** and its pro-drug were able to reduce lipid accumulation in HepG2 and  
 426 promote lipolysis with comparable effects to those elicited by T3, used as reference drug. These

427 results were associated with a safe off-target and ADME-Tox profile. Importantly, *in vivo* studies  
428 confirmed the apparent lack of toxicity of our thyromimetics. Indeed, no liver injury, as assayed  
429 by serum levels of ALT, AST and bilirubin and no cardiac hypertrophy, a critical side effect of  
430 T3, could be observed in thyromimetic-treated rats. Interestingly, we found a significant decrease  
431 in blood triglyceride content following administration of both TR $\beta$  agonists, suggesting their  
432 possible effect on lipid metabolism. Future *in vivo* studies will be needed to investigate the effect  
433 of both compounds in experimental models of NAFLD in order to validate them as new tools to  
434 treat hepatic diseases and to confirm that **1** is an efficient pro-drug of TR $\beta$  selective agonist **3**,  
435 with higher affinity toward the liver.

436

## 437 **EXPERIMENTAL SECTION**

### 438 **Chemistry**

#### 439 *General Material and Methods*

440 Melting points were determined on a Kofler hot-stage apparatus and are uncorrected. Chemical  
441 shifts ( $\delta$ ) are reported in parts per million downfield from tetramethylsilane and referenced from  
442 solvent references; coupling constants *J* are reported in hertz. <sup>1</sup>H-NMR, <sup>13</sup>C-NMR and <sup>19</sup>F-NMR  
443 spectra were obtained with a Bruker TopSpin 3.2 400 MHz spectrometer and were recorded at  
444 400, 101 and 376 MHz, respectively. <sup>19</sup>F and <sup>13</sup>C NMR spectra are <sup>1</sup>H decoupled. <sup>19</sup>F NMR  
445 spectra are unreferenced, corrected from Trifluoroacetic Acid (TFA) as external standard (-76.2  
446 ppm). Signal spectra were fully decoupled. The following abbreviations are used: singlet (s),  
447 doublet (d), triplet (t), double-doublet (dd), and multiplet (m). The elemental compositions of  
448 the compounds agreed to within  $\pm 0.4$  % of the calculated values. Chromatographic separation  
449 was performed on silica gel columns by flash (Kieselgel 40, 0.040–0.063 mm; Merck) or gravity  
450 column (Kieselgel 60, 0.063–0.200 mm; Merck) chromatography. The  $\geq 95$  % purity of the tested  
451 compounds was confirmed by combustion analysis. Reactions were followed by thin-layer  
452 chromatography (TLC) on Merck aluminum silica gel (60 F254) sheets that were visualized  
453 under a UV lamp. The microwave-assisted procedures were carried out with a Biotage Initiator+  
454 microwave. Evaporation was performed *in vacuo* (rotating evaporator). Sodium sulfate was  
455 always used as the drying agent. Commercially available chemicals were purchased from Sigma-  
456 Aldrich or Fluorochem.

457 *Synthesis of 2-(4-(4-acetamido-3-isopropylbenzyl)-3,5-dimethylphenoxy)acetic acid (1)*

458 A solution of phenolic derivative **19** (0.29 mmol) in DMF was treated with Cs<sub>2</sub>CO<sub>3</sub> (473 mg;  
459 1.45 mmol) and BrCH<sub>2</sub>COOH (0.29 mmol). The mixture obtained was stirred for 1 h at rt and  
460 then, quenched with water. After extraction with DCM, aqueous phase was acidified with HCl  
461 10 % and extracted again with DCM. Organic phases were then collected, dried, filtered and  
462 concentrated to obtain a crude which was washed in hexane, providing final compound **1**. Yield:  
463 82 % (white powder). <sup>1</sup>H-NMR (CD<sub>3</sub>OD-d<sub>4</sub>): δ 1.12 (d, 6H, *J* = 6.8 Hz, CH<sub>3</sub>); 2.12 (s, 3H,  
464 CH<sub>3</sub>CO); 2.18 (s, 6H, CH<sub>3</sub>); 3.05–3.08 (m, 1H, CH); 3.98 (s, 2H, CH<sub>2</sub>); 4.35 (s, 2H, CH<sub>2</sub>); 6.67  
465 (s, 2H, Ar); 6.76 (dd, 1H, *J* = 2.0, 8.0 Hz, Ar); 7.00–7.08 (m, 2H, Ar) ppm. <sup>13</sup>C-NMR (CD<sub>3</sub>OD-  
466 d<sub>4</sub>): δ 180.44 (C=O); 172.91 (CH<sub>3</sub>C=O); [158.17, 145.59, 140.71, 139.23, 132.96, 130.42,  
467 128.55, 126.41, 126.32, 115.34] Ar; 68.49 (OCH<sub>2</sub>); 34.84 (CH<sub>2</sub>); 29.06 (CH); 24.18 (CHCH<sub>3</sub>);  
468 23.70 (CH<sub>3</sub>); 22.81 (CH<sub>3</sub>CO); 20.52 (CH<sub>3</sub>) ppm. Anal. Calcd for C<sub>22</sub>H<sub>27</sub>NO<sub>4</sub>: C, 71.52 %; H,  
469 7.37 %; N, 3.79 %. Found: C, 71.41 %; H, 7.42 %; N, 3.59 %.

470

#### 471 *Synthesis of 2-(4-(4-acetamido-3-isopropylbenzyl)phenoxy)acetic acid (2)*

472 The crude product was obtained following the same synthetic procedure reported for compound  
473 **1**. The crude was purified by suspension in hexane. Yield: 64 % (grey powder). <sup>1</sup>H NMR  
474 (CD<sub>3</sub>OD): δ 1.64 (d, 6H, *J* = 6.8 Hz, CH<sub>3</sub>); 2.13 (s, 3H, CH<sub>3</sub>CO); 3.08 (m, 1H, *J* = 6.8 Hz, CH);  
475 3.89 (s, 2H, CH<sub>2</sub>); 4.61 (s, 2H, CH<sub>2</sub>COOH); 6.83 (d, 2H, *J* = 8.4 Hz, Ar); 6.98 (dd, 1H, *J* = 2.0,  
476 8.0 Hz, Ar); 7.08 (d, 1H, *J* = 8 Hz, Ar); 7.12 (d, 2H, *J* = 8.4 Hz, Ar); 7.17 (d, 1H, *J* = 2 Hz, Ar)  
477 ppm. <sup>13</sup>C NMR (CD<sub>3</sub>OD): δ 172.81 (C=O); 172.71 (C=OCH<sub>3</sub>); [157.74, 145.62, 142.06, 135.55,  
478 133.10, 130.74, 128.54, 127.48, 127.16, 115.51] Ar; 65.88 (CH<sub>2</sub>COOH); 41.56 (CH<sub>2</sub>); 29.02  
479 (CH); 23.59 (CH<sub>3</sub>); 22.67 (CH<sub>3</sub>CO) ppm. Anal. Calcd for C<sub>20</sub>H<sub>23</sub>NO<sub>4</sub>: C, 70.36 %; H, 6.79 %; N,  
480 4.10 %. Found: C, 70.43 %; H, 6.69 %; N, 4.21 %.

481

#### 482 *Synthesis of 2-(4-(4-amino-3-isopropylbenzyl)-3,5-dimethylphenoxy)acetic acid (3)*

483 Compound **1** (103 mg, 0.279 mmol) and HCl conc. (8 mL) were mixed with 2 mL of water and  
484 refluxed at 120 °C for 4 h. Upon cooling a solid was formed, mainly constituted by compound **3**.  
485 Crude obtained was washed in HCl 10 % and hexane under vigorous stirring. Yield: 52 % (grey  
486 powder). <sup>1</sup>H-NMR (CD<sub>3</sub>OD-d<sub>4</sub>): δ 1.15 (d, *J* = 6.8 Hz, 6H, CH<sub>3</sub>); 2.19 (s, 6H, CH<sub>3</sub>); 2.92–2.99  
487 (m, 1H, CH); 3.87 (s, 2H, CH<sub>2</sub>); 4.67 (s, 2H, OCH<sub>2</sub>); 6.52 (dd, 1H, *J* = 1.8, 8.0 Hz, Ar); 6.61 (d,  
488 1H, *J* = 8.0 Hz, Ar); 6.62 (s, 2H, Ar); 6.79 (d, 1H, *J* = 1.8 Hz, Ar) ppm. <sup>13</sup>C NMR (CD<sub>3</sub>OD-d<sub>4</sub>):

489  $\delta$ 171.77, 157.28, 142.51, 139.50, 134.79, 132.24, 131.59, 126.44, 125.77, 117.72, 115.03, 66.02,  
490 52.53, 34.52, 28.32, 23.05, 20.52 ppm. Anal. Calcd for  $C_{20}H_{25}NO_3$ : C, 73.37 %; H, 7.70 %; N,  
491 4.28 %. Found: C, 73.52 %; H, 7.68 %; N, 4.19 %.

492

493 *Synthesis of 2-(4-(4-amino-3-isopropylbenzyl)phenoxy)acetic acid (4)*

494 The crude product was obtained following the same synthetic procedure reported for compound  
495 **3** and purified by resuspension in hexane. Yield: 96 % (grey powder).  $^1H$  NMR ( $CD_3OD-d_4$ ):  $\delta$   
496 1.26 (d, 6H,  $J = 6.8$  Hz,  $CH_3$ ); 3.04 (m, 1H,  $J = 6.8$  Hz, CH); 3.94 (s, 2H,  $CH_2$ ); 4.62 (s, 2H,  
497  $CH_2COOH$ ); 6.86 (d, 2H,  $J = 8.4$  Hz, Ar); 7.12 (d, 3H,  $J = 8.8$  Hz, Ar); 7.25 (d, 1H,  $J = 2.0, 8.0$   
498 Hz, Ar); 7.34 (s, 1H, Ar); 7.91 (s, 1H, COOH) ppm.  $^{13}C$  NMR ( $CD_3OD-d_4$ ):  $\delta$  171.44 (COOH);  
499 (157.82, 144.57, 143.37, 135.01, 130.83, 128.63, 128.60, 124.20, 115.67) Ar; 66.03  
500 ( $CH_2COOH$ ); 41.29 ( $CH_2$ ); 28.64 (CH); 23.79 ( $CH_3$ ) ppm. Anal. Calcd for  $C_{18}H_{21}NO_3$ : C, 72.22  
501 %; H, 7.07 %; N, 4.68 %. Found: C, 72.27 %; H, 7.12 %; N, 4.39 %.

502

503 *General procedure for synthesis of compounds 5, 6 and 8*

504 Under nitrogen atmosphere,  $AlCl_3$  (1.35 mmol) was added to a solution of  $LiAlH_4$  (1.35 mmol)  
505 in THF. The mixture was stirred at rt for 5 min; then, a solution of the proper cyanoderivative **22**,  
506 **23** or **31** (0.15 mmol) in THF was added dropwise, and the mixture refluxed for 12 h. After  
507 cooling at 0 °C, the mixture was diluted with water, acidified with HCl 10 % and washed with  
508  $Et_2O$ . Aqueous phase was alkalized with NaOH 1N and extracted with chloroform; then,  
509 organic phase was filtered through celite, washed with brine, dried over  $Na_2SO_4$  and  
510 concentrated.

511

512 *Synthesis of 4-(4-(2-aminoethoxy)-2,6-dimethylbenzyl)-N-ethyl-2-isopropylaniline (5)*

513 The crude product was transformed in the corresponding hydrochloride salt. Yield: 15 % (grey  
514 powder)  $^1H$ -NMR ( $CD_3OD-d_4$ ):  $\delta$  1.23 (d, 6H,  $J = 6.8$  Hz,  $CH_3$ ); 1.36 (t, 3H,  $J = 7.4$  Hz,  $CH_2$ );  
515 2.20 (s, 6H,  $CH_3$ ); 3.02-3.06 (m, 1H, CH); 3.36-3.40 (m, 4H,  $CH_2NH_2$ ,  $CH_2$ ); 4.07 (s, 2H,  $CH_2$ );  
516 4.22 (t,  $J = 4.8$  Hz, 2H,  $OCH_2$ ); 6.77 (s, 2H, Ar); 6.97 (dd, 1H,  $J = 1.4, 8.0$  Hz, Ar); 7.21 (d, 1H,  $J$   
517 = 1.4 Hz, Ar); 7.27 (d, 1H,  $J = 8.0$  Hz, Ar) ppm.  $^{13}C$  NMR ( $CD_3OD-d_4$ ):  $\delta$  157.89, 144.36,  
518 143.49, 139.71, 130.74, 130.50, 128.61, 127.99, 124.54, 115.19, 65.06, 40.42, 34.67, 28.66,  
519 24.46, 20.43, 20.36, 11.36 ppm. Anal. Calcd for  $C_{22}H_{33}ClN_2O$ : C, 70.10 %; H, 8.82 %; N, 7.43



520 %; Found: C, 70.24 %; H, 8.75 %; N, 7.56 %.

521

522 *Synthesis of 4-(4-(2-aminoethoxy)-2-(trifluoromethyl)benzyl)-N-ethyl-2-isopropylaniline (6)*

523 The crude was purified by transformation in hydrochloric salt and subsequent re-crystallization  
524 in isopropanol/diisopropyl ether. Yield: 17 % (yellow oil). <sup>1</sup>H-NMR (CD<sub>3</sub>OD-d<sub>4</sub>): δ 1.27 (d, *J* =  
525 6.4 Hz, 6H, CH<sub>3</sub>); 1.36 (t, *J* = 7.4 Hz, 3H, CH<sub>3</sub>); 3.03–3.04 (m, 1H, CH); 3.38–3.41 (m, 4H,  
526 CH<sub>2</sub>NH<sub>2</sub>, CH<sub>2</sub>); 4.19 (s, 2H, CH<sub>2</sub>); 4.29 (t, 2H, *J* = 8.0 Hz, CH<sub>2</sub>O); 7.11 (dd, *J* = 2.0, 8.4 Hz, 1H,  
527 Ar); 7.23 (dd, 2H, *J* = 2.4, 8.4 Hz, 1H, Ar); 7.28–7.37 (m, 4H, Ar) ppm. <sup>13</sup>C-NMR (CD<sub>3</sub>OD-d<sub>4</sub>):  
528 δ 158.10, 143.52, 135.03, 134.77, 132.28, 131.02, 130.72, 129.55, 128.94, 124.40, 124.19,  
529 119.09, 113.96, 65.76, 40.20, 37.67, 28.74, 24.41, 17.28, 11.42 ppm. Anal. Calcd for  
530 C<sub>21</sub>H<sub>28</sub>ClF<sub>3</sub>N<sub>2</sub>O: C, 60.50 %; H, 6.77 %; N, 6.72 %; Found: C, 60.51 %; H, 6.72 %; N, 6.71 %.

531

532 *Synthesis of 4-(4-(2-aminoethoxy)-2,6-dimethylbenzyl)phenol (7)*

533 Aniline derivative **34** (0.17 mmol, 48 mg) was solubilized in water and treated with H<sub>2</sub>SO<sub>4</sub> (0.05  
534 mL). The mixture obtained was stirred for 20 min at 0 °C. Then, a solution of NaNO<sub>2</sub> (0.17  
535 mmol; 12 mg) in H<sub>2</sub>O was added and the reaction refluxed for 1 h. After this time, reaction  
536 mixture was cooled at RT and diluted with AcOEt. Organic phase was then washed with a  
537 saturated solution of NaCl, dried, filtered and concentrated. The crude obtained was purified by  
538 precipitation in MeOH/Et<sub>2</sub>O. Yield 42% (dark yellow powder). <sup>1</sup>H-NMR (CD<sub>3</sub>OD-d<sub>6</sub>): δ 2.19 (s,  
539 6H, CH<sub>3</sub>); 3.09 (t, *J* = 5.0 Hz; 2H, CH<sub>2</sub>NH<sub>2</sub>); 3.88 (s, 2H, CH<sub>2</sub>); 3.99 (t, *J* = 5.0 Hz; 2H, OCH<sub>2</sub>);  
540 6.61 (s, 2H, Ar); 6.69 (d, *J* = 8.6, 2H, Ar); 6.83 (d, *J* = 8.6, 2H, Ar) ppm. <sup>13</sup>C-NMR (CD<sub>3</sub>OD-d<sub>6</sub>):  
541 δ 158.24, 156.33, 139.34, 132.20, 131.26, 129.62, 116.09, 115.11, 69.76, 41.84, 34.21, 20.54  
542 ppm. Anal. Calcd for C<sub>17</sub>H<sub>21</sub>NO<sub>2</sub>: C, 75.25 %; H, 7.80 %; N, 5.16 %; Found: C, 75.19 %; H,  
543 7.66 %; N, 4.88 %.

544

545 *Synthesis of 4-(4-(2-aminoethoxy)-2-(trifluoromethyl)benzyl)aniline (8)*

546 The crude product was transformed in the corresponding hydrochloride salt. Yield: 10 % (yellow  
547 oil). <sup>1</sup>H-NMR (CD<sub>3</sub>OD-d<sub>4</sub>): δ 3.39(t, *J*=4.8 Hz, 2H, CH<sub>2</sub>NH<sub>2</sub>); 4.19 (s, 2H, CH<sub>2</sub>); 4.29 (t, *J* =  
548 4.8, 2H CH<sub>2</sub>); 7.23 (dd, *J* = 2.4, 8.4 Hz, 1H Ar); 7.27–7.35 (m, 6H Ar) ppm. <sup>13</sup>C-NMR (CD<sub>3</sub>OD-  
549 d<sub>4</sub>): δ 158.09, 143.25, 135.05, 132.29, 131.44, 130.89, 130.10, 126.97, 124.13, 119.10, 113.98,  
550 65.78, 40.21, 37.53 ppm. Anal. Calcd for C<sub>16</sub>H<sub>17</sub>F<sub>3</sub>N<sub>2</sub>O: C, 61.93 %; H, 5.52 %; N, 9.03 %;

551 Found: C, 62.07 %; H, 5.42 %; N, 9.26 %.

552

553 *Synthesis of 2-(4-(4-aminobenzyl)-3-fluorophenoxy)acetic acid (9)*

554 A solution of derivative **35** (28 mg, 0.109 mmol) in H<sub>2</sub>O was acidified with HCl 37 % and  
555 refluxed at 100 °C for 4 h. Then the mixture was concentrated affording the crude **9**, which was  
556 purified by formation of the corresponding hydrochloride salt. Yield: 77 % (grey powder). <sup>1</sup>H  
557 NMR (CD<sub>3</sub>OD-d<sub>4</sub>): δ 3.98 (s, 2H, CH<sub>2</sub>); 4.66 (s, 2H, CH<sub>2</sub>COOH); 6.69-6.74 (m, 2H, Ar); 7.15  
558 (d, 1H, J=8.4 Hz, Ar); 7.31-7.37 (m, 4H, Ar) ppm. <sup>13</sup>C NMR (CD<sub>3</sub>OD-d<sub>4</sub>): δ 172.21(COOH);  
559 [161.28, 159.50, 143.21, 132.57, 131.21, 129.81, 124.10, 121.30, 111.53, 103.49] Ar; 66.03  
560 (CH<sub>2</sub>COOH); 34.51 (CH<sub>2</sub>) ppm. Anal. Calcd for C<sub>15</sub>H<sub>14</sub>FNO<sub>3</sub>: C, 65.45 %; H, 5.13 %; N, 5.09  
561 %; Found: C, 65.27 %; H, 5.18 %; N, 5.21 %.

562

563 *Synthesis of 2-(4-(4-aminobenzyl)-3,5-dimethylphenoxy)acetic acid (10)*

564 Ester **36** (0.12 mmol; 39 mg) solubilized in MeOH was treated with an aqueous solution of  
565 NaOH 10% (0.02 mL). Mixture was then refluxed for 1h and then, concentrated *in vacuo*. The  
566 crude obtained was purified by precipitation in MeOH/Et<sub>2</sub>O providing compound **10**. Yield: 42  
567 % (pale yellow). <sup>1</sup>H-NMR (CD<sub>3</sub>OD-d<sub>4</sub>): δ 2.17 (s, 6H, CH<sub>3</sub>); 3.85 (s, 2H, CH<sub>2</sub>); 4.34 (s, 2H,  
568 CH<sub>2</sub>COOH); 6.61 (d, 2H, J = 8.4 Hz, Ar); 6.65 (s, 2H, Ar); 6.72 (d, 2H, J = 8.4 Hz, Ar) ppm.  
569 <sup>13</sup>C-NMR (CD<sub>3</sub>OD-d<sub>4</sub>): δ 177.01, 157.94, 146.00, 139.15, 131.39, 131.25, 129.36, 117.00,  
570 115.25, 68.47, 34.27, 20.54 ppm. Anal. Calcd for C<sub>17</sub>H<sub>19</sub>NO<sub>3</sub>: C, 71.56 %; H, 6.71 %; N, 4.91 %;  
571 Found: C, 71.38 %; H, 6.92 %; N, 5.07 %.

572

573 *Synthesis of 2-(4-(4-hydroxybenzyl)-3,5-dimethylphenoxy)acetic acid (11)*

574 Aniline **10** (0.20 mmol; 64 mg) was dissolved in H<sub>2</sub>O, added to a solution of H<sub>2</sub>SO<sub>4</sub> at  
575 concentrated grade (0.05 mL), and left under stirring at 0 °C for 20 min. Then, a solution of  
576 NaNO<sub>2</sub> (0.20 mmol; 14 mg) in H<sub>2</sub>O was added, and the mixture was refluxed for 1 h. After this  
577 time, the reaction was allowed to cold down to rt and then diluted with AcOEt. Organic phase  
578 was washed with a saturated solution of NaCl, then dried, filtered and evaporated. The crude  
579 product was purified by precipitation in AcOEt/Hexane. Yield: 35 % (brown powder). <sup>1</sup>H-NMR  
580 (CD<sub>3</sub>OD-d<sub>4</sub>): δ 2.17 (s, 6H, CH<sub>3</sub>); 3.87 (s, 2H, CH<sub>2</sub>); 4.59 (s, 2H, CH<sub>2</sub>COOH); 6.60–6.67 (m,  
581 4H, Ar); 6.77 (d, 2H, J = 8.4 Hz, Ar) ppm. <sup>13</sup>C-NMR (CD<sub>3</sub>OD-d<sub>4</sub>): δ 173.18, 157.42, 156.32,

582 139.45, 132.10, 131.86, 129.64, 116.09, 115.12, 65.94, 34.21, 20.53 ppm. Anal. Calcd for  
583 C<sub>17</sub>H<sub>18</sub>O<sub>4</sub>: C, 71.31 %; H, 6.34 %. Found: C, 71.46 %; H, 6.47 %.

584

### 585 **X-ray selection**

586 To date, many X-ray structures of TR $\alpha$  and TR $\beta$  in complex with T3, GC-1, KB131084 and  
587 other thyromimetics, are available in the Protein Data Bank (PDB). A superposition on the  $\alpha$ -  
588 carbon atoms of all these structures, showed that the general protein folding is highly preserved,  
589 with a good conservation of both the secondary structure and the side chain orientation,  
590 especially within the LBC. Thus, among the crystals with highest resolution, those co-  
591 crystallized with our ligands progenitor GC-1 were chosen for our docking calculations: PDB  
592 codes 3ILZ and 3IMY, for TR $\alpha$  and TR $\beta$ , respectively.

593

### 594 **Docking calculations**

595 The ligands tridimensional structure were generated with the Maestro Build Panel and prepared  
596 using Ligprep predicting all tautomeric and protonation states at physiological pH (7.4  $\pm$  1.5).  
597 The receptor structures were prepared using the Protein Preparation Wizard implemented in  
598 Maestro Suite (Schrödinger Release 2019-2: Schrödinger Suite 2019-1), deleting all water  
599 molecules with the exception of those within 3 Å from the ligand, adding missing hydrogen  
600 atoms and minimizing the complexes. The docking grid was calculated through the grid  
601 generation tool in Glide 6.7<sup>37,38, 39</sup> and centered around the crystallized ligand using default  
602 settings. The OPLS3E force field was employed for docking. The results of calculations were  
603 evaluated and ranked based on the Glide SP scoring function.

604

### 605 ***In vitro* studies**

#### 606 *Activity against thyroid hormone receptors*

607 Assays on selected compounds were performed by SelectScreen™ Biochemical Nuclear  
608 Receptor Profiling Service (Thermofisher Scientific, US) using the LanthaScreen™ TR-FRET  
609 Nuclear Receptor Coregulator Assay (service provided by Invitrogen Corporation, USA), as  
610 reported on the company's website. ([https://www.thermofisher.com/it/en/home/products-and-  
611 services/services/custom-services/screening-and-profiling-services/selectscreen-profiling-  
612 service/selectscreen-cell-based-nuclear-receptor-profiling-services.html](https://www.thermofisher.com/it/en/home/products-and-services/services/custom-services/screening-and-profiling-services/selectscreen-profiling-service/selectscreen-cell-based-nuclear-receptor-profiling-services.html)).

613

614 *Human hepatocellular carcinoma (HepG2) cell culture and treatment with compounds 1 and 3*

615 The human hepatocellular carcinoma HepG2 cells line was purchased from the American Type  
616 Culture Collection (ATCC HB-8065, Rockville, MD, USA) and cultured in low glucose (LG)  
617 DMEM supplemented with 10 % FBS, 100 IU/mL penicillin G sodium and 100 µg/mL  
618 streptomycin sulfate (Invitrogen, Paisley, UK) incubating in a humidified atmosphere with 5 %  
619 CO<sub>2</sub> at 37 °C. These cells were then treated with 1 and 10 µM concentrations of test compounds  
620 for 24 h. After treatments, cells were lysed in a buffer containing 20 mM Tris-HCl (pH 7.5), 0.9  
621 % NaCl, 0.2 % Triton X-100, and 1 % of the protease inhibitor cocktail (Sigma-Aldrich, Milan,  
622 Italy) and then stored at -80 °C for further western blot analysis. All the analyses were  
623 conducted on cells between the third and the sixth passage.

624

625 *Oil red O (ORO) staining of lipid accumulation in HepG2 cells*

626 Total lipid accumulation was evaluated according to the method previously described by Liu et  
627 al.<sup>40</sup> Cells were seeded at a density of  $3.5 \times 10^4$  cells/well in 1 mL of lipogenic growth medium  
628 (HG-DMEM) and treated for 24 h with compound **1** or **3**, at 1 and 10 µM. Cloroquine (25 µM)  
629 was used as positive control. Subsequently, after collecting the growth media to be used to  
630 perform glycerol level measurements (as detailed below), cells were rinsed twice with PBS and  
631 fixed in 4 % paraformaldehyde in PBS at 4 °C for 30 min. After 3 washes with cold PBS, cells  
632 were stained with ORO working solution, prepared as described above, for 30 min at room  
633 temperature and subsequently rinsed again with PBS.

634

635 *Determination of glycerol release from HepG2 cells*

636 After treatment with test compounds, cell culture supernatants were collected from each well and  
637 placed in glycerol-free containers. A 125µg/mL Glycerol Standard Solution (Abcam, Milan,  
638 Italy) was used to make a #1 through #8 standard curve. 25 µL of each supernatant and standard  
639 were then transferred into a 96-well plate and 100µL of either Free Glycerol Assay Reagent  
640 (Abcam, Milan, Italy) or MilliQ water added to each well. After incubation at rt for 15 min,  
641 glycerol levels were measured by reading absorbance at 540 nm (Bio-Rad 680, Milan, Italy).

642

643 *Western Blotting Analysis*

644 Proteins (20–30 µg) were separated on CriterionTGX™ gel (4-20 %) and transferred on  
645 Immuno-PVDF membrane (Biorad, Milan, Italy) for 30 min. The membranes were then  
646 incubated overnight at 4 °C with one of the following the specific primary antibodies: anti-p-  
647 AMPK $\alpha$ 1-thr172, anti-AMPK, anti-p-ACC-ser79, anti-ACC (Cell Signaling Technology,  
648 Danvers, MA, USA). Then, blots were washed 3 times for 10 min with 1X TBS, 0.1 %  
649 Tween<sup>®</sup>20 and incubated for 2 h with secondary antibody (peroxidase-coupled anti rabbit in 1X  
650 TBS, 0.1 % Tween<sup>®</sup>20). After washing 3 times for 10 min, the reactive signals were revealed by  
651 an enhanced ECL Western Blotting analysis system (Amersham, Milan, Italy). Band  
652 densitometric analysis was performed using Image Lab Software (Biorad, Milan, Italy).

653

#### 654 *In vivo Studies*

655 Five-week-old male F-344 rats purchased from Charles River (Milano, Italy) were maintained on  
656 a standard laboratory diet (Ditta Mucedola, Milano, Italy). The animals were given food and  
657 water ad libitum with a 12 h light/dark daily cycle and were acclimated for 1 week before the  
658 start of the experiment. All procedures were performed in accordance with the Guidelines for the  
659 Care and Use of Laboratory Animals and were approved by the Italian Ministry of Health.  
660 Animals were treated with daily intragastric (IG) injections for 3 days of **1** or **3** (50, 75 and 100  
661 µg/100 g b.w) or T3 (20 µg/100 g b. wt). A control group received the vehicle (DMSO 5 % in  
662 corn oil). Additional two groups received daily injections of either **1** or **3** at the dose of 75  
663 µg/100 g b. wt. intraperitoneally for 3 days

664

665 *Analysis of Serum Aspartate aminotransferase (AST), Alanine aminotransferase (ALT),*  
666 *Triglycerides (TGs) and Cholesterol (CH).*

667 Immediately after sacrifice, blood samples were collected from the abdominal aorta, serum was  
668 separated by centrifugation (2000 g for 20 minutes) and tested for triglycerides, cholesterol,  
669 aspartate aminotransferase and alanine aminotransferase using a commercially available kit from  
670 Boehringer (Mannheim, Germany).

671

#### 672 *Statistical Analysis*

673 Statistical analyses were performed using GraphPad Prism version 6.0 for Windows (GraphPad  
674 Software, San Diego, CA, USA). Data were subjected to One-Way analysis of variance for mean

675 comparison, and significant differences among different treatments were calculated according to  
676 Tukey's HSD (honest significant difference) multiple range test. Data are reported as mean  $\pm$   
677 SEM. Differences at  $p < 0.05$  were considered statistically significant.

678

## 679 **ASSOCIATED CONTENT**

680 The Supporting Information is available free of charge on the Elsevier website at DOI:

681

## 682 **AUTHOR INFORMATION**

683 Corresponding Author:

684 For S.R.: phone, +39 050 2219582; fax, +39 050 2219577; Email, [simona.rapposelli@unipi.it](mailto:simona.rapposelli@unipi.it).

685 \*For G.C.: phone, +39 050 2218677; E-mail, [grazia.chiellini@unipi.it](mailto:grazia.chiellini@unipi.it).

686

687 Author Contributions:

688 MR and SS carried out the synthesis. LB and GC carried out the experiments in HepG2 and  
689 adipocytes and analyzed the data. VLP, VMD and LM carried out the computational studies. AP,  
690 MAK and AC carried out the in vivo experiments and the data analysis. MR and SG carried out  
691 the off-target and ADME-Tox profiling assays and analyzed the data. SR and GC design and  
692 coordinate the project. All authors discussed the results and contributed to the final manuscript.  
693 MR, SR, AC and GC wrote the manuscript.

694

695 Funding Sources: This work was supported by grants from International Society of Drug  
696 Discovery (ISDD) (Milan), from the University of Pisa [Progetti di Ricerca di Ateneo  
697 PRA\_2017\_55 (to GC) and PRA\_2018\_20 (to SR)], from Associazione Italiana Ricerca sul  
698 Cancro (AIRC, IG-20176 to AC) and from Regione Autonoma Sardegna (RAS to AC).

699

700 Notes: The authors declare no conflict of interest

701

## 702 **ACKNOWLEDGMENT**

703 We thank the COST action CA15135 (Multitarget Paradigm for Innovative Ligand Identification  
704 in the Drug Discovery Process MuTaLig) for support the working experience of MR at the  
705 Fraunhofer-IME SP (Hamburg, Germany). We also thank POR FSE 2014-2020 – Regione

706 Toscana and the University of Pisa for financing the fellowship to SS and Fondazione Umberto  
707 Veronesi for financing to MAK the fellowship.

708

## 709 ABBREVIATIONS

710 THs, thyroid hormones; TR $\alpha$ , thyroid hormone receptor  $\alpha$ ; TR $\beta$ , thyroid hormone receptor  $\beta$ ;  
711 NAFLD, non-alcoholic fatty-liver disease.

712

## 713 REFERENCES

- 714 1. Yen, P. M. Physiological and molecular basis of thyroid hormone action. *Physiological*  
715 *reviews* **2001**, 81, 1097-1142.
- 716 2. Brent, G. A. Mechanisms of thyroid hormone action. *The Journal of clinical investigation*  
717 **2012**, 122, 3035-3043.
- 718 3. Kapoor, R.; Fanibunda, S. E.; Desouza, L. A.; Guha, S. K.; Vaidya, V. A. Perspectives on  
719 thyroid hormone action in adult neurogenesis. *Journal of neurochemistry* **2015**, 133, 599-  
720 616.
- 721 4. Baxi, E. G.; Schott, J. T.; Fairchild, A. N.; Kirby, L. A.; Karani, R.; Uapinyoying, P.;  
722 Pardo- Villamizar, C.; Rothstein, J. R.; Bergles, D. E.; Calabresi, P. A. A selective thyroid  
723 hormone  $\beta$  receptor agonist enhances human and rodent oligodendrocyte differentiation.  
724 *Glia* **2014**, 62, 1513-1529.
- 725 5. Vaitkus, J.; Farrar, J.; Celi, F. Thyroid hormone mediated modulation of energy expenditure.  
726 *Int J Mol Sci* **2015**, 16, 16158-16175.
- 727 6. Tancevski, I.; Eller, P.; Patsch, J. R.; Ritsch, A. The resurgence of thyromimetics as lipid-  
728 modifying agents. *Current opinion in investigational drugs (London, England: 2000)* **2009**,  
729 10, 912.
- 730 7. Gullberg, H.; Rudling, M.; Saltó, C.; Forrest, D.; Angelin, B.; Vennström, B. r. Requirement  
731 for thyroid hormone receptor  $\beta$  in T3 regulation of cholesterol metabolism in mice.  
732 *Molecular Endocrinology* **2002**, 16, 1767-1777.
- 733 8. Kowalik, M. A.; Columbano, A.; Perra, A. Thyroid hormones, thyromimetics and their  
734 metabolites in the treatment of liver disease. *Frontiers in endocrinology* **2018**, 9.
- 735 9. Chiellini, G.; Apriletti, J. W.; Al Yoshihara, H.; Baxter, J. D.; Ribeiro, R. C.; Scanlan, T. S.  
736 A high-affinity subtype-selective agonist ligand for the thyroid hormone receptor. *Chemistry*  
737 *& biology* **1998**, 5, 299-306.
- 738 10. Erion, M. D.; Cable, E. E.; Ito, B. R.; Jiang, H.; Fujitaki, J. M.; Finn, P. D.; Zhang, B. H.;  
739 Hou, J.; Boyer, S. H.; van Poelje, P. D.; Linemeyer, D. L. Targeting thyroid hormone  
740 receptor-beta agonists to the liver reduces cholesterol and triglycerides and improves the  
741 therapeutic index. *Proceedings of the National Academy of Sciences of the United States of*  
742 *America* **2007**, 104, 15490-5.
- 743 11. Berkenstam, A.; Kristensen, J.; Mellstrom, K.; Carlsson, B.; Malm, J.; Rehnmark, S.; Garg,  
744 N.; Andersson, C. M.; Rudling, M.; Sjoberg, F.; Angelin, B.; Baxter, J. D. The thyroid  
745 hormone mimetic compound KB2115 lowers plasma LDL cholesterol and stimulates bile  
746 acid synthesis without cardiac effects in humans. *Proceedings of the National Academy of*  
747 *Sciences of the United States of America* **2008**, 105, 663-7.

- 748 12. Johansson, L.; Rudling, M.; Scanlan, T. S.; Lundasen, T.; Webb, P.; Baxter, J.; Angelin, B.;  
749 Parini, P. Selective thyroid receptor modulation by GC-1 reduces serum lipids and  
750 stimulates steps of reverse cholesterol transport in euthyroid mice. *Proceedings of the*  
751 *National Academy of Sciences of the United States of America* **2005**, 102, 10297-302.
- 752 13. Tancevski, I.; Rudling, M.; Eller, P. Thyromimetics: a journey from bench to bed-side.  
753 *Pharmacology & therapeutics* **2011**, 131, 33-9.
- 754 14. Meruvu, S.; Ayers, S. D.; Winnier, G.; Webb, P. Thyroid hormone analogues: where do we  
755 stand in 2013? *Thyroid : official journal of the American Thyroid Association* **2013**, 23,  
756 1333-44.
- 757 15. Elbers, L. P.; Kastelein, J. J.; Sjouke, B. Thyroid hormone mimetics: the past, current status  
758 and future challenges. *Current atherosclerosis reports* **2016**, 18, 14.
- 759 16. Zhou, J.; Waskowicz, L. R.; Lim, A.; Liao, X.-H.; Lian, B.; Masamune, H.; Refetoff, S.;  
760 Tran, B.; Koeberl, D. D.; Yen, P. M. A liver-specific thyromimetic, VK2809, decreases  
761 hepatosteatosis in glycogen storage disease type Ia (GSD Ia). *Thyroid : official journal of*  
762 *the American Thyroid Association* **2019**.
- 763 17. Chiellini, G.; Nesi, G.; Sestito, S.; Chiarugi, S.; Runfola, M.; Espinoza, S.; Sabatini, M.;  
764 Bellusci, L.; Laurino, A.; Cichero, E.; Gainetdinov, R. R.; Fossa, P.; Raimondi, L.; Zucchi,  
765 R.; Rapposelli, S. Hit-to-Lead Optimization of Mouse Trace Amine Associated Receptor 1  
766 (mTAAR1) Agonists with a Diphenylmethane-Scaffold: Design, Synthesis, and Biological  
767 Study. *J Med Chem* **2016**, 59, 9825-9836.
- 768 18. Bellusci, L.; Laurino, A.; Sabatini, M.; Sestito, S.; Lenzi, P.; Raimondi, L.; Rapposelli, S.;  
769 Biagioni, F.; Fornai, F.; Salvetti, A.; Rossi, L.; Zucchi, R.; Chiellini, G. New Insights into  
770 the Potential Roles of 3-Iodothyronamine (TIAM) and Newly Developed Thyronamine-  
771 Like TAAR1 Agonists in Neuroprotection. *Frontiers in pharmacology* **2017**, 8, 905.
- 772 19. Yoshihara, H. A.; Apreletti, J. W.; Baxter, J. D.; Scanlan, T. S. Structural determinants of  
773 selective thyromimetics. *Journal of medicinal chemistry* **2003**, 46, 3152-3161.
- 774 20. Chiellini, G.; Nesi, G.; Digiacomio, M.; Malvasi, R.; Espinoza, S.; Sabatini, M.; Frascarelli,  
775 S.; Laurino, A.; Cichero, E.; Macchia, M.; Gainetdinov, R. R.; Fossa, P.; Raimondi, L.;  
776 Zucchi, R.; Rapposelli, S. Design, Synthesis, and Evaluation of Thyronamine Analogues as  
777 Novel Potent Mouse Trace Amine Associated Receptor 1 (mTAAR1) Agonists. *J Med*  
778 *Chem* **2015**, 58, 5096-107.
- 779 21. Evans, W. E.; Relling, M. V. Pharmacogenomics: translating functional genomics into  
780 rational therapeutics. *science* **1999**, 286, 487-491.
- 781 22. Cote, I. L.; McCullough, S. D.; Hines, R. N.; Vandenberg, J. J. Application of epigenetic  
782 data in human health risk assessment. *Current opinion in toxicology* **2017**, 6, 71-78.
- 783 23. Gul, S. Epigenetic assays for chemical biology and drug discovery. *Clinical epigenetics*  
784 **2017**, 9, 41.
- 785 24. Dietrich, S. W.; Bolger, M. B.; Kollman, P. A.; Jorgensen, E. C. Thyroxine analogues. 23.  
786 Quantitative structure-activity correlation studies of in vivo and in vitro thyromimetic  
787 activities. *J Med Chem* **1977**, 20, 863-80.
- 788 25. Bleicher, L.; Aparicio, R.; Nunes, F. M.; Martinez, L.; Gomes Dias, S. M.; Figueira, A. C.;  
789 Santos, M. A.; Venturelli, W. H.; da Silva, R.; Donate, P. M.; Neves, F. A.; Simeoni, L. A.;  
790 Baxter, J. D.; Webb, P.; Skaf, M. S.; Polikarpov, I. Structural basis of GC-1 selectivity for  
791 thyroid hormone receptor isoforms. *BMC structural biology* **2008**, 8, 8.
- 792 26. Martinez, L.; Nascimento, A. S.; Nunes, F. M.; Phillips, K.; Aparicio, R.; Dias, S. M.;  
793 Figueira, A. C.; Lin, J. H.; Nguyen, P.; Apreletti, J. W.; Neves, F. A.; Baxter, J. D.; Webb,



- 794 P.; Skaf, M. S.; Polikarpov, I. Gaining ligand selectivity in thyroid hormone receptors via  
795 entropy. *Proceedings of the National Academy of Sciences of the United States of America*  
796 **2009**, 106, 20717-22.
- 797 27. Hangeland, J. J.; Doweiko, A. M.; Dejneka, T.; Friends, T. J.; Devasthale, P.; Mellstrom,  
798 K.; Sandberg, J.; Grynfarb, M.; Sack, J. S.; Einspahr, H.; Farnegardh, M.; Husman, B.;  
799 Ljunggren, J.; Koehler, K.; Sheppard, C.; Malm, J.; Ryono, D. E. Thyroid receptor ligands.  
800 Part 2: Thyromimetics with improved selectivity for the thyroid hormone receptor beta.  
801 *Bioorganic & medicinal chemistry letters* **2004**, 14, 3549-53.
- 802 28. Li, Y. L.; Litten, C.; Koehler, K. F.; Mellstrom, K.; Garg, N.; Garcia Collazo, A. M.;  
803 Farnegard, M.; Grynfarb, M.; Husman, B.; Sandberg, J.; Malm, J. Thyroid receptor ligands.  
804 Part 4: 4'-amido bioisosteric ligands selective for the thyroid hormone receptor beta.  
805 *Bioorganic & medicinal chemistry letters* **2006**, 16, 884-6.
- 806 29. Ipsen, D. H.; Lykkesfeldt, J.; Tveden-Nyborg, P. Molecular mechanisms of hepatic lipid  
807 accumulation in non-alcoholic fatty liver disease. *Cell Mol Life Sci* **2018**, 75, 3313-3327.
- 808 30. Singh, R.; Kaushik, S.; Wang, Y.; Xiang, Y.; Novak, I.; Komatsu, M.; Tanaka, K.; Cuervo,  
809 A. M.; Czaja, M. J. Autophagy regulates lipid metabolism. *Nature* **2009**, 458, 1131-5.
- 810 31. Sinha, R. A.; Singh, B. K.; Yen, P. M. Direct effects of thyroid hormones on hepatic lipid  
811 metabolism. *Nat Rev Endocrinol* **2018**, 14, 259-269.
- 812 32. Chi, H.-C.; Tsai, C.-Y.; Tsai, M.-M.; Yeh, C.-T.; Lin, K.-H. Molecular functions and clinical  
813 impact of thyroid hormone-triggered autophagy in liver-related diseases. *J Biomed Sci* **2019**,  
814 26, 24-24.
- 815 33. Gasparrini, M.; Giampieri, F.; Alvarez Suarez, J. M.; Mazzoni, L.; T, Y. F. H.; Quiles, J. L.;  
816 Bullon, P.; Battino, M. AMPK as a New Attractive Therapeutic Target for Disease  
817 Prevention: The Role of Dietary Compounds AMPK and Disease Prevention. *Current drug*  
818 *targets* **2016**, 17, 865-89.
- 819 34. Wakil, S. J.; Abu-Elheiga, L. A. Fatty acid metabolism: target for metabolic syndrome.  
820 *Journal of lipid research* **2009**, 50 Suppl, S138-43.
- 821 35. Zhang, D.; Wang, W.; Sun, X.; Xu, D.; Wang, C.; Zhang, Q.; Wang, H.; Luo, W.; Chen, Y.;  
822 Chen, H.; Liu, Z. AMPK regulates autophagy by phosphorylating BECN1 at threonine 388.  
823 *Autophagy* **2016**, 12, 1447-1459.
- 824 36. Tamargo-Gómez, I.; Mariño, G. AMPK: Regulation of Metabolic Dynamics in the Context  
825 of Autophagy. *Int J Mol Sci* **2018**, 19, 3812.
- 826 37. Friesner, R. A.; Murphy, R. B.; Repasky, M. P.; Frye, L. L.; Greenwood, J. R.; Halgren, T.  
827 A.; Sanschagrin, P. C.; Mainz, D. T. Extra precision glide: docking and scoring  
828 incorporating a model of hydrophobic enclosure for protein-ligand complexes. *J Med Chem*  
829 **2006**, 49, 6177-96.
- 830 38. Halgren, T. A.; Murphy, R. B.; Friesner, R. A.; Beard, H. S.; Frye, L. L.; Pollard, W. T.;  
831 Banks, J. L. Glide: a new approach for rapid, accurate docking and scoring. 2. Enrichment  
832 factors in database screening. *J Med Chem* **2004**, 47, 1750-9.
- 833 39. Friesner, R. A.; Banks, J. L.; Murphy, R. B.; Halgren, T. A.; Klicic, J. J.; Mainz, D. T.;  
834 Repasky, M. P.; Knoll, E. H.; Shelley, M.; Perry, J. K.; Shaw, D. E.; Francis, P.; Shenkin, P.  
835 S. Glide: a new approach for rapid, accurate docking and scoring. 1. Method and assessment  
836 of docking accuracy. *J Med Chem* **2004**, 47, 1739-49.
- 837 40. Liu, T. F.; Vachharajani, V. T.; Yoza, B. K.; McCall, C. E. NAD<sup>+</sup>-dependent sirtuin 1 and 6  
838 proteins coordinate a switch from glucose to fatty acid oxidation during the acute  
839 inflammatory response. *Journal of biological chemistry* **2012**, 287, 25758-25769.

## **Design, synthesis and biological evaluation of novel TR $\beta$ selective agonists sustained by ADME-Toxicity analysis**

Massimiliano Runfola<sup>1#</sup>, Simona Sestito<sup>1#</sup>, Lorenza Bellusci<sup>2</sup>, Valeria La Pietra<sup>3</sup>, Vincenzo Maria D'Amore<sup>3</sup>, Marta Anna Kowalik<sup>4</sup>, Grazia Chiellini<sup>2\*</sup>, Sheraz Gul<sup>5</sup>, Andrea Perra<sup>4</sup>, Amedeo Columbano<sup>4</sup>, Luciana Marinelli<sup>3</sup>, Ettore Novellino<sup>3</sup>, Simona Rapposelli<sup>1,6\*</sup>

<sup>1</sup>Department of Pharmacy, University of Pisa, Pisa, 56126, Italy;

<sup>2</sup>Department of Pathology, University of Pisa, Pisa, 56126, Italy;

<sup>3</sup>Department of Pharmacy, University of Naples Federico II, Italy;

<sup>4</sup>Department of Biomedical Sciences, Unit of Oncology and Molecular Pathology, University of Cagliari, Cagliari, Italy;

<sup>5</sup>Fraunhofer Institute for Molecular Biology & Applied Ecology – ScreeningPort, Hamburg, Germany;

<sup>6</sup>Interdepartmental Research Centre for Biology and Pathology of Aging, University of Pisa, Pisa, Italy.

# M.R and S.S equally contributed;

\*For S.R.: phone, +39 050 2219582; fax, +39 050 2219577; Email: [simona.rapposelli@unipi.it](mailto:simona.rapposelli@unipi.it)

\*For G.C.: phone, +39 050 2218662; E-mail, [grazia.chiellini@unipi.it](mailto:grazia.chiellini@unipi.it)

## HIGHLIGHTS

- A novel series of thyromimetics was developed and their ADME-Toxicity profile was assessed.
- To simulate the interaction of selected compounds with the putative receptor-binding site in silico docking-studies were performed
- Compounds **1** and **3** proved to be TR $\beta$  selective agonists and promote lipolysis through the activation of AMPK/ACC pathway
- Preliminary in vivo studies of thyromimetics **1** and **3** confirm a safe-profile of both compounds, lacking both cardio- and hepatotoxicity.

## ABSTRACT

Although triiodothyronine (T3) induces several beneficial effects on lipid metabolism, its use is hampered by toxic side-effects, such as tachycardia, arrhythmia, heart failure, bone and muscle catabolism and mood disturbances. Since the  $\alpha$  isoform of thyroid hormone receptors (TRs) is the main cause of T3-related harmful effects, several efforts have been made to develop selective agonists of the  $\beta$  isoform that could induce some beneficial effects (i.e. lowering triglyceride and cholesterol levels reducing obesity and improving metabolic syndrome), while overcoming most of the adverse T3-dependent side effects. Herein, we describe the drug discovery process sustained by ADME-Toxicity analysis that led us to identify novel agonists with selectivity for the isoform TR $\beta$  and an acceptable off-target and absorption, distribution metabolism, excretion and toxicity (ADME-Tox) profile. Within the small series of compounds synthesized, derivatives **1** and **3**, emerge from this analysis as “potentially safe” to be engaged in preclinical studies. In in vitro investigation proved that both compounds were able to reduce lipid accumulation in HepG2 and promote lipolysis with comparable effects to those elicited by T3, used as reference drug. Moreover, a preliminary in vivo study confirmed the apparent lack of toxicity, thus suggesting compounds **1** and **3** as new potential TR $\beta$ -selective thyromimetics.

**KEYWORDS:** Triiodothyronine, thyronamine, TR $\beta$  selective agonist, fatty-liver disorder, liver regeneration

## INTRODUCTION

Thyroid hormones (THs) are essential regulatory molecules for normal growth and development and for maintaining metabolic homeostasis [1]. Most of the activities elicited by THs are mediated by nuclear thyroid hormones receptors (TRs), which are members of the nuclear hormone receptor family and act as ligand-activated transcription factors. There are two main TR isoforms encoded on separate genes, namely TR $\alpha$  and TR $\beta$ . Both TR isoforms bind 3,5,3'-triiodothyronine (T3) and mediate TH-regulated gene expression through interactions with DNA response elements and with a complex array of transcriptional cofactors, including corepressors (CoRs), coactivators (CoAs), integrators like CREB-binding protein (CBP), and general transcription factors (GTFs) [2]. TH/TR binding exerts profound effects in several physiological processes. In the central nervous system (CNS) THs signaling is involved in development and maintenance of brain function, influencing various activities such as neuronal and glial cell differentiation, myelination, and neurogenesis [3, 4]. In the liver, THs influence hepatic lipid metabolism through multiple pathways, with insightful effects on energy expenditure [5], fat oxidation [6] and cholesterol metabolism [7]. Conversely, alteration of cellular TH signaling in the liver plays a key role in the onset or progression of several liver-associated diseases, such as non-alcoholic fatty liver disease (NAFLD), and hepatocellular carcinoma (HCC) [8]. Therefore, modulating the function of THs offers the potential to treat a wide variety of liver diseases and cancer, as well. Unfortunately, the use of THs as therapeutic agents is hampered by the lack of selectivity and the consequent adverse side effects (such as increased heart rate, cardiac hypertrophy, muscle wasting, and reduced bone density) that are mainly due to their binding to TR $\alpha$  receptors. In order to overcome these drawbacks, selective activation of the  $\beta$  thyroid hormone receptor (TR $\beta$ ) is an appropriate method to develop new treatments for several chronic diseases with a reduced side effect profile.

During the past two decades, a number of selective TR $\beta$  agonists have been developed. These include the analogues Sobetirome (GC-1), KB-141 and the Hep-Direct prodrug VK2809 that exhibits most of the beneficial properties of T3 in the absence of deleterious effects [9-11]. GC-1 emerged in 1995 [9] as the first halogen free thyromimetics. It was shown to bind preferentially to TR $\beta$  vs TR $\alpha$  and was initially studied as an hypocholesterolemic compound able to stimulate hepatic pathways without harmful side effects [12]. Due to the beneficial effects of GC-1 and KB2115, the latter known as Eprotirome, entered human clinical trials for dyslipidaemia, and yielded encouraging results in the absence of harmful effects typically associated with THs high levels (for reviews, see Tancevski et al. 2011 [13], Meruvu et al. 2013 [14]). The progression of GC-1 was discontinued despite a promising phase I trial for the treatment of lipid metabolism disorders and obesity, with no phase II trials being planned. Additional applications of GC-1 have

been proposed in orphan indications and this drug is now in phase I/II trial for a rare disease (X-Linked Adrenoleukodystrophy) (Clinicaltrial.gov Identifier: NCT03196765). Eprotirome, progressed to phase III clinical trial but was terminated due to unexpected side effects in animal studies [15]. Another selective thyromimetic, namely Resmetirom (MGL-3196) was designed as a liver-specific TR $\beta$  agonist able to reduce hepatic lipid synthesis and has progressed to phase II trials (ClinicalTrials.gov Identifier: NCT02912260). In addition, VK2809 is a novel liver-directed thyroid receptor beta agonist pro-drug [16] that possesses selectivity for liver tissue, and after undergoing cleavage by a cytochrome P450 enzyme, is able to release the selective thyromimetic MB07344 which binds to TR $\beta$  receptor (Figure 1). Currently, VK2809 has progressed to Phase 2 clinical trial in patients with primary hypercholesterolemia and non-alcoholic fatty liver disease (NAFLD). (ClinicalTrials.gov identifier: NCT02927184). Although many thyromimetics are currently in clinical trials, none have been approved by FDA (Figure 1).

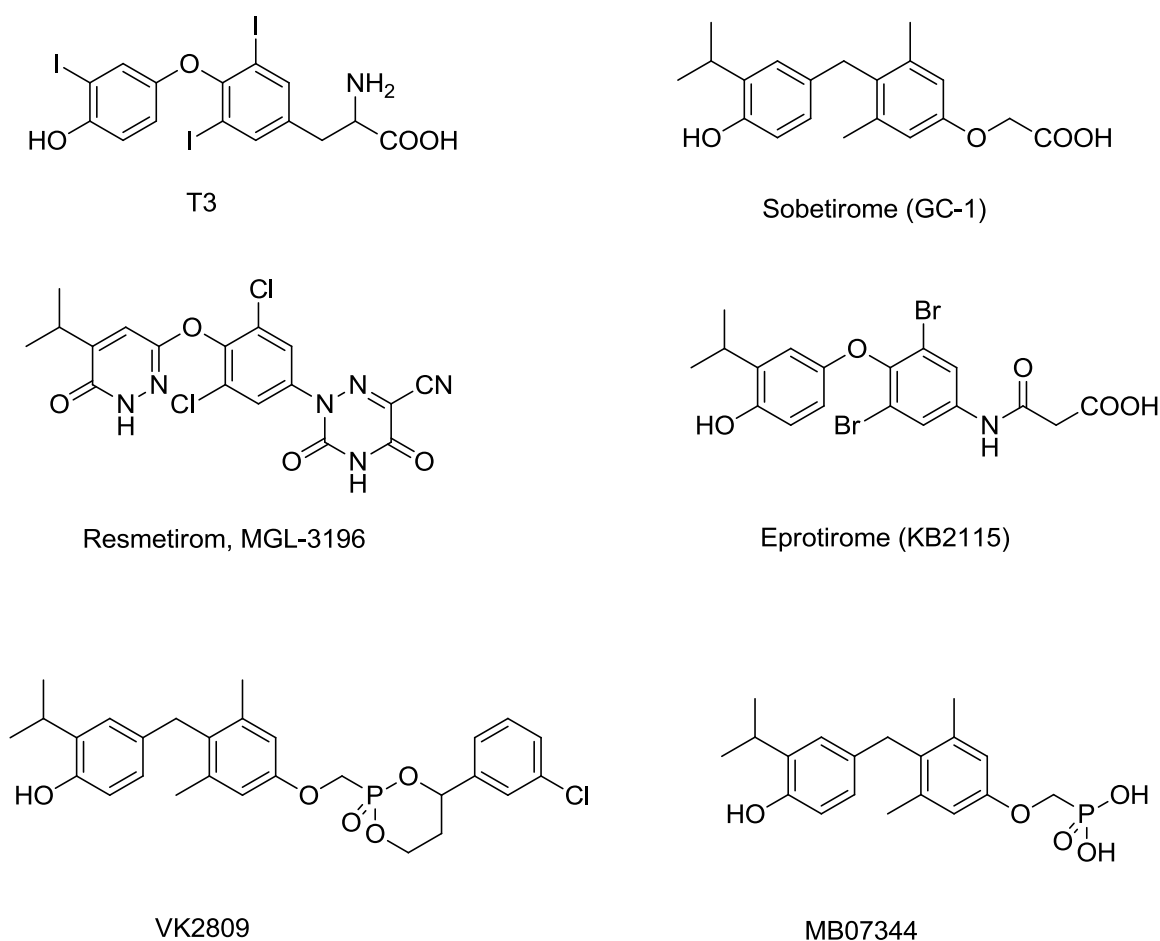


**Figure 1.** Structures of TR $\beta$  agonists which have been progressed in drug discovery.

Despite the challenges with progressing TR $\beta$  selective agonists due to their side effect profiles, their use to treat other human pathologies could be explored as part of drug repositioning strategies. Accordingly, the identification of novel agonists with selectivity for both the TR $\beta$  and the liver could represent a valid strategy to regulate metabolic disorders. This paper reports the results of the design and synthesis of a novel series of TR $\beta$  agonists. The thyromimetic-analogues were evaluated for their off-target and ADME-Tox properties and the most optimal compounds progressed to in vitro profiling in a nuclear receptor coregulator assay (Thermofisher®) and for their ability to promote lipolysis in human hepatoma cells (HepG2). Further investigation to determine the cellular pathways involved in their lipid-lowering ability was also carried-out. Additionally, to rationalize the pharmacological results, in silico docking studies on selected compounds were also performed in order to simulate their interaction with the putative receptor-binding site. Finally, we performed preliminary in vivo studies to assess the effect of two thyromimetics (compound **3** and its pro-drug **1**), which were shown to be associated with the most optimal off-target and ADME-Tox profile, to determine their ability to modulate cholesterol serum levels, triglycerides, glucose, bilirubin and transaminases in rats.

## RESULTS & DISCUSSION

### Rational design of new thyromimetic molecules

Our search for therapeutic agents focused on the design and synthesis of agonists endowed with high selectivity for TR $\beta$  and enhanced hepato-specificity. To this end, we designed and synthesized a new class of thyromimetics based on a diphenylmethane scaffold. This moiety has been widely recognized as an effective replacement for the biaryl-ether core of THs [16-20]. Notably, in previously developed diphenylmethane-based thyromimetics, the oxyacetic acid side chain was shown to have a critical role in conferring TR $\beta$  selectivity [19]. On the basis of this finding, we designed compounds **1-4** and **9-11** (Figure 2). In compounds **3**, **4**, **9** and **10**, the hydroxyl group at the 4'-position in T3 was replaced by an amino group. This type of modification generates the zwitterion that could be detrimental for the bioavailability of the molecule. Hence, we synthesized the corresponding acetamide-analogues of **3** and **4**, namely **1** and **2**, which could represent potential pro-drugs with improved drug-like properties. Oral administration of these pro-drugs, by first pass metabolism through the liver, should lead to an efficient generation of the corresponding parent compounds. Based on our previous experience gained during the development of SG-compounds as thyronamine analogues of T1AM, it is known that the oxyethylamine sidechain represents a valid

precursor of the oxyacetic group that is formed following the metabolic activation by MAOs [18]. Therefore, we synthesized the derivatives **5-8** as possible precursors of the corresponding thyromimetics with an oxyacetic structure. The two iodine atoms present in the T3 inner ring have been replaced with hydrogen atoms (**2** and **4**), with two methyl groups (**1**, **3**, **5**, **7**, **10** and **11**) or with a hydrogen and CF<sub>3</sub> (or H and F) as in compounds **6**, **8** and **9**. As to the iodine atom in the outer ring of T3, it has been replaced by an isopropyl group (**1-6**) or by a hydrogen atom (**7-11**).

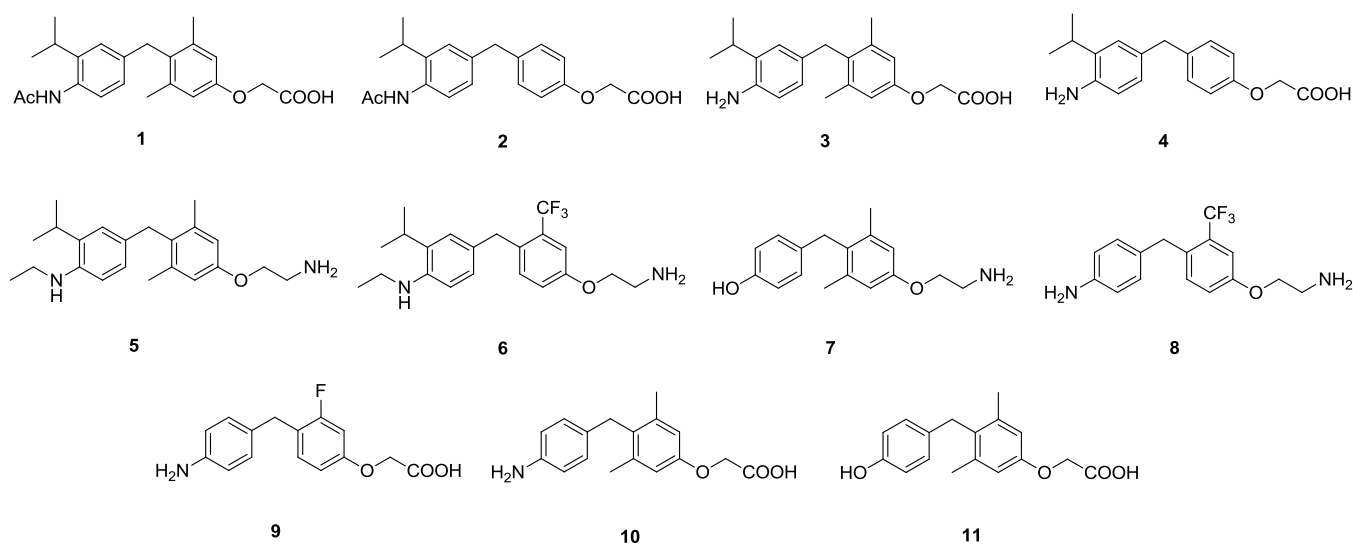
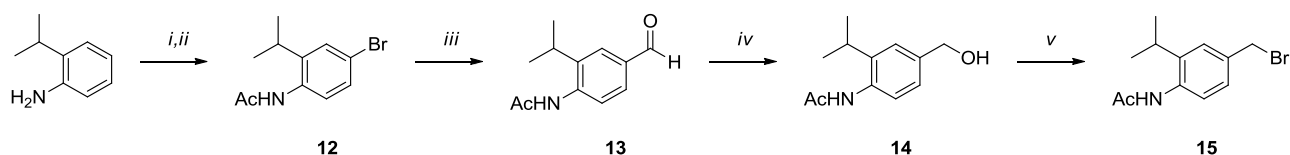


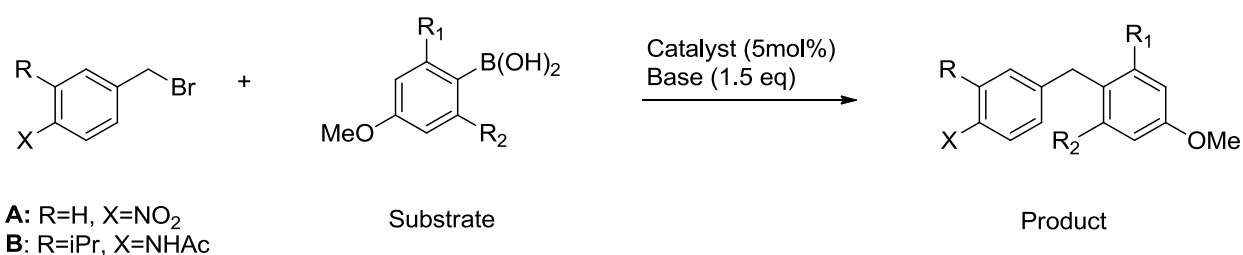
**Figure 2.** Structures of novel thyromimetics **1-11** with a biphenylmethane scaffold.

## Chemistry

A crucial component in our synthetic procedures is the synthesis of the biphenylmethane scaffold which was obtained with the palladium (0)-catalyzed Suzuki-Miyaura cross coupling reaction between the substituted benzylbromide and selected phenyl boronic acid derivatives. The Suzuki-Miyaura reaction was performed under standard or microwave-assisted conditions, with yields ranging from 22% and 60% as reported in **Table 1**. In particular, benzylbromide **15**, which was not commercially available, was obtained as shown in **Scheme 1**. A one-pot reaction between 2-isopropylaniline, acetic anhydride, and bromine was carried out in acetic acid providing the bromobenzene derivative **12** with high yields. Then, formylation of **12** with n-BuLi and DMF at –78 °C led to benzaldehyde-derivative **13**, which was reduced with NaBH<sub>4</sub> to provide the benzylic alcohol **14**. Finally, **15** was obtained by bromination of **14**, using CBr<sub>4</sub> and PPh<sub>3</sub> (Appel reaction).



**Scheme 1.** Synthesis of benzylbromide **15**. *Reagents and conditions.* *i:* Ac<sub>2</sub>O, AcOH, 117-118 °C, 1 h; *ii:* Br<sub>2</sub>, AcOH, 65 °C, 30' ; *iii:* n-BuLi, DMF, THF, -78 °C → rt, 3 h; *iv:* NaBH<sub>4</sub>, MeOH, 0 °C → rt, 12 h; *v:* CBr<sub>4</sub>, PPh<sub>3</sub>, DCM, 0 °C → rt, 12 h.

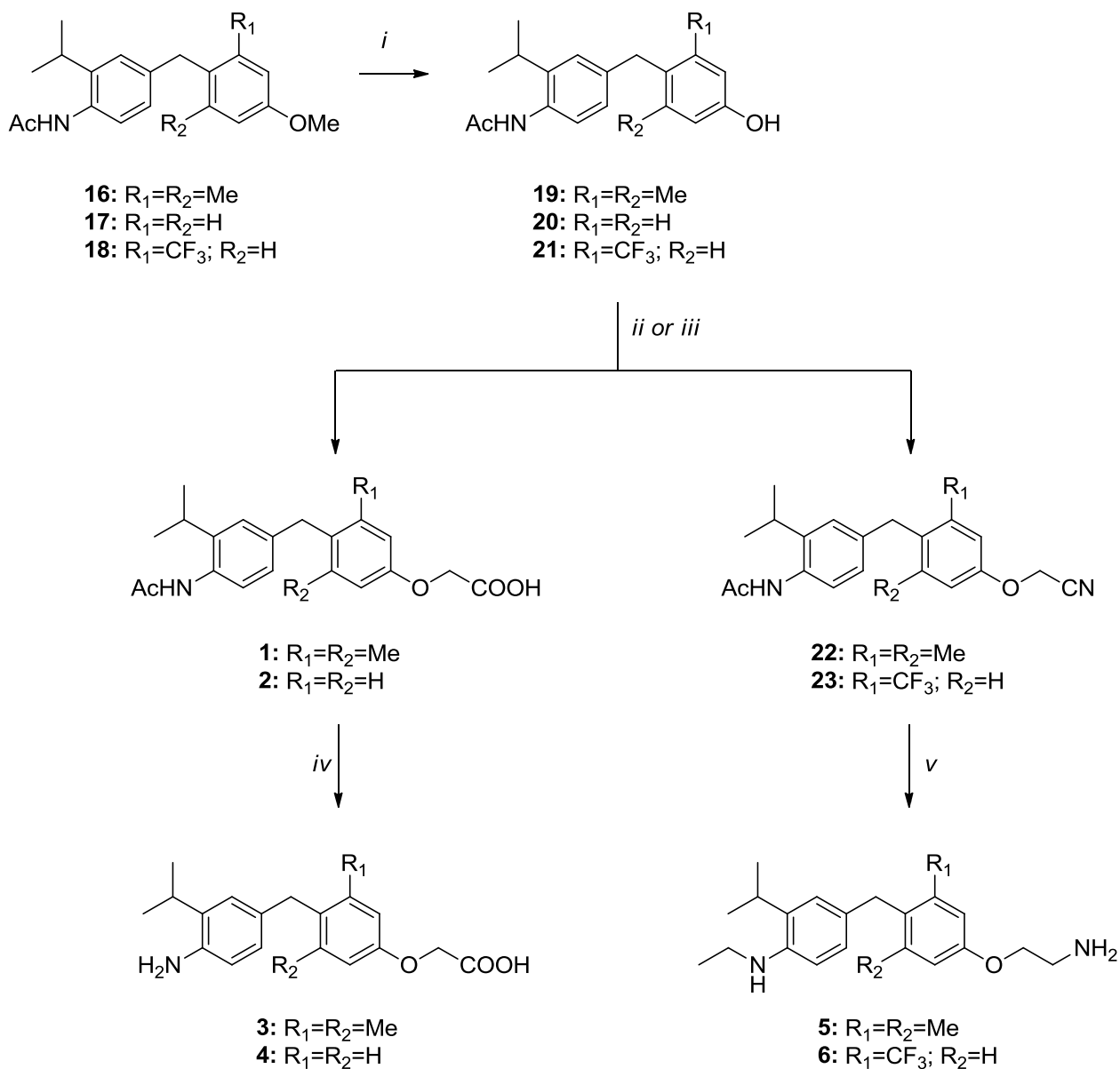


Entry	Substrate <sup>a</sup>		Product	Base	Catalyst	Solvent	Temp.	Time	Yield <sup>d</sup>
	R <sub>1</sub>	R <sub>2</sub>							
<b>B<sup>b</sup></b>	Me	Me	<b>16</b>	K <sub>2</sub> CO <sub>3</sub>	PdCl <sub>2</sub>	acetone/H <sub>2</sub> O	40 °C	6h	60%
<b>B<sup>b</sup></b>	H	H	<b>17</b>	K <sub>2</sub> CO <sub>3</sub>	PdCl <sub>2</sub>	Acetone/H <sub>2</sub> O	100 °C	10 <sup>c</sup>	30%
<b>B<sup>b</sup></b>	CF <sub>3</sub>	H	<b>18</b>	K <sub>2</sub> CO <sub>3</sub>	Pd(PPh <sub>3</sub> ) <sub>4</sub>	1,4 dioxane	90 °C	12h	22%
<b>A<sup>a</sup></b>	F	H	<b>24</b>	Ba(OH) <sub>2</sub> *8H <sub>2</sub> O	Pd(PPh <sub>3</sub> ) <sub>4</sub>	1,2-DME/H <sub>2</sub> O	110 °C	20 <sup>c</sup>	39%
<b>A<sup>a</sup></b>	CF <sub>3</sub>	H	<b>25</b>	K <sub>2</sub> CO <sub>3</sub>	Pd(PPh <sub>3</sub> ) <sub>4</sub>	1,4 dioxane	90 °C	6h	52%
<b>A<sup>a</sup></b>	Me	Me	<b>26</b>	K <sub>2</sub> CO <sub>3</sub>	PdCl <sub>2</sub>	acetone/H <sub>2</sub> O	rt	72h	32%

**Table 1.** Cross-Coupling Reactions. <sup>a</sup>commercially available starting material; <sup>b</sup>compound **15**; <sup>c</sup>reaction was performed using a microwave reactor; <sup>d</sup>yields refer to products after compound purification which was performed by flash chromatography (for further information on eluent mixture, consult supplementary material).



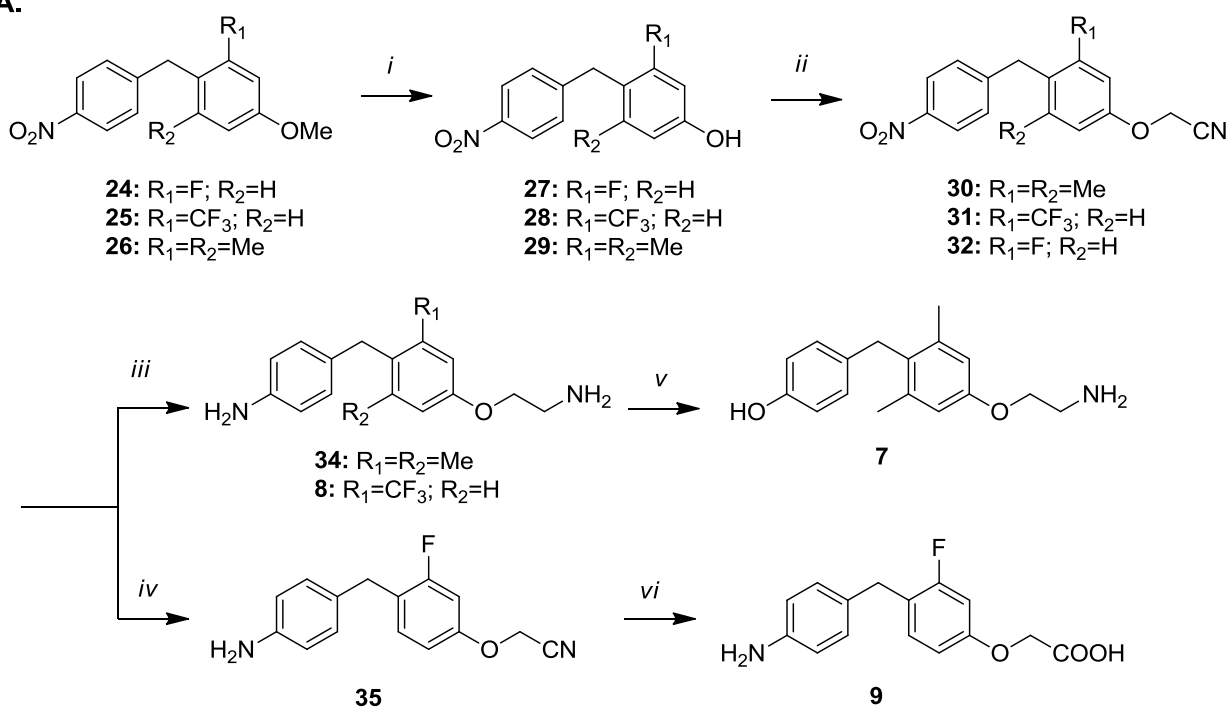
Scheme 2 illustrates the synthetic procedure to obtain compounds **1-6**. Briefly, phenol derivatives **19-21** were obtained by demethylation of purified cross coupling products **16-18** by using  $\text{BBr}_3$ . The following O-alkylation reaction of **20** and **21** with bromoacetic acid led to compound **1** and **2**, which have undergone deacetylation in presence of hydrochloric acid at concentrated grade to provide desired compound **3** or **4**. Compounds **5** and **6** were obtained by reaction of phenolic derivative **19** or **21** with bromoacetonitrile, followed by reduction of intermediates **22** and **23** in presence of  $\text{LiAlH}_4$  and  $\text{AlCl}_3$ .



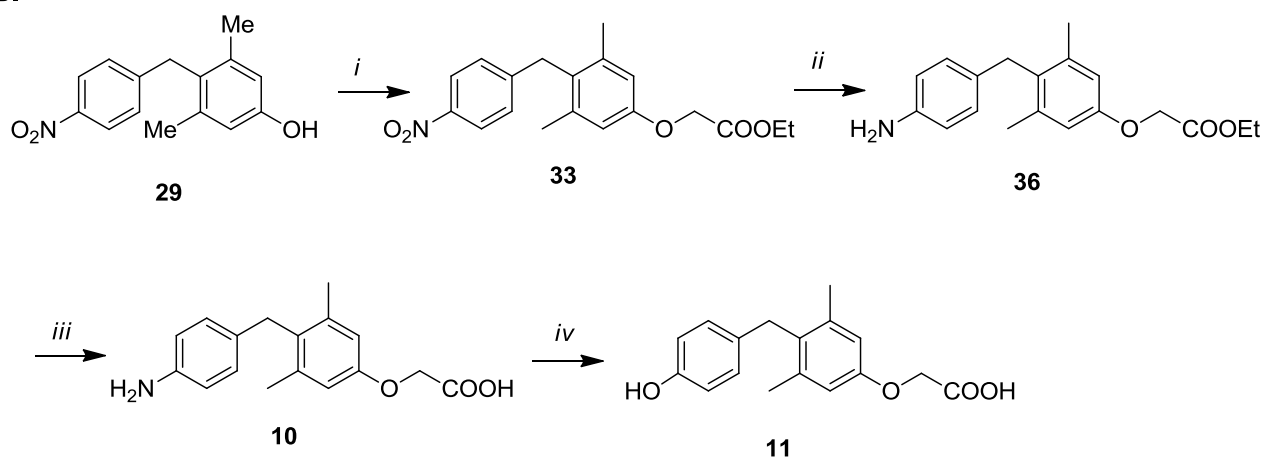
**Scheme 2.** Synthesis of final compounds **1-6**. *Reagents and conditions.* (i)  $\text{BBr}_3$ , DCM,  $-10\text{ }^\circ\text{C}$ , 1 h; (ii)  $\text{BrCH}_2\text{COOH}$ , DMF,  $\text{Cs}_2\text{CO}_3$ , rt, 1 h; (iii)  $\text{BrCH}_2\text{CN}$ , DMF,  $\text{Cs}_2\text{CO}_3$ , rt, 30'; (iv)  $\text{HCl}$  37%,  $\text{H}_2\text{O}$ ,  $120\text{ }^\circ\text{C}$ , 12 h; (v)  $\text{LiAlH}_4$ ,  $\text{AlCl}_3$ , THF, rt  $\rightarrow$   $66\text{ }^\circ\text{C}$ , 12 h.

Compounds **7-11** were obtained according to the synthetic procedure reported in Scheme 3. Briefly, purified cross-coupling products **24-26** were treated with  $\text{BBr}_3$  to afford the phenol derivatives **27-29** which have undergone O-alkylation reaction with bromoacetonitrile or ethyl bromoacetate leading to intermediates **30-32** and **33**, respectively. Compound **9** was obtained by selective nitro-group reduction (**35**), followed by acid hydrolysis with  $\text{HCl}$  at concentrated grade. Treatment of **33** with hydrazine and  $\text{FeCl}_3$  led to ethyl ester **36** which was converted to compound **10** by mild saponification. Finally, the conversion of amine moiety of **10** to a phenolic group using diazonium salt led to compound **11**.

**A.**



**B.**



**Scheme 3** Synthesis of final compounds **7-11**. *Reagents and conditions:* **A.** (i)  $\text{BBr}_3$ ,  $\text{DCM}$ ,  $-10^\circ\text{C}$ , 1 h; (ii)  $\text{BrCH}_2\text{CN}$ ,  $\text{DMF}$ ,  $\text{Cs}_2\text{CO}_3$ ,  $\text{rt}$ , 20', 1 h; (iii)  $\text{LiAlH}_4$ ,  $\text{AlCl}_3$ ,  $\text{THF}$ ,  $\text{rt} \rightarrow 66^\circ\text{C}$ , 12 h; (iv)  $\text{H}_2$ ,

Pd/C, MeOH, 12 h; (v) H<sub>2</sub>SO<sub>4</sub>, NaNO<sub>2</sub>, H<sub>2</sub>O, 100 °C, 1 h; (vi) HCl 37%, H<sub>2</sub>O, 100 °C, 4 h; **B.** (i) BrCH<sub>2</sub>COOEt, DMF, Cs<sub>2</sub>CO<sub>3</sub>, rt, 1 h; (ii) H<sub>2</sub>, Pd/C, EtOH, 150', rt (iii) NaOH 10%, MeOH, 66 °C, 1 h; (iv) H<sub>2</sub>SO<sub>4</sub>, NaNO<sub>2</sub>, H<sub>2</sub>O, 100 °C, 1 h.

### Off-target and ADME-Tox profiling

In order to identify the most promising compound for progression in the drug discovery process, the novel thymomimetics **1-11** were screened in vitro at 10 µM against a panel of early ADME-Tox assays comprising cytotoxicity (U2OS, HEK, hTERT and MCF-7), cardiotoxicity (*h*ERG), cytochrome P450 inhibition (CYP1A2, CYP2C9, CYP2C19, CYP2D6 and CYP3A4), and off-targets such as Aurora B kinase and phosphodiesterase (PDE4C1), and epigenetic enzymes (SIRT7, HDAC4, HDAC6, HDAC8 and HDAC9), see Figure 3. At first, the cytotoxicity of **1-11** were determined after 24 h or 48 h of treatment in the four cell-lines. Reassuringly, only compound **6** was associated with a low degree of cytotoxicity at 10 µM (65% at 24 h and 53% at 48 h) towards MCF-7 cell-line (see “paper data in brief” for details). [Ref]

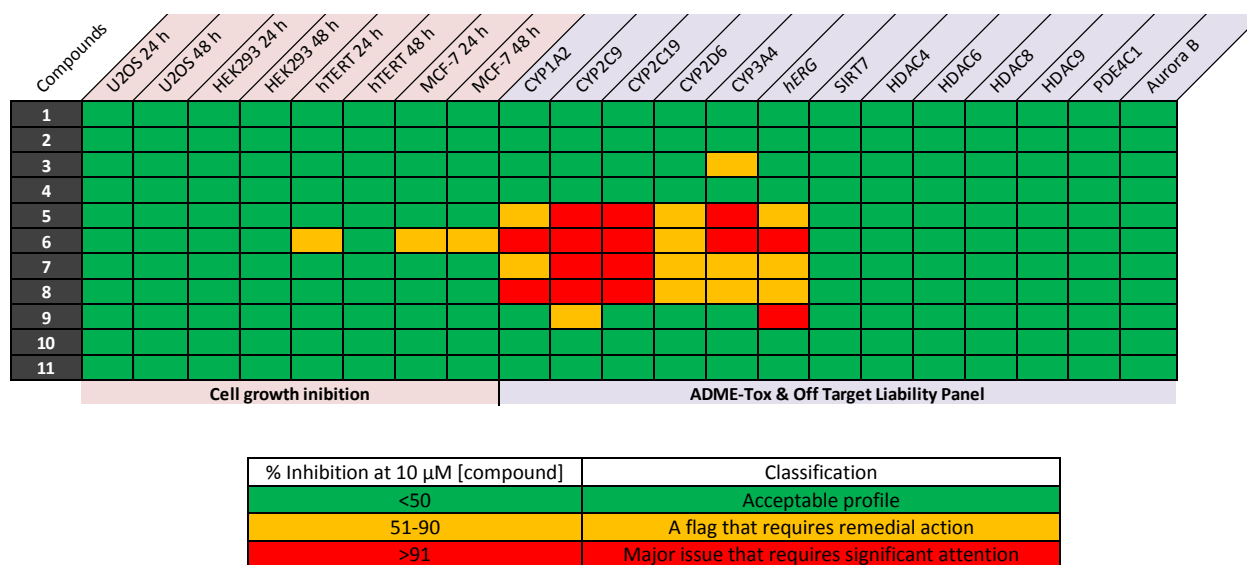


**Figure 3.** Off-target and ADME-Tox profile of compounds **1-11**. All compounds were screened at 10 µM in triplicate. A traffic-light system was used to characterize the effect of the new thymomimetics in the in vitro off-target and ADME-Tox assays.

The ADME-Tox profile of a compound is a major factor when selecting the best candidate(s) to progress in the drug discovery value chain. Among several enzymes responsible for xenobiotic transformation, the cytochrome P450 (CYP450) enzyme plays a key role in phase I oxidative

metabolism and most of drug biotransformation are essentially achieved by five isoforms: CYP1A2, CYP2C9, CYP2C19, CYP2D6, and CYP3A4 [21]. Interestingly, while the carboxylic compounds were associated with minimal adverse effect on CYP450 enzyme activity, compounds **5-8** yielded considerably more inhibition against all CYP450 enzymes, probably as a consequence of the oxyethylamine moiety. In order to assess the off-target liability of newly synthesized molecules, all compounds were tested against several well-known off-targets. For this study, enzymes belonging to different classes were selected. SIRT7, HDAC4, HDAC6, HDAC8 and HDAC9 were chosen as representatives of an undesirable epigenetic modulation [22, 23]. No compounds were associated with adverse inhibition of these targets. Moreover, the new synthesized molecules were also shown to be inactive against Aurora B kinase and PDE4C1 enzymes which are known to be essential for cell growth and whose inhibition has been involved in tumorigenesis. Finally, the ability of the newly synthesized molecules to modulate hERG ion-channel activity was assessed using the Predictor hERG FP assay (Thermofisher®). The hERG ion-channel plays a key role in cardiac action potential and represents one of the main reasons for failure of clinical candidates or, even worse, a cause for withdrawal of drugs from the market. For this reason, it is considered important to assess the effect of compounds on hERG ion-channel activity at an early stage of drug discovery process. Compounds **1-4**, **10** and **11** did not significantly alter the hERG ion-channel activity, such that the percentage of inhibition was <40 % at 10  $\mu$ M. More importantly, compound **1**, **10**, and **11** were shown to inhibit hERG ion-channel activity <25 % at 10  $\mu$ M (Figure 4). Overall, the off-target and ADME-Tox profiling led to the identification of 6 compounds (**1-4**, **10**, **11**) with the most optimal profiles for progression. Next, we proceeded with biological evaluation to assess their agonist activity against TR $\alpha$  and TR $\beta$ .

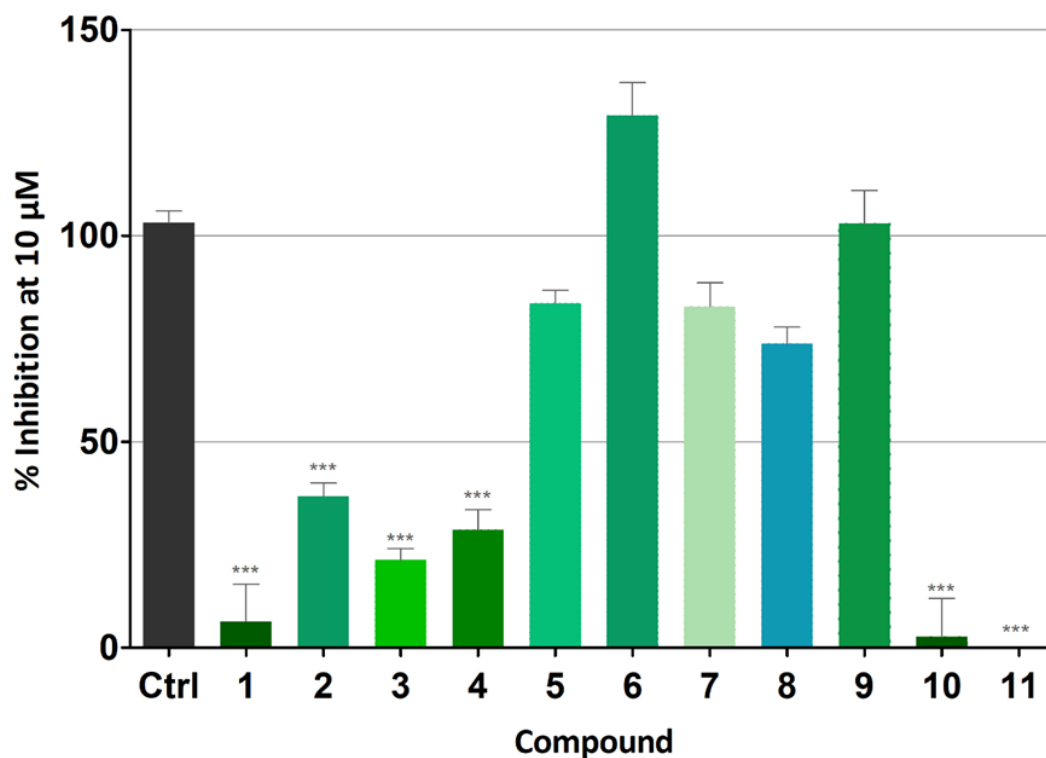


**Figure 4.** hERG ion-channel inhibition profile of compounds **1-11**. All compounds were tested at 10 μM in triplicate, and raw data were normalized to positive control (Ctrl = Compound E-4051) and negative control (DMSO) and the % Inhibition of the hERG ion-channel activity calculated. Results were compared to control using the One-Way ANOVA test. \*\*\* p<0.005.

### Nuclear receptor activation

The activity of compounds **1-4** and **10-11** on TRα and TRβ was assessed using the LanthaScreen™ TR-FRET Nuclear Receptor Coregulator Assay (service provided by Invitrogen Corporation, USA) in 10-point dose-response experiments for each compound. Among the tested compounds, only **3** and **11** were active against TRα and TRβ. Interestingly, compound **11** activated both TR isoforms with EC50 towards TRα and TRβ of respectively 54 and 32 nM. Apart from ability to activate the receptors, the selectivity towards the TRβ isoform is pivotal in order to avoid side effects related to TRα activation in vivo. Above all, compound **3** was shown to be a TRβ agonist with EC50 value 458 nM, whereas it only activated TRα to 30 % (at 1μM) (see Supporting Information for details). Based upon these results, compound **3** was selected for further biological investigations. In addition, compound **1** was also selected for further study, as it was originally designed as pro-drug of compound **3**, and more importantly, it was also found to possess an acceptable off-target and ADME-Tox profile.

## Computational studies

In order to elucidate the activity and the preferential binding of compound **3** for TR $\beta$  with respect to TR $\alpha$ , docking calculations were carried out with the aid of Glide 6.7 (Maestro packaging) into the ligand-binding-cavity (LBC) of the two receptors, using the structures co-crystallized with GC-1, PDB: 3ILZ and 3IMY, respectively (See Experimental Section for X-ray selection). Bearing in mind the importance of water-mediated interactions for GC-1, which is a potent thyromimetic as well as a very close analogue of **3**, our calculations were performed retaining crystal water molecules within 3 Å of the ligand. As for TR $\beta$ , the best ranked docking pose predicted for **3** (Figure 5) is highly superimposable with the crystal structure of GC-1 into the thyroid receptor. Specifically, the ligand carboxylate forms a H-bond with the backbone NH group of the N331 and engages two charge-reinforced H-bonds with the guanidinium group of R282. Moreover, water-mediated contacts are found with the R316 and R320 side chains. As for the dimethyl phenyl moiety, it establishes many van der Waals interactions with the LBC lipophilic side chains of L330, I275, I353, M313 and M310 and, thanks to the 3,5 di-methyl substitutions, it is locked in the active perpendicular conformation with respect to the terminal phenyl ring [24]. Other profitable lipophilic interactions are detected between the latter and the L341, F272, I276, L346 side chains and between the iso-propyl substituent with the residues F269, F272, M442, L346 and F451. Finally, the **3** amino group H-bonds the imidazoline nitrogen atom of the H435. Of note, when the zwitterionic form of **3** is docked into the receptor, numerous bad contacts are found between the cationic amino group and the surrounding lipophilic residues of the LBC, which might be responsible of the lower activity of **3** with respect to its hydroxyl analogue GC-1 (data from the literature). Moreover, the bulkiness of the residues F269, F455 and F439 does not allow a proper accommodation of the 4'-NH-acetyl group of compound **1**, generating intramolecular steric clashes and hampering the formation of an H-bond with H435, justifying the loss of activity of this prodrug (see Figure SI2 together with comments on the other derivatives of the series that can be found in Supporting Information).

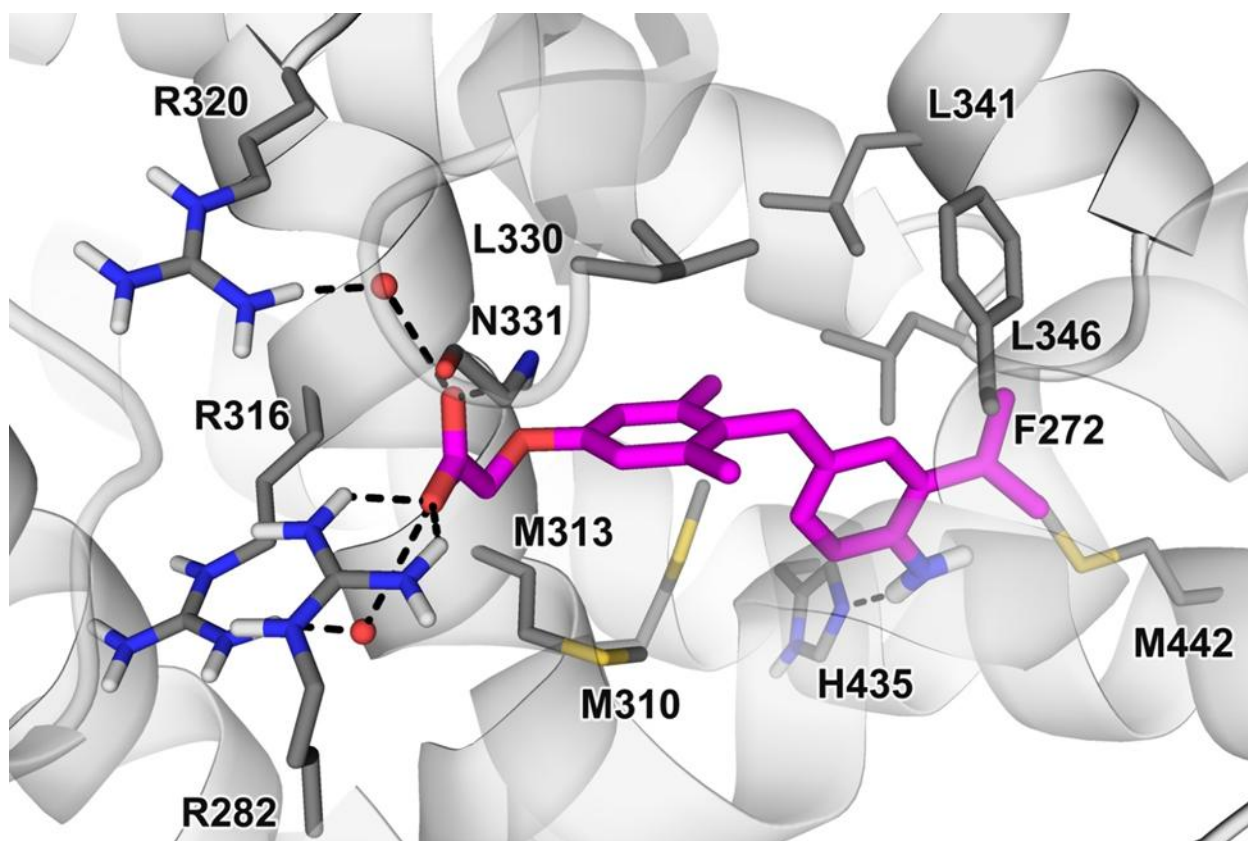


**Figure 5.** Binding mode of compound **3** in the TR $\beta$  LBC. The receptor is displayed in grey cartoon, while the ligand and the main protein residues are depicted in magenta and gray sticks respectively. H3 helix and the N331 loop are in transparency and non-polar hydrogens are omitted for sake of clarity. H-bonds are shown as black dashed lines.

As for the selectivity profile of **3**, in TR $\alpha$  a pose very similar to the co-crystallized structure of GC-1 with the receptor is found. This outcome is not surprising since it is known that only a single residue mutation (S277 in TR $\alpha$  versus N331 in TR $\beta$ ) differentiates within the TR $\alpha$  and TR $\beta$  binding pockets, and this mutation does not alter the overall shape and characteristics of the two clefts. However, a deeper analysis shows that our ligand is not able to interact with R262 (R316 in TR $\beta$ ) and just one water-mediated contact is found with the R228 side chain (R282 in TR $\beta$ ). In this regards, crystallographic analysis and MD studies [25, 26], have demonstrated that this single mutation is able to affect the orientation of one of the interacting arginines (R228 in TR $\alpha$  and R282 in TR $\beta$ ). Specifically, in TR $\beta$ , the N331 side chain interacts with the R282 guanidinium, which in turn is permanently and optimally oriented toward the ligand carboxylate allowing GC-1 to stabilize a rich H-bonds network with the three surrounding arginines, justifying its preferential binding to TR $\beta$ . As described above, analogously to GC-1, thyromimetic compound **3** is able to establish a broad and stable interaction pattern with TR $\beta$  arginines, including strong and direct contacts with

R282, while part of these interactions are lost in TR $\alpha$ . Reasonably, this might in part justify the preferential binding of **3** to TR $\beta$  with respect to TR $\alpha$ . Also, it is known that in TR $\beta$  LBC, the residues lining the outer ring of thyromimetics (especially the M442 residue) [27], are more flexible with respect to their corresponding TR $\alpha$  residues, so that large 3'-substituents and certain 4'-substituents [28], increment selectivity toward this isoform. Thus, it is possible that **3**, possessing the novel combination of 3'-iPr e 4'-NH<sub>2</sub> substituents on the outer ring, it is better accommodated within the TR $\beta$  pocket.

### Effects on lipid metabolism

Abnormal accumulation of lipids in hepatocytes is a prominent aspect in several liver diseases such as NAFLD (non-alcoholic fatty liver spectrum disease) and alcoholic steato-hepatitis (ASH) [29]. In order to investigate whether the new thyromimetic molecules **1** and **3** could promote lipolysis, and whether derivative **1** is capable of efficiently delivering the corresponding parent compound **3**, we evaluated their effect on lipid metabolism in the human hepatoma cells HepG2. Initially HepG2 cells were incubated for 24 h with **1** and **3** at 1  $\mu$ M and 10  $\mu$ M, with T3 as reference drug (Figure 6). Oil-red O staining was used to monitor intracellular lipid accumulation (Figure 7). Cloroquine (CLO) 25  $\mu$ M was used as positive controls.

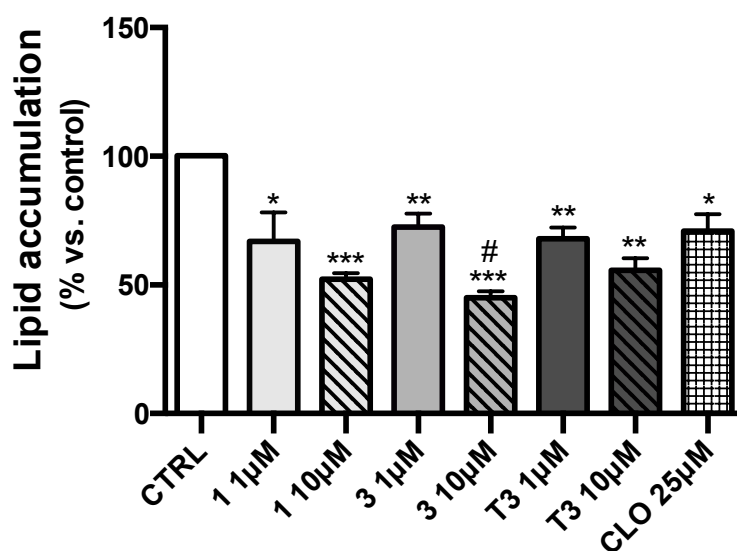


**Figure 6.** Effects of **1** and **3** on total lipid accumulation in HepG2 cells. Cells were treated for 24 h with **1**, **3** or T3 at 1 and 10  $\mu$ M. 25  $\mu$ M Cloroquine (CLO) was used as positive control. Oil red O stained intercellular oil droplets were eluted with isopropanol and quantified by spectrophotometry analysis at 510 nm. Values represent the mean  $\pm$  SEM of 4 to 8 experiments. The groups were



compared using the One-Way ANOVA followed by Tukey's range test. \* $p < 0.05$  vs. Ctrl; \*\* $p < 0.01$  vs. Ctrl; \*\*\* $p < 0.005$  vs. Ctrl; # $p < 0.05$  vs. **3** 1  $\mu$ M.

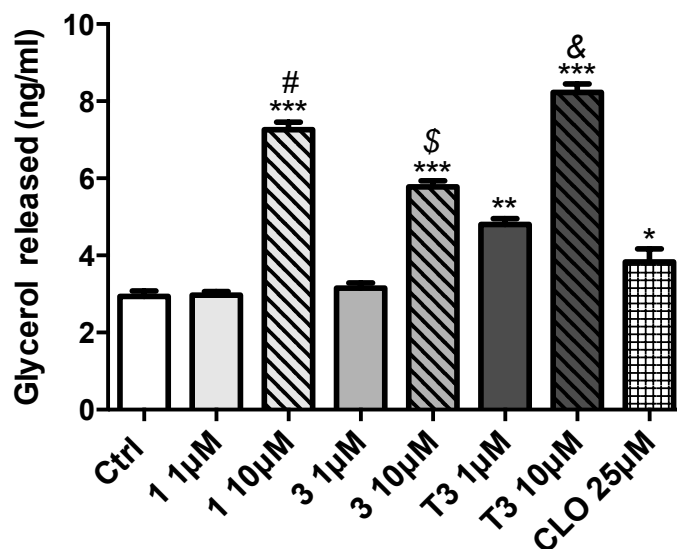


**Figure 7.** Thyromimetic-derivatives **1** and **3** induce lipolysis in HepG2 cells. Glycerol released in the culture medium (0.5 ml) of HepG2 cells after 24 h treatment with **1**, **3** and **T3** at 1 and 10  $\mu$ M. 25  $\mu$ M Cloroquine (CLO) was used as positive control. Values represent the mean  $\pm$  SEM of 4 to 8 experiments. The groups were compared using the One-Way ANOVA followed by Tukey's range test. \* $p < 0.05$  vs. Ctrl; \*\* $p < 0.01$  vs. Ctrl; \*\*\* $p < 0.005$  vs. Ctrl; # $p < 0.005$  vs. compound **1** 1  $\mu$ M; \$ $p < 0.01$  vs. compound **3** 1  $\mu$ M; & $p < 0.01$  vs. **T3** 1  $\mu$ M.

Oil Red O staining revealed that the newly designed compound **3** reduced total lipid accumulation into lipid droplets with a potency comparable or even higher than equimolar doses of **T3** (Figure 6). This result also shows that compound **1** exerts the same effect of **3** in reducing lipid accumulation, whereas the increase in glycerol released levels seems to be more efficient when compared with **3**. This result let us to speculate that thyromimetic derivative **1** is a pro-drug which possesses improved drug-like properties when compared to **3** (zwitterionic molecule) and this contributes to increase the bioavailability of the molecule inside the hepatocytes. Further pharmacokinetic investigations need to be carried out in the near future to confirm our hypothesis.

### Effects on AMPK/ACC pathway

Thyroid hormone mediates lipogenesis, fatty acid  $\beta$ -oxidation, cholesterol synthesis and the reverse cholesterol transport pathway through different mechanisms such as (a) the induction of genes transcription involved in metabolism as well as (b) the activation of alternative cellular pathways

implicated in the direct catabolism of fatty acids, such as autophagy [30, 31]. Hepatic autophagy regulates lipid metabolism through elimination of triglyceride accumulation in liver and prevents the development of steatosis [30, 32]. The 5' AMP-activated protein kinase (AMPK) is a serine/threonine protein kinase which plays a central role in regulating cellular metabolism and energy balance in mammalian cells [33]. Once activated, AMPK triggers several pathways such as glycolysis, fatty acid oxidation, and lipolysis. The overall effect on lipid metabolism is stimulation of fatty acid oxidation (FAO) and inhibition of cholesterol and triglycerides synthesis [34]. Since AMPK is a regulator of autophagy [35, 36], we investigated AMPK as a possible target of thyromimetic analogues **1** and **3**. In particular, we examined the protein levels of phosphorylated AMPK (p-AMPK), and its target phosphorylated acetyl-CoA carboxylase (p-ACC), a rate-limiting enzyme in cholesterol and fatty acid biosynthesis. As shown in Figure 8, both compounds, when tested at the higher concentration (i.e. 10  $\mu$ M), induced a significant enhancement of p-AMPK/AMPK and p-ACC/ACC ratios. Consistently, the effect induced by thyromimetic analogue **1** in the p-ACC/ACC ratio was more pronounced than that observed with the thyroid hormone T3.

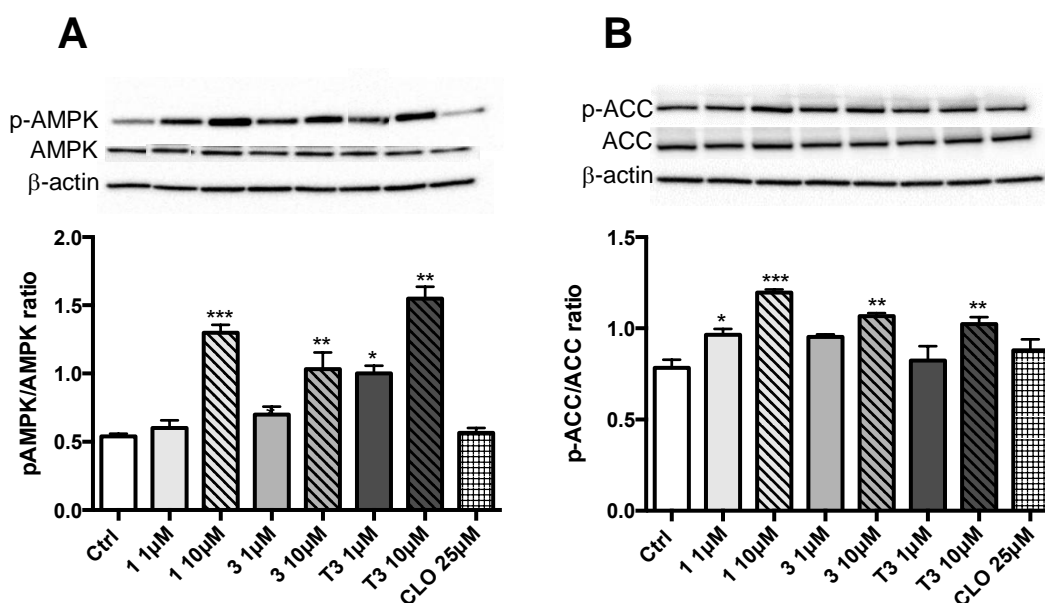


**Figure 8.** Derivatives **1** and **3** regulate metabolism in HepG2 cells via AMPK/ACC pathway. (A) Representative immunoblotting images and quantitative analysis of AMPK phosphorylation. (B) Representative immunoblotting images and quantitative analysis of ACC phosphorylation. \*  $p < 0.05$  vs. Ctrl; \*\*  $p < 0.01$  vs. Ctrl; \*\*\*  $p < 0.005$  vs. Ctrl.

### Lack of hepatic toxicity and cardiac hypertrophy in thyromimetics-treated rats

Our in vitro results showed that compound **3** and its pro-drug **1** efficiently reduced lipid accumulation, suggesting their potential therapeutic use in pathological conditions, such as NAFLD.

To assess their effect in vivo we treated F344 male rats for 3 days with daily intragastric (IG) administrations of **1** or **3** (50, 75 and 100 µg/100g b.w.). Two additional groups treated with the vehicle or with T3 (20 µg/100g b.w.) were included. As shown in Figure 9A, despite the brief exposure, T3 caused a significant increase of heart weight, as well as of the heart/body weight ratio. No such effect was found in the heart of animals treated with **1** or **3** at all doses used (Figure 9A), showing that the preferential binding to - and activation of - TRβ does not result in cardiac hypertrophy. As to the liver, while T3 treatment caused a significant reduction of the liver weight/body weight ratio, neither **1** nor **3** caused change in liver weight. Similar results were obtained when the two thyromimetics were administered at the dose of 75 µg/100 g b.w. intraperitoneally for 3 days (Figure 9B). Notably, no change in the serum levels of markers of liver injury, such as transaminases or bilirubin was observed following administration of the two thyromimetics. Interestingly, the two novel drugs did not exhibit any significant effect on serum levels of cholesterol and glucose, whereas compound **1** induces a significant reduction of triglycerides when compared to controls and to T3 (Table 2).

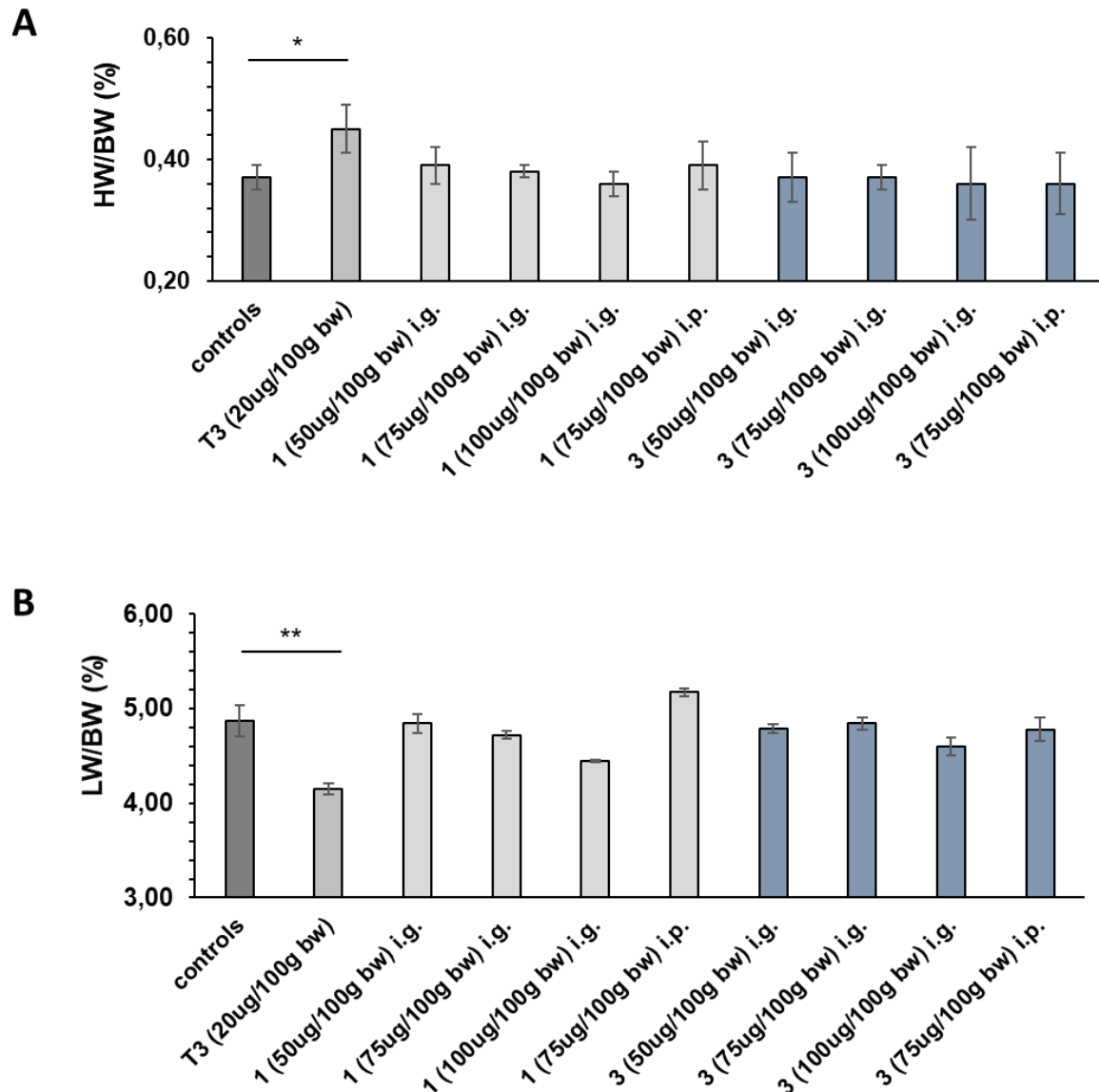


**Figure 9.** Effect of T3, **1** and **3** on liver/body weight ratio. F344 male rats were treated for 3 days with daily intragastric (IG) injections of **1** or **3** (50, 75 and 100 µg/100 g b.w.) or T3 (20 µg/100 g b.w.). A control group received the vehicle (DMSO 5% in corn oil). Additional two groups received daily injections of either **1** or **3** at the dose of 75 ug/100 g b.w. intraperitoneally for 3 days. \*\*P<0.01.

Treatment	AST/GOT (U/L)	ALT/GPT (U/L)	Bilirubin (mg/dl)	Glucose (mg/dl)	Cholesterol (mg/dl)	TGs (mg/dl)
Controls	153 ± 11	46 ± 4	1.4 ± 0.2	151 ± 13.5	67.2 ± 2.5	86.8 ± 10.4
T3	159 ± 11	53 ± 4.1	1.4 ± 0.3	139 ± 4.4	65.2 ± 7.1	90.2 ± 9.3
<b>1</b> i.g. (50 ug/100 g)	141 ± 11	46 ± 3.1	1.1 ± 0.3	129 ± 14	68.0 ± 5.2	70.4 ± 7.6
<b>1</b> i.g. (75 ug/100 g)	133 ± 8	46 ± 1.7	0.9 ± 0.1	132 ± 7.6	71.4 ± 6.6	67.0 ± 12.0
<b>1</b> i.g. (100 ug/100 g)	108 ± 7	37 ± 2.5	1.1 ± 0.2	164 ± 12	67.6 ± 8.1	62.8 ± 6.1*
<b>3</b> i.g. (50 ug/100 g)	134 ± 6	41 ± 2.1	1.3 ± 0.3	136 ± 6	69.5 ± 9.4	68.3 ± 9.1
<b>3</b> i.g. (75 ug/100 g)	119 ± 6	43 ± 3.3	1.6 ± 0.2	153 ± 18	68.6 ± 5.6	74.0 ± 12.8
<b>3</b> i.g. (100 ug/100 g)	102 ± 5	42 ± 4.6	1.0 ± 0.2	166 ± 5.1	70.2 ± 7.0	67.8 ± 12.5
<b>1</b> i.p. (75 ug/100 g)	134 ± 10	38 ± 2.9	1.5 ± 0.4	132 ± 14	71.4 ± 3.1	74.2 ± 9.0
<b>3</b> i.p. (75 ug/100 g)	123 ± 10	36 ± 1.7	1.1 ± 0.2	129 ± 9	69.6 ± 1.2	79.6 ± 9.7

Values are expressed as means ± S.D. of 3 to 4 animals per group. \*Significantly different from Controls for at least;  $p < 0.05$ .

**Table 2.** Effect of thyromimetics **1** and **3** and **T3** on rat Serum Levels of AST/GOT, ALT/GPT, Bilirubin, Cholesterol and Triglycerides (TGs) after the treatment with **1** or **3** (i.g., 50, 75 and 100  $\mu\text{g}/100\text{ g b.w.}$ ; or i.p. 75  $\mu\text{g}/100\text{ g b.w.}$ ) or T3 (20  $\mu\text{g}/100\text{ g b.w.}$ ) for 3 days.

## CONCLUSION

Compound **3** and its pro-drug **1** showed encouraging off-target and ADME-Tox profile that prompted us to explore them as TR $\beta$  selective thyromimetics. The biochemical-based nuclear receptor assay allowed us to consider compound **3** as a potential TR $\beta$  selective agonist able to influence lipid metabolism and fat oxidation in hepatocytes. Indeed, our in vitro assays showed that both compound **3** and its pro-drug (**1**) were able to reduce lipid accumulation in HepG2 and promote lipolysis with comparable effects to those elicited by T3, used as reference drug. These results were associated with a safe off-target and ADME-Tox profile. Importantly, in vivo studies confirmed the apparent lack of toxicity of our thyromimetics. Indeed, no liver injury, as assayed by serum levels of ALT, AST and bilirubin and no cardiac hypertrophy, a critical side effect of T3, could be observed in thyromimetic-treated rats. Interestingly, we found a significant decrease in blood triglyceride content following administration of both TR $\beta$  agonists, suggesting their possible effect on lipid metabolism. Future in vivo studies will be needed to investigate the effect of both compounds in experimental models of NAFLD in order to validate them as new tools to treat

hepatic diseases and to confirm that **1** is an efficient pro-drug of TR $\beta$  selective agonist **3**, with higher affinity toward the liver.

## EXPERIMENTAL SECTION

### Chemistry

**General Material and Methods.** Melting points were determined on a Kofler hot-stage apparatus and are uncorrected. Chemical shifts ( $\delta$ ) are reported in parts per million downfield from tetramethylsilane and referenced from solvent references; coupling constants  $J$  are reported in hertz.  $^1\text{H-NMR}$ ,  $^{13}\text{C-NMR}$  and  $^{19}\text{F-NMR}$  spectra were obtained with a Bruker TopSpin 3.2 400 MHz spectrometer and were recorded at 400, 101 and 376 MHz, respectively.  $^{19}\text{F}$  and  $^{13}\text{C}$  NMR spectra are  $^1\text{H}$  decoupled.  $^{19}\text{F}$  NMR spectra are unreferenced, corrected from Trifluoroacetic Acid (TFA) as external standard (-76.2 ppm). Signal spectra were fully decoupled. The following abbreviations are used: singlet (s), doublet (d), triplet (t), double-doublet (dd), and multiplet (m). The elemental compositions of the compounds agreed to within  $\pm 0.4$  % of the calculated values. Chromatographic separation was performed on silica gel columns by flash (Kieselgel 40, 0.040–0.063 mm; Merck) or gravity column (Kieselgel 60, 0.063–0.200 mm; Merck) chromatography. The  $\geq 95$  % purity of the tested compounds was confirmed by combustion analysis. Reactions were followed by thin-layer chromatography (TLC) on Merck aluminum silica gel (60 F254) sheets that were visualized under a UV lamp. The microwave-assisted procedures were carried out with a Biotage Initiator+ microwave. Evaporation was performed in vacuo (rotating evaporator). Sodium sulfate was always used as the drying agent. Commercially available chemicals were purchased from Sigma-Aldrich or Fluorochem.

**Synthesis of 2-(4-(4-acetamido-3-isopropylbenzyl)-3,5-dimethylphenoxy)acetic acid (**1**).** A solution of phenolic derivative **19** (0.29 mmol) in DMF was treated with  $\text{Cs}_2\text{CO}_3$  (473 mg; 1.45 mmol) and  $\text{BrCH}_2\text{COOH}$  (0.29 mmol). The mixture obtained was stirred for 1 h at rt and then, quenched with water. After extraction with DCM, aqueous phase was acidified with HCl 10% and extracted again with DCM. Organic phases were then collected, dried, filtered and concentrated to obtain a crude which was washed in hexane, providing final compound **1**. Yield: 82 % (white powder).  $^1\text{H-NMR}$  ( $\text{CD}_3\text{OD-d}_4$ ):  $\delta$  1.12 (d, 6H,  $J = 6.8$  Hz,  $\text{CH}_3$ ); 2.12 (s, 3H,  $\text{CH}_3\text{CO}$ ); 2.18 (s, 6H,  $\text{CH}_3$ ); 3.05–3.08 (m, 1H, CH); 3.98 (s, 2H,  $\text{CH}_2$ ); 4.35 (s, 2H,  $\text{CH}_2$ ); 6.67 (s, 2H, Ar); 6.76 (dd, 1H,  $J = 2.0, 8.0$  Hz, Ar); 7.00–7.08 (m, 2H, Ar) ppm.  $^{13}\text{C-NMR}$  ( $\text{CD}_3\text{OD-d}_4$ ):  $\delta$  180.44 (COOH); 172.91 ( $\text{CH}_3\text{CO}$ ); [158.17, 145.59, 140.71, 139.23, 132.96, 130.42, 128.55, 126.41, 126.32, 115.34] Ar;

68.49 (OCH<sub>2</sub>); 34.84 (CH<sub>2</sub>); 29.06 (CH); 24.18 (CHCH<sub>3</sub>); 23.70 (CH<sub>3</sub>); 22.81 (CH<sub>3</sub>CO); 20.52 (CH<sub>3</sub>) ppm. Anal. Calcd for C<sub>22</sub>H<sub>27</sub>NO<sub>4</sub>: C, 71.52 %; H, 7.37 %; N, 3.79 %. Found: C, 71.41 %; H, 7.42 %; N, 3.59 %.

**Synthesis of 2-(4-(4-acetamido-3-isopropylbenzyl)phenoxy)acetic acid (2).** The crude product was obtained following the same synthetic procedure reported for compound **1**. The crude was purified by suspension in hexane. Yield: 64 % (grey powder). <sup>1</sup>H NMR (CD<sub>3</sub>OD): δ 1.64 (d, 6H, *J* = 6.8 Hz, CH<sub>3</sub>); 2.13 (s, 3H, CH<sub>3</sub>CO); 3.08 (m, 1H, *J* = 6.8 Hz, CH); 3.89 (s, 2H, CH<sub>2</sub>); 4.61 (s, 2H, CH<sub>2</sub>COOH); 6.83 (d, 2H, *J* = 8.4 Hz, Ar); 6.98 (dd, 1H, *J* = 2.0, 8.0 Hz, Ar); 7.08 (d, 1H, *J* = 8 Hz, Ar); 7.12 (d, 2H, *J* = 8.4 Hz, Ar); 7.17 (d, 1H, *J* = 2 Hz, Ar) ppm. <sup>13</sup>C NMR (CD<sub>3</sub>OD): δ 172.81 (COOH); 172.71 (COCH<sub>3</sub>); [157.74, 145.62, 142.06, 135.55, 133.10, 130.74, 128.54, 127.48, 127.16, 115.51] Ar; 65.88 (CH<sub>2</sub>COOH); 41.56 (CH<sub>2</sub>); 29.02 (CH); 23.59 (CH<sub>3</sub>); 22.67 (CH<sub>3</sub>CO) ppm. Anal. Calcd for C<sub>20</sub>H<sub>23</sub>NO<sub>4</sub>: C, 70.36 %; H, 6.79 %; N, 4.10 %. Found: C, 70.43 %; H, 6.69 %; N, 4.21 %.

**Synthesis of 2-(4-(4-amino-3-isopropylbenzyl)-3,5-dimethylphenoxy)acetic acid (3).** Compound **1** (103 mg, 0.279 mmol) and HCl conc. (8 mL) were mixed with 2 mL of water and refluxed at 120 °C for 4 h. Upon cooling a solid was formed, mainly constituted by compound **3**. Crude obtained was washed in HCl 10 % and hexane under vigorous stirring. Yield: 52 % (grey powder). <sup>1</sup>H-NMR (CD<sub>3</sub>OD-d<sub>4</sub>): δ 1.15 (d, *J* = 6.8 Hz, 6H, CH<sub>3</sub>); 2.19 (s, 6H, CH<sub>3</sub>); 2.92–2.99 (m, 1H, CH); 3.87 (s, 2H, CH<sub>2</sub>); 4.67 (s, 2H, OCH<sub>2</sub>); 6.52 (dd, 1H, *J* = 1.8, 8.0 Hz, Ar); 6.61 (d, 1H, *J* = 8.0 Hz, Ar); 6.62 (s, 2H, Ar); 6.79 (d, 1H, *J* = 1.8 Hz, Ar) ppm. <sup>13</sup>C NMR (CD<sub>3</sub>OD-d<sub>4</sub>): δ 171.77, 157.28, 142.51, 139.50, 134.79, 132.24, 131.59, 126.44, 125.77, 117.72, 115.03, 66.02, 52.53, 34.52, 28.32, 23.05, 20.52 ppm. Anal. Calcd for C<sub>20</sub>H<sub>25</sub>NO<sub>3</sub>: C, 73.37 %; H, 7.70 %; N, 4.28 %. Found: C, 73.52 %; H, 7.68 %; N, 4.19 %.

**Synthesis of 2-(4-(4-amino-3-isopropylbenzyl)phenoxy)acetic acid (4).** The crude product was obtained following the same synthetic procedure reported for compound **3** and purified by resuspension in hexane. Yield: 96 % (grey powder). <sup>1</sup>H NMR (CD<sub>3</sub>OD-d<sub>4</sub>): δ 1.26 (d, 6H, *J* = 6.8 Hz, CH<sub>3</sub>); 3.04 (m, 1H, *J* = 6.8 Hz, CH); 3.94 (s, 2H, CH<sub>2</sub>); 4.62 (s, 2H, CH<sub>2</sub>COOH); 6.86 (d, 2H, *J* = 8.4 Hz, Ar); 7.12 (d, 3H, *J* = 8.8 Hz, Ar); 7.25 (d, 1H, *J* = 2.0, 8.0 Hz, Ar); 7.34 (s, 1H, Ar); 7.91 (s, 1H, COOH) ppm. <sup>13</sup>C NMR (CD<sub>3</sub>OD-d<sub>4</sub>): δ 171.44 (COOH); (157.82, 144.57, 143.37, 135.01, 130.83, 128.63, 128.60, 124.20, 115.67) Ar; 66.03 (CH<sub>2</sub>COOH); 41.29 (CH<sub>2</sub>); 28.64 (CH); 23.79 (CH<sub>3</sub>) ppm. Anal. Calcd for C<sub>18</sub>H<sub>21</sub>NO<sub>3</sub>: C, 72.22 %; H, 7.07 %; N, 4.68 %. Found: C, 72.27 %; H, 7.12 %; N, 4.39 %.

**General procedure for synthesis of compounds 5, 6 and 8.** Under nitrogen atmosphere,  $\text{AlCl}_3$  (1.35 mmol) was added to a solution of  $\text{LiAlH}_4$  (1.35 mmol) in THF. The mixture was stirred at rt for 5 min; then, a solution of the proper cyanoderivative **22**, **23** or **31** (0.15 mmol) in THF was added dropwise, and the mixture refluxed for 12 h. After cooling at 0 °C, the mixture was diluted with water, acidified with HCl 10 % and washed with  $\text{Et}_2\text{O}$ . Aqueous phase was alkalized with NaOH 1N and extracted with chloroform; then, organic phase was filtered through celite, washed with brine, dried over  $\text{Na}_2\text{SO}_4$  and concentrated.

**Synthesis of 4-(4-(2-aminoethoxy)-2,6-dimethylbenzyl)-N-ethyl-2-isopropylaniline (5).** The crude product was transformed in the corresponding hydrochloride salt. Yield: 15 % (grey powder)  $^1\text{H-NMR}$  ( $\text{CD}_3\text{OD-d}_4$ ):  $\delta$  1.23 (d, 6H,  $J = 6.8$  Hz,  $\text{CH}_3$ ); 1.36 (t, 3H,  $J = 7.4$  Hz,  $\text{CH}_2$ ); 2.20 (s, 6H,  $\text{CH}_3$ ); 3.02-3.06 (m, 1H, CH); 3.36-3.40 (m, 4H,  $\text{CH}_2\text{NH}_2$ ,  $\text{CH}_2$ ); 4.07 (s, 2H,  $\text{CH}_2$ ); 4.22 (t,  $J = 4.8$  Hz, 2H,  $\text{OCH}_2$ ); 6.77 (s, 2H, Ar); 6.97 (dd, 1H,  $J = 1.4, 8.0$  Hz, Ar); 7.21 (d, 1H,  $J = 1.4$  Hz, Ar); 7.27 (d, 1H,  $J = 8.0$  Hz, Ar) ppm.  $^{13}\text{C NMR}$  ( $\text{CD}_3\text{OD-d}_4$ ):  $\delta$  157.89, 144.36, 143.49, 139.71, 130.74, 130.50, 128.61, 127.99, 124.54, 115.19, 65.06, 40.42, 34.67, 28.66, 24.46, 20.43, 20.36, 11.36 ppm. Anal. Calcd for  $\text{C}_{22}\text{H}_{33}\text{ClN}_2\text{O}$ : C, 70.10 %; H, 8.82 %; N, 7.43 %; Found: C, 70.24 %; H, 8.75 %; N, 7.56 %.

**Synthesis of 4-(4-(2-aminoethoxy)-2-(trifluoromethyl)benzyl)-N-ethyl-2-isopropylaniline (6).** The crude was purified by transformation in hydrochloric salt and subsequent re-crystallization in isopropanol/diisopropyl ether. Yield: 17 % (yellow oil).  $^1\text{H-NMR}$  ( $\text{CD}_3\text{OD-d}_4$ ):  $\delta$  1.27 (d,  $J = 6.4$  Hz, 6H,  $\text{CH}_3$ ); 1.36 (t,  $J = 7.4$  Hz, 3H,  $\text{CH}_3$ ); 3.03–3.04 (m, 1H, CH); 3.38–3.41 (m, 4H,  $\text{CH}_2\text{NH}_2$ ,  $\text{CH}_2$ ); 4.19 (s, 2H,  $\text{CH}_2$ ); 4.29 (t, 2H,  $J = 8.0$  Hz,  $\text{CH}_2\text{O}$ ); 7.11 (dd,  $J = 2.0, 8.4$  Hz, 1H, Ar); 7.23 (dd, 2H,  $J = 2.4, 8.4$  Hz, 1H, Ar); 7.28-7.37 (m, 4H, Ar) ppm.  $^{13}\text{C-NMR}$  ( $\text{CD}_3\text{OD-d}_4$ ):  $\delta$  158.10, 143.52, 135.03, 134.77, 132.28, 131.02, 130.72, 129.55, 128.94, 124.40, 124.19, 119.09, 113.96, 65.76, 40.20, 37.67, 28.74, 24.41, 17.28, 11.42 ppm. Anal. Calcd for  $\text{C}_{21}\text{H}_{28}\text{ClF}_3\text{N}_2\text{O}$ : C, 60.50 %; H, 6.77 %; N, 6.72 %; Found: C, 60.51 %; H, 6.72 %; N, 6.71 %.

**Synthesis of 4-(4-(2-aminoethoxy)-2,6-dimethylbenzyl)phenol (7).** Aniline derivative **34** (0.17 mmol, 48 mg) was solubilized in water and treated with  $\text{H}_2\text{SO}_4$  (0.05 mL). The mixture obtained was stirred for 20 min at 0 °C. Then, a solution of  $\text{NaNO}_2$  (0.17 mmol; 12 mg) in  $\text{H}_2\text{O}$  was added and the reaction refluxed for 1 h. After this time, reaction mixture was cooled at RT and diluted with AcOEt. Organic phase was then washed with a saturated solution of NaCl, dried, filtered and concentrated. The crude obtained was purified by precipitation in MeOH/ $\text{Et}_2\text{O}$ . Yield 42% (dark yellow powder).  $^1\text{H-NMR}$  ( $\text{CD}_3\text{OD-d}_6$ ):  $\delta$  2.19 (s, 6H,  $\text{CH}_3$ ); 3.09 (t,  $J = 5.0$  Hz; 2H,  $\text{CH}_2\text{NH}_2$ ); 3.88 (s, 2H,  $\text{CH}_2$ ); 3.99 (t,  $J = 5.0$  Hz; 2H,  $\text{OCH}_2$ ); 6.61 (s, 2H, Ar); 6.69 (d,  $J = 8.6$ , 2H, Ar); 6.83 (d,  $J =$



8.6, 2H, Ar) ppm.  $^{13}\text{C}$ -NMR ( $\text{CD}_3\text{OD-d}_6$ ):  $\delta$  158.24, 156.33, 139.34, 132.20, 131.26, 129.62, 116.09, 115.11, 69.76, 41.84, 34.21, 20.54 ppm. Anal. Calcd for  $\text{C}_{17}\text{H}_{21}\text{NO}_2$ : C, 75.25 %; H, 7.80 %; N, 5.16 %; Found: C, 75.19 %; H, 7.66 %; N, 4.88 %.

**Synthesis of 4-(4-(2-aminoethoxy)-2-(trifluoromethyl)benzyl)aniline (8).** The crude product was transformed in the corresponding hydrochloride salt. Yield: 10 % (yellow oil).  $^1\text{H}$ -NMR ( $\text{CD}_3\text{OD-d}_4$ ):  $\delta$  3.39 (t,  $J=4.8$  Hz, 2H,  $\text{CH}_2\text{NH}_2$ ); 4.19 (s, 2H,  $\text{CH}_2$ ); 4.29 (t,  $J = 4.8$  Hz, 2H,  $\text{CH}_2$ ); 7.23 (dd,  $J = 2.4, 8.4$  Hz, 1H Ar); 7.27–7.35 (m, 6H Ar) ppm.  $^{13}\text{C}$ -NMR ( $\text{CD}_3\text{OD-d}_4$ ):  $\delta$  158.09, 143.25, 135.05, 132.29, 131.44, 130.89, 130.10, 126.97, 124.13, 119.10, 113.98, 65.78, 40.21, 37.53 ppm. Anal. Calcd for  $\text{C}_{16}\text{H}_{17}\text{F}_3\text{N}_2\text{O}$ : C, 61.93 %; H, 5.52 %; N, 9.03 %; Found: C, 62.07 %; H, 5.42 %; N, 9.26 %.

**Synthesis of 2-(4-(4-aminobenzyl)-3-fluorophenoxy)acetic acid (9).** A solution of derivative **35** (28 mg, 0.109 mmol) in  $\text{H}_2\text{O}$  was acidified with HCl 37 % and refluxed at 100 °C for 4 h. Then the mixture was concentrated affording the crude **9**, which was purified by formation of the corresponding hydrochloride salt. Yield: 77 % (grey powder).  $^1\text{H}$  NMR ( $\text{CD}_3\text{OD-d}_4$ ):  $\delta$  3.98 (s, 2H,  $\text{CH}_2$ ); 4.66 (s, 2H,  $\text{CH}_2\text{COOH}$ ); 6.69-6.74 (m, 2H, Ar); 7.15 (d, 1H,  $J=8.4$  Hz, Ar); 7.31-7.37 (m, 4H, Ar) ppm.  $^{13}\text{C}$  NMR ( $\text{CD}_3\text{OD-d}_4$ ):  $\delta$  172.21(COOH); [161.28, 159.50, 143.21, 132.57, 131.21, 129.81, 124.10, 121.30, 111.53, 103.49] Ar; 66.03 ( $\text{CH}_2\text{COOH}$ ); 34.51 ( $\text{CH}_2$ ) ppm. Anal. Calcd for  $\text{C}_{15}\text{H}_{14}\text{FNO}_3$ : C, 65.45 %; H, 5.13 %; N, 5.09 %; Found: C, 65.27 %; H, 5.18 %; N, 5.21 %.

**Synthesis of 2-(4-(4-aminobenzyl)-3,5-dimethylphenoxy)acetic acid (10).** Ester **36** (0.12 mmol; 39 mg) solubilized in MeOH was treated with an aqueous solution of NaOH 10% (0.02 mL). Mixture was then refluxed for 1h and then, concentrated in vacuo. The crude obtained was purified by precipitation in MeOH/ $\text{Et}_2\text{O}$  providing compound **10**. Yield: 42 % (pale yellow).  $^1\text{H}$ -NMR ( $\text{CD}_3\text{OD-d}_4$ ):  $\delta$  2.17 (s, 6H,  $\text{CH}_3$ ); 3.85 (s, 2H,  $\text{CH}_2$ ); 4.34 (s, 2H,  $\text{CH}_2\text{COOH}$ ); 6.61 (d, 2H,  $J = 8.4$  Hz, Ar); 6.65 (s, 2H, Ar); 6.72 (d, 2H,  $J = 8.4$  Hz, Ar) ppm.  $^{13}\text{C}$ -NMR ( $\text{CD}_3\text{OD-d}_4$ ):  $\delta$  177.01, 157.94, 146.00, 139.15, 131.39, 131.25, 129.36, 117.00, 115.25, 68.47, 34.27, 20.54 ppm. Anal. Calcd for  $\text{C}_{17}\text{H}_{19}\text{NO}_3$ : C, 71.56 %; H, 6.71 %; N, 4.91 %; Found: C, 71.38 %; H, 6.92 %; N, 5.07 %.

**Synthesis of 2-(4-(4-hydroxybenzyl)-3,5-dimethylphenoxy)acetic acid (11).** Aniline **10** (0.20 mmol; 64 mg) was dissolved in  $\text{H}_2\text{O}$ , added to a solution of  $\text{H}_2\text{SO}_4$  at concentrated grade (0.05 mL), and left under stirring at 0 °C for 20 min. Then, a solution of  $\text{NaNO}_2$  (0.20 mmol; 14 mg) in  $\text{H}_2\text{O}$  was added, and the mixture was refluxed for 1 h. After this time, the reaction was allowed to cold down to rt and then diluted with AcOEt. Organic phase was washed with a saturated solution of

NaCl, then dried, filtered and evaporated. The crude product was purified by precipitation in AcOEt/Hexane. Yield: 35 % (brown powder). <sup>1</sup>H-NMR (CD<sub>3</sub>OD-d<sub>4</sub>): δ 2.17 (s, 6H, CH<sub>3</sub>); 3.87 (s, 2H, CH<sub>2</sub>); 4.59 (s, 2H, CH<sub>2</sub>COOH); 6.60–6.67 (m, 4H, Ar); 6.77 (d, 2H, *J* = 8.4 Hz, Ar) ppm. <sup>13</sup>C-NMR (CD<sub>3</sub>OD-d<sub>4</sub>): δ 173.18, 157.42, 156.32, 139.45, 132.10, 131.86, 129.64, 116.09, 115.12, 65.94, 34.21, 20.53 ppm. Anal. Calcd for C<sub>17</sub>H<sub>18</sub>O<sub>4</sub>: C, 71.31 %; H, 6.34 %. Found: C, 71.46 %; H, 6.47 %.

**X-ray selection.** To date, many X-ray structures of TR $\alpha$  and TR $\beta$  in complex with T3, GC-1, KB131084 and other thyromimetics, are available in the Protein Data Bank (PDB). A superposition on the  $\alpha$ -carbon atoms of all these structures, showed that the general protein folding is highly preserved, with a good conservation of both the secondary structure and the side chain orientation, especially within the LBC. Thus, among the crystals with highest resolution, those co-crystallized with our ligands progenitor GC-1 were chosen for our docking calculations: PDB codes 3ILZ and 3IMY, for TR $\alpha$  and TR $\beta$ , respectively.

**Docking calculations** The ligands tridimensional structure were generated with the Maestro Build Panel and prepared using Ligprep predicting all tautomeric and protonation states at physiological pH (7.4  $\pm$  1.5). The receptor structures were prepared using the Protein Preparation Wizard implemented in Maestro Suite (Schrödinger Release 2019-2: Schrödinger Suite 2019-1), deleting all water molecules with the exception of those within 3 Å from the ligand, adding missing hydrogen atoms and minimizing the complexes. The docking grid was calculated through the grid generation tool in Glide 6.7 [37-39] and centered around the crystallized ligand using default settings. The OPLS3E force field was employed for docking. The results of calculations were evaluated and ranked based on the Glide SP scoring function.

## **In vitro studies**

**Activity against thyroid hormone receptors.** Assays on selected compounds were performed by SelectScreen™ Biochemical Nuclear Receptor Profiling Service (ThermoFisher Scientific, US) using the LanthaScreen™ TR-FRET Nuclear Receptor Coregulator Assay (service provided by Invitrogen Corporation, USA), as reported on the company's website. (<https://www.thermofisher.com/it/en/home/products-and-services/services/custom-services/screening-and-profiling-services/selectscreen-profiling-service/selectscreen-cell-based-nuclear-receptor-profiling-services.html>).

### **Human hepatocellular carcinoma (HepG2) cell culture and treatment with compounds 1 and 3.**

The human hepatocellular carcinoma HepG2 cells line was purchased from the American Type Culture Collection (ATCC HB-8065, Rockville, MD, USA) and cultured in low glucose (LG) DMEM supplemented with 10 % FBS, 100 IU/mL penicillin G sodium and 100 µg/mL streptomycin sulfate (Invitrogen, Paisley, UK) incubating in a humidified atmosphere with 5 % CO<sub>2</sub> at 37 °C. These cells were then treated with 1 and 10 µM concentrations of test compounds for 24 h. After treatments, cells were lysed in a buffer containing 20 mM Tris-HCl (pH 7.5), 0.9 % NaCl, 0.2 % Triton X-100, and 1 % of the protease inhibitor cocktail (Sigma-Aldrich, Milan, Italy) and then stored at -80 °C for further western blot analysis. All the analyses were conducted on cells between the third and the sixth passage.

**Oil red O (ORO) staining of lipid accumulation in HepG2 cells.** Total lipid accumulation was evaluated according to the method previously described by Liu et al. [40] Cells were seeded at a density of  $3.5 \times 10^4$  cells/well in 1 mL of lipogenic growth medium (HG-DMEM) and treated for 24 h with compound **1** or **3**, at 1 and 10 µM. Cloroquine (25 µM) was used as positive control. Subsequently, after collecting the growth media to be used to perform glycerol level measurements (as detailed below), cells were rinsed twice with PBS and fixed in 4 % paraformaldehyde in PBS at 4 °C for 30 min. After 3 washes with cold PBS, cells were stained with ORO working solution, prepared as described above, for 30 min at room temperature and subsequently rinsed again with PBS.

**Determination of glycerol release from HepG2 cells.** After treatment with test compounds, cell culture supernatants were collected from each well and placed in glycerol-free containers. A 125µg/mL Glycerol Standard Solution (Abcam, Milan, Italy) was used to make a #1 through #8 standard curve. 25 µL of each supernatant and standard were then transferred into a 96-well plate and 100µL of either Free Glycerol Assay Reagent (Abcam, Milan, Italy) or MilliQ water added to each well. After incubation at rt for 15 min, glycerol levels were measured by reading absorbance at 540 nm (Bio-Rad 680, Milan, Italy).

**Western Blotting Analysis.** Proteins (20–30 µg) were separated on CriterionTGX™ gel (4–20 %) and transferred on Immuno-PVDF membrane (Biorad, Milan, Italy) for 30 min. The membranes were then incubated overnight at 4 °C with one of the following the specific primary antibodies: anti-p-AMPKα1-thr172, anti-AMPK, anti-p-ACC-ser79, anti-ACC (Cell Signaling Technology, Danvers, MA, USA). Then, blots were washed 3 times for 10 min with 1X TBS, 0.1 % Tween®20 and incubated for 2 h with secondary antibody (peroxidase-coupled anti rabbit in 1X TBS, 0.1 % Tween®20). After washing 3 times for 10 min, the reactive signals were revealed by an enhanced

ECL Western Blotting analysis system (Amersham, Milan, Italy). Band densitometric analysis was performed using Image Lab Software (Biorad, Milan, Italy).

**In vivo Studies.** Five-week-old male F-344 rats purchased from Charles River (Milano, Italy) were maintained on a standard laboratory diet (Ditta Mucedola, Milano, Italy). The animals were given food and water ad libitum with a 12 h light/dark daily cycle and were acclimated for 1 week before the start of the experiment. All procedures were performed in accordance with the Guidelines for the Care and Use of Laboratory Animals and were approved by the Italian Ministry of Health. Animals were treated with daily intragastric (IG) injections for 3 days of **1** or **3** (50, 75 and 100  $\mu\text{g}/100$  g b.w) or T3 (20  $\mu\text{g}/100$  g b. wt). A control group received the vehicle (DMSO 5 % in corn oil). Additional two groups received daily injections of either **1** or **3** at the dose of 75  $\mu\text{g}/100$  g b. wt. intraperitoneally for 3 days

**Analysis of Serum Aspartate aminotransferase (AST), Alanine aminotransferase (ALT), Triglycerides (TGs) and Cholesterol (CH).** Immediately after sacrifice, blood samples were collected from the abdominal aorta, serum was separated by centrifugation (2000 g for 20 minutes) and tested for triglycerides, cholesterol, aspartate aminotransferase and alanine aminotransferase using a commercially available kit from Boehringer (Mannheim, Germany).

**Statistical Analysis.** Statistical analyses were performed using GraphPad Prism version 6.0 for Windows (GraphPad Software, San Diego, CA, USA). Data were subjected to One-Way analysis of variance for mean comparison, and significant differences among different treatments were calculated according to Tukey's HSD (honest significant difference) multiple range test. Data are reported as mean  $\pm$  SEM. Differences at  $p < 0.05$  were considered statistically significant.

## ASSOCIATED CONTENT

The Supporting Information is available free of charge on the Elsevier website at DOI:

## AUTHOR INFORMATION

Corresponding Author: For S.R.: phone, +39 050 2219582; fax, +39 050 2219577; Email, [simona.rapposelli@unipi.it](mailto:simona.rapposelli@unipi.it). \*For G.C.: phone, +39 050 2218677; E-mail, [grazia.chiellini@unipi.it](mailto:grazia.chiellini@unipi.it).

### **Author Contributions:**

MR and SS carried out the synthesis. LB and GC carried out the experiments in HepG2 and adipocytes and analyzed the data. VLP, VMD and LM carried out the computational studies. AP, MAK and AC carried out the in vivo experiments and the data analysis. MR and SG carried out the off-target and ADME-Tox profiling assays and analyzed the data. SR and GC design and coordinate the project. All authors discussed the results and contributed to the final manuscript. MR, SR, AC and GC wrote the manuscript.

**Funding Sources:** This work was supported by grants from International Society of Drug Discovery (ISDD) (Milan), from the University of Pisa [Progetti di Ricerca di Ateneo PRA\_2017\_55 (to GC) and PRA\_2018\_20 (to SR)], from Associazione Italiana Ricerca sul Cancro (AIRC, IG-20176 to AC) and from Regione Autonoma Sardegna (RAS to AC).

**Notes:** The authors declare no conflict of interest

### **ACKNOWLEDGMENT**

We thank the COST action CA15135 (Multitarget Paradigm for Innovative Ligand Identification in the Drug Discovery Process MuTaLig) for support the working experience of MR at the Fraunhofer-IME SP (Hamburg, Germany). We also thank POR FSE 2014-2020 – Regione Toscana and the University of Pisa for financing the fellowship to SS and Fondazione Umberto Veronesi for financing to MAK the fellowship.

### **ABBREVIATIONS**

THs, thyroid hormones; TR $\alpha$ , thyroid hormone receptor  $\alpha$ ; TR $\beta$ , thyroid hormone receptor  $\beta$ ; NAFLD, non-alcoholic fatty-liver disease.

## References

- [1] P.M. Yen, Physiological and molecular basis of thyroid hormone action, *Physiological reviews*, 81 (2001) 1097-1142.
- [2] G.A. Brent, Mechanisms of thyroid hormone action, *The Journal of clinical investigation*, 122 (2012) 3035-3043.
- [3] R. Kapoor, S.E. Fanibunda, L.A. Desouza, S.K. Guha, V.A. Vaidya, Perspectives on thyroid hormone action in adult neurogenesis, *Journal of neurochemistry*, 133 (2015) 599-616.
- [4] E.G. Baxi, J.T. Schott, A.N. Fairchild, L.A. Kirby, R. Karani, P. Uapinyoying, C. Pardo-Villamizar, J.R. Rothstein, D.E. Bergles, P.A. Calabresi, A selective thyroid hormone  $\beta$  receptor agonist enhances human and rodent oligodendrocyte differentiation, *Glia*, 62 (2014) 1513-1529.
- [5] J.A. Vaitkus, J.S. Farrar, F.S. Celi, Thyroid Hormone Mediated Modulation of Energy Expenditure, *International journal of molecular sciences*, 16 (2015) 16158-16175.
- [6] I. Tancevski, P. Eller, J.R. Patsch, A. Ritsch, The resurgence of thyromimetics as lipid-modifying agents, *Current opinion in investigational drugs (London, England : 2000)*, 10 (2009) 912-918.
- [7] H. Gullberg, M. Rudling, C. Salto, D. Forrest, B. Angelin, B. Vennstrom, Requirement for thyroid hormone receptor beta in T3 regulation of cholesterol metabolism in mice, *Molecular endocrinology (Baltimore, Md.)*, 16 (2002) 1767-1777.
- [8] M.A. Kowalik, A. Columbano, A. Perra, Thyroid Hormones, Thyromimetics and Their Metabolites in the Treatment of Liver Disease, *Frontiers in endocrinology*, 9 (2018) 382-382.
- [9] G. Chiellini, J.W. Apriletti, H. Al Yoshihara, J.D. Baxter, R.C. Ribeiro, T.S. Scanlan, A high-affinity subtype-selective agonist ligand for the thyroid hormone receptor, *Chemistry & biology*, 5 (1998) 299-306.
- [10] M.D. Erion, E.E. Cable, B.R. Ito, H. Jiang, J.M. Fujitaki, P.D. Finn, B.H. Zhang, J. Hou, S.H. Boyer, P.D. van Poelje, D.L. Linemeyer, Targeting thyroid hormone receptor-beta agonists to the liver reduces cholesterol and triglycerides and improves the therapeutic index, *Proceedings of the National Academy of Sciences of the United States of America*, 104 (2007) 15490-15495.
- [11] A. Berkenstam, J. Kristensen, K. Mellstrom, B. Carlsson, J. Malm, S. Rehnmark, N. Garg, C.M. Andersson, M. Rudling, F. Sjoberg, B. Angelin, J.D. Baxter, The thyroid hormone mimetic compound KB2115 lowers plasma LDL cholesterol and stimulates bile acid synthesis without cardiac effects in humans, *Proceedings of the National Academy of Sciences of the United States of America*, 105 (2008) 663-667.
- [12] L. Johansson, M. Rudling, T.S. Scanlan, T. Lundåsen, P. Webb, J. Baxter, B. Angelin, P. Parini, Selective thyroid receptor modulation by GC-1 reduces serum lipids and stimulates steps of reverse cholesterol transport in euthyroid mice, *Proceedings of the National Academy of Sciences*, 102 (2005) 10297-10302.
- [13] I. Tancevski, M. Rudling, P. Eller, Thyromimetics: a journey from bench to bed-side, *Pharmacology & therapeutics*, 131 (2011) 33-39.
- [14] S. Meruvu, S.D. Ayers, G. Winnier, P. Webb, Thyroid hormone analogues: where do we stand in 2013?, *Thyroid*, 23 (2013) 1333-1344.
- [15] L.P. Elbers, J.J. Kastelein, B. Sjouke, Thyroid hormone mimetics: the past, current status and future challenges, *Current atherosclerosis reports*, 18 (2016) 14.
- [16] J. Zhou, L.R. Waskowicz, A. Lim, X.-H. Liao, B. Lian, H. Masamune, S. Refetoff, B. Tran, D.D. Koeberl, P.M. Yen, A Liver-Specific Thyromimetic, VK2809, Decreases Hepatosteatosis in Glycogen Storage Disease Type Ia, *Thyroid*, 29 (2019) 1158-1167.
- [17] G. Chiellini, G. Nesi, S. Sestito, S. Chiarugi, M. Runfola, S. Espinoza, M. Sabatini, L. Bellusci, A. Laurino, E. Cichero, Hit-to-lead optimization of mouse Trace Amine Associated Receptor 1 (mTAAR1) agonists with a diphenylmethane-scaffold: Design, Synthesis, and biological study, *Journal of Medicinal Chemistry*, 59 (2016) 9825-9836.

- [18] L. Bellusci, A. Laurino, M. Sabatini, S. Sestito, P. Lenzi, L. Raimondi, S. Rapposelli, F. Biagioni, F. Fornai, A. Salvetti, New insights into the potential roles of 3-iodothyronamine (TIAM) and newly developed thyronamine-like TAAR1 agonists in neuroprotection, *Frontiers in pharmacology*, 8 (2017) 905.
- [19] H.A. Yoshihara, J.W. Apriletti, J.D. Baxter, T.S. Scanlan, Structural determinants of selective thyromimetics, *Journal of medicinal chemistry*, 46 (2003) 3152-3161.
- [20] G. Chiellini, G. Nesi, M. Digiacomio, R. Malvasi, S. Espinoza, M. Sabatini, S. Frascarelli, A. Laurino, E. Cichero, M. Macchia, R.R. Gainetdinov, P. Fossa, L. Raimondi, R. Zucchi, S. Rapposelli, Design, Synthesis, and Evaluation of Thyronamine Analogues as Novel Potent Mouse Trace Amine Associated Receptor 1 (mTAAR1) Agonists, *Journal of Medicinal Chemistry*, 58 (2015) 5096-5107.
- [21] W.E. Evans, M.V. Relling, Pharmacogenomics: Translating Functional Genomics into Rational Therapeutics, *Science*, 286 (1999) 487.
- [22] I.L. Cote, S.D. McCullough, R.N. Hines, J.J. Vandenberg, Application of epigenetic data in human health risk assessment, *Current opinion in toxicology*, 6 (2017) 71-78.
- [23] S. Gul, Epigenetic assays for chemical biology and drug discovery, *Clinical epigenetics*, 9 (2017) 41.
- [24] S.W. Dietrich, M.B. Bolger, P.A. Kollman, E.C. Jorgensen, Thyroxine analogs. 23. Quantitative structure-activity correlation studies of in vivo and in vitro thyromimetic activities, *Journal of Medicinal Chemistry*, 20 (1977) 863-880.
- [25] L. Bleicher, R. Aparicio, F.M. Nunes, L. Martinez, S.M.G. Dias, A.C.M. Figueira, M.A.M. Santos, W.H. Venturelli, R. Da Silva, P.M. Donate, Structural basis of GC-1 selectivity for thyroid hormone receptor isoforms, *BMC structural biology*, 8 (2008) 8.
- [26] L. Martínez, A.S. Nascimento, F.M. Nunes, K. Phillips, R. Aparicio, S.M.G. Dias, A.C.M. Figueira, J.H. Lin, P. Nguyen, J.W. Apriletti, Gaining ligand selectivity in thyroid hormone receptors via entropy, *Proceedings of the National Academy of Sciences*, 106 (2009) 20717-20722.
- [27] J.J. Hangeland, A.M. Doweiko, T. Dejneka, T.J. Friends, P. Devasthale, K. Mellström, J. Sandberg, M. Grynfarb, J.S. Sack, H. Einspahr, Thyroid receptor ligands. Part 2: Thyromimetics with improved selectivity for the thyroid hormone receptor beta, *Bioorganic & medicinal chemistry letters*, 14 (2004) 3549-3553.
- [28] Y.-L. Li, C. Litten, K.F. Koehler, K. Mellström, N. Garg, A.M.G. Collazo, M. Färnegård, M. Grynfarb, B. Husman, J. Sandberg, Thyroid receptor ligands. Part 4: 4'-amido bioisosteric ligands selective for the thyroid hormone receptor beta, *Bioorganic & medicinal chemistry letters*, 16 (2006) 884-886.
- [29] D.H. Ipsen, J. Lykkesfeldt, P. Tveden-Nyborg, Molecular mechanisms of hepatic lipid accumulation in non-alcoholic fatty liver disease, *Cellular and molecular life sciences*, 75 (2018) 3313-3327.
- [30] R. Singh, S. Kaushik, Y. Wang, Y. Xiang, I. Novak, M. Komatsu, K. Tanaka, A.M. Cuervo, M.J. Czaja, Autophagy regulates lipid metabolism, *Nature*, 458 (2009) 1131-1135.
- [31] R.A. Sinha, B.K. Singh, P.M. Yen, Direct effects of thyroid hormones on hepatic lipid metabolism, *Nature Reviews Endocrinology*, 14 (2018) 259.
- [32] H.-C. Chi, C.-Y. Tsai, M.-M. Tsai, C.-T. Yeh, K.-H. Lin, Molecular functions and clinical impact of thyroid hormone-triggered autophagy in liver-related diseases, *Journal of biomedical science*, 26 (2019) 24.
- [33] M. Gasparri, F. Giampieri, J.M. Alvarez Suarez, L. Mazzoni, Y.F.H. T, J.L. Quiles, P. Bullon, M. Battino, AMPK as a New Attractive Therapeutic Target for Disease Prevention: The Role of Dietary Compounds AMPK and Disease Prevention, *Current drug targets*, 17 (2016) 865-889.
- [34] S.J. Wakil, L.A. Abu-Elheiga, Fatty acid metabolism: target for metabolic syndrome, *Journal of lipid research*, 50 Suppl (2009) S138-143.

- [35] D. Zhang, W. Wang, X. Sun, D. Xu, C. Wang, Q. Zhang, H. Wang, W. Luo, Y. Chen, H. Chen, AMPK regulates autophagy by phosphorylating BECN1 at threonine 388, *Autophagy*, 12 (2016) 1447-1459.
- [36] I. Tamargo-Gomez, G. Marino, AMPK: Regulation of Metabolic Dynamics in the Context of Autophagy, *Int J Mol Sci*, 19 (2018).
- [37] R.A. Friesner, R.B. Murphy, M.P. Repasky, L.L. Frye, J.R. Greenwood, T.A. Halgren, P.C. Sanschagrin, D.T. Mainz, Extra precision glide: docking and scoring incorporating a model of hydrophobic enclosure for protein-ligand complexes, *J Med Chem*, 49 (2006) 6177-6196.
- [38] T.A. Halgren, R.B. Murphy, R.A. Friesner, H.S. Beard, L.L. Frye, W.T. Pollard, J.L. Banks, Glide: a new approach for rapid, accurate docking and scoring. 2. Enrichment factors in database screening, *J Med Chem*, 47 (2004) 1750-1759.
- [39] R.A. Friesner, J.L. Banks, R.B. Murphy, T.A. Halgren, J.J. Klicic, D.T. Mainz, M.P. Repasky, E.H. Knoll, M. Shelley, J.K. Perry, D.E. Shaw, P. Francis, P.S. Shenkin, Glide: a new approach for rapid, accurate docking and scoring. 1. Method and assessment of docking accuracy, *J Med Chem*, 47 (2004) 1739-1749.
- [40] T.F. Liu, V.T. Vachharajani, B.K. Yoza, C.E. McCall, NAD<sup>+</sup>-dependent sirtuin 1 and 6 proteins coordinate a switch from glucose to fatty acid oxidation during the acute inflammatory response, *J Biol Chem*, 287 (2012) 25758-25769.



**Supplementary Material - For Publication Online**

[Click here to download Supplementary Material - For Publication Online: EurJMedChem\\_supplementary material SR.docx](#)

**Data in Brief**

[Click here to download Data in Brief: DatainBrief.zip](#)

**Manuscript EJMECH-D-19-02351**

**Design, synthesis and biological evaluation of novel TR $\beta$  selective agonists sustained by ADME-Toxicity analysis**

Massimiliano Runfola, Simona Sestito, Lorenza Bellusci, Valeria La Pietra, Vincenzo Maria D'Amore, Marta Anna Kowalik, Grazia Chiellini, Sheraz Gul, Andrea Perra, Amedeo Columbano, Luciana Marinelli, Ettore Novellino, Simona Rapposelli

**Declaration of interests**

The authors declare that they have no known competing financial interests or personal relationships that could have appeared to influence the work reported in this paper.

The authors declare the following financial interests/personal relationships which may be considered as potential competing interests: